

University of Naples “Federico II”



Department of Biology

**Doctorate School in Biology
Cycle XXIX**

**MYC proteins in human cancer: epigenetic changes and
molecular targeting**

Susanna Ambrosio

**Coordinator
Prof. Salvatore Cozzolino**

**Tutor
Prof. Barbara Majello**

INDEX

1. INTRODUCTION	1
1.1 MYC proteins in cancer, an overview	1
1.1.1 Cell proliferation and metabolism.....	2
1.1.2 Genomic instability.....	3
1.1.3 Tumor environment and metastasis	4
1.2 MYC and chromatin	5
1.2.1 MYC proteins and histone acetylation	5
1.2.2 MYC proteins and histone methylation.....	6
1.3 LSD1	6
1.3.1 MYCN/LSD1 complex in neuroblastoma	7
2 MYC IMPAIRS RESOLUTION OF SITE-SPECIFIC DNA DOUBLE-STRAND BREAKS REPAIRCELL CYCLE-DEPENDENT RESOLUTION OF DNA DOUBLE-STRAND BREAKS	9
3 CELL CYCLE-DEPENDENT RESOLUTION OF DNA DOUBLE-STRAND BREAKS	18
4 LSD1 MEDIATES MYCN CONTROL OF EPITHELIAL-MESENCHYMAL TRANSITION THROUGH SILENCING OF METASTATIC SUPPRESSOR NDRG1 GENE	31
5 LYSINE-SPECIFIC DEMETHYLASE LSD1 INHIBITORS INDUCE AUTOPHAGY THROUGH SESN2-DEPENDENT PATHWAY	48
6 CONCLUSIONS	78
7 BIBLIOGRAPHY	86

CHAPTER 1
INTRODUCTION

Introduction

1.1 MYC proteins in cancer, an overview

MYC proteins are a group of transcription factors that includes c-MYC, N-MYC and L-MYC. MYC transcription factors have highly homologous structures and contain a bHLH/LZ (basic Helix-Loop-Helix/Leucine Zipper) domain: through the bHLH domain MYC proteins bind to DNA, while the leucine zipper domain allows dimerization with the Max co-factor; the heterodimer MYC/MAX binds consensus sequences (CANNTG) named E-box in the regulatory regions of its target genes and recruit transcriptional co-factors (1, 2).

Myc is considered a master regulatory transcription factor that has been estimated to bind to over 10% of gene promoters in different cellular types. MYC activates gene transcription through the release of the RNA polymerase II by recruiting to the promoters the transcription elongating factor b (P-TEFb) (3), but it has been also describes to negatively regulate target genes transcription through the interaction with the transcription factors Myc interacting zinc protein 1 (Miz-1) or SP1 (4, 5).

MYC family proteins are overexpressed in several cancers such as lymphoma, melanoma, multiple myeloma and neuroblastoma, as well as colon, breast and lung cancers (6-9). On average, 70% of human tumors show an increased MYC expression, feature that usually correlates with high-grade premalignancy and invasive cancers, and associates with poor prognosis (10-13). Pathological MYC over-expression is frequently achieved by transcriptional up-regulation due to chromosomal translocation (14-18), gene amplification (19, 20) or by virus mediated insertional mutagenesis (21, 22). Although the increase in MYC gene copy number is not always related to MYC overexpression, the frequent correlation of this event with metastasis and poor survival of patients indicate his direct role in many human cancers (23). MYC overexpression is involved in all aspects of tumor cell biology by promoting proliferation, cell survival, differentiation blockage, angiogenesis and metastasis. Furthermore, cell proliferation, metabolic boost and survival promoted by MYC produce cells with highly unstable genomes and, consequently, a higher chance to accumulate additional mutations, which may contribute to tumor progression and maintenance. These processes provide cancer cells with a long-term proliferative

Introduction

advantage; on the other hand each of them represents a possible target to develop innovative therapeutic approaches to counteract Myc overexpressing tumors.

1.1.1 Cell proliferation and metabolism

MYC has a critical role in different physiological processes and its overexpression may alter transcription of its target genes involved in cell cycle, replication, metabolism, and RNA biogenesis. MYC has the ability to stimulate tumor progression by promoting proliferative and pro-survival pathways, which could give cancer cells a long-term advantage. MYC proteins can profoundly influence cell cycle progression. It has been shown that MYC ectopic expression is sufficient to drive the quiescent cells in S phase, independent of any growth stimulus (24, 25). MYC promotes cell cycle progression directly by controlling cell cycle regulator factors expression. Indeed, MYC activates transcription of genes essential for cell cycle progression, such as CDKs, cyclins and E2F1 (26, 27). MYC also can indirectly induce the activation of complex cyclin/Cdk through the activation of Cdk activating kinase (CAK) and Cdc25 phosphatases (28). On the other hand, Myc can also antagonize antiproliferative genes, such as p21 (29, 30) and p27 (31). Moreover, Myc stimulates DNA replication by the upregulation of genes encoding proteins essential for replication initiation and by its interaction with the pre-replicative complex and localization to early sites of DNA synthesis.

Rapidly dividing cells need a constant flow of nutrients, energy and protein to sustain a high rate of replication and division and MYC promotes the metabolic adaptation in tumor, regulating mitochondrial biogenesis, glucose and glutamine metabolism (32). In addition to these processes, MYC amplification activates the expression of genes encoding proteins involved in ribosome biogenesis and translation of mRNAs and promotes mRNA capping (33). MYC also increases the translational capacity of cells through the activation of transcription by RNA polymerase I (34, 35) and III (36), which increase the synthesis of rRNA and tRNA, respectively. Finally, MYC cooperates with mTOR, master regulator of protein synthesis, by directly stimulating the activity of factors such as eIF4E, which increases the efficiency of mRNA to occupy ribosomes (37).

Introduction

1.1.2 Genomic instability

MYC overexpression is associated with activation of DNA damage response (DDR) (38-40) and increased genomic instability (41, 42), suggesting that high levels of MYC expression lead to accumulation of DNA damage. First, enhanced mitochondrial biogenesis and cellular metabolism induced by MYC overexpression are not accompanied by the appropriate compensatory mechanism that normally reduces the oxygen free radicals (ROS), exposing cell to a ROS accumulation with consequent oxidative DNA damage (43).

Another potential source of genomic instability may arise from the MYC ability to regulate the biology of telomeres; there is evidence that MYC activation leads to end-to-end chromosomes fusion, promoting breakage-fusion-bridge cycles and subsequently chromosomal rearrangements (44).

Aberrant proliferation induced by oncogenes disconnects DNA replication events by other processes that normally are closely coordinated to ensure faithful duplication of chromosomes. This anomaly results in a phenomenon called "replication stress", a condition that generates aberrant DNA replication intermediates that induce a DNA damage response on sites of active replication and determine chromosomal instability. MYC overexpression is associated with an increase of active replication origins and premature origin firing, which could lead to the physical clashing of the replication fork along with the RNA polymerase, causing replication fork collapse and DNA damage (45).

Myc seems to be also involved in the regulation of DNA repair. Indeed, it has been demonstrated that enhanced MYC expression inhibits DSB repair in γ -irradiated cells, increasing genomic instability (46, 47).

1.1.3 Tumor environment and metastasis

Myc activation is also associated with global changes in tumor microenvironment, which may also contribute to tumorigenesis. Enhanced MYC expression leads to release of numerous tumor associated cytokines, chemokines and other inflammatory mediators that activate inflammatory responses and lead to alterations in immune surveillance mechanisms (48). MYC contributes to tumor vascularization by the induction of vascular endothelial growth factor

Introduction

(VEGF) expression (49) and the repression of thrombospondin-1, leading to adjacent endothelial cells to proliferate and form the vascular network (50).

Myc can also increase cancer cells ability to metastasize, stimulating the expression of factors which enhance tumor invasion and reduce cell adhesion. Indeed, Myc activates epithelial-to-mesenchymal transition (EMT) through the regulation of a miRNA, miR-9, which targets E-cadherin, a key mediator of cell adhesion (51, 52). MYC also promotes TGF β -mediated activation of the SNAIL transcription factor, both directly and indirectly through a micro-RNA network involving a LIN28B/let-7/HMGA2 pathway (53). Similarly, MYC represses N-Myc Downstream-Regulated Gene 1 (NDRG1) expression (54), a protein that has been widely implicated in promoting cancer cell migration and invasion. Beyond direct transcriptional regulation of EMT-related genes, MYC could facilitate metastasis by its ability to promote a stem-like state, by blocking differentiation pathways and enhancing self-renewal and pluripotency factors (55, 56).

1.2 MYC and chromatin

In the recent years has emerged the notion that tumors in which MYC activation occurred appear to be “addicted” to MYC high levels to sustain the malignant state, including in cases where MYC is not the primary oncogenic driver (57). Accordingly, several reports suggest that suppression of MYC expression via RNA interference, short hairpin and antisense oligonucleotides, in a wide variety of MYC-amplified tumors, increases apoptosis and differentiation, and restores the normal tissue architecture (58-60), suggesting that targeting MYC activity may be a possible therapeutic strategy in MYC-amplified cancers. However, MYC itself, as most transcription factors, is difficult to drug. Given the pivotal involvement of chromatin in MYC expression and activity, a promising approach to circumvent blocking MYC is directly targeting chromatin modifiers that drive MYC-dependent transcription.

1.2.1 MYC proteins and histone acetylation

The histone acetylation acts on transcriptional regulation through at least two

Introduction

mechanisms: while on the one hand promotes the opening of chromatin structure, on the other it generates binding sites for specific protein-protein interaction that recruit specific acetylation-dependent chromatin reader, such as the acetyl lysine-binding bromodomain.

MYC-mediated transcription is correlated to a plethora of acetylation events at target gene loci, mediated by a large number of histone acetyltransferases (HATs) and HAT-containing complexes including GCN5/PCAF, Tip60, and p300/CBP, as well as the adaptor protein TRRAP, component of many HAT complexes (61-63).

Although less studied, control of histone acetylation has also been implicated in transcriptional repression by MYC. Associations have been reported between MYC and histone deacetylases (HDACs); indeed, MYC has been shown to recruit HDAC-containing co-repressor complexes to target loci, correlating with a reduction in histone acetylation and repression of gene activity (64-67).

1.2.2 MYC proteins and histone methylation

In contrast to histone acetylation, the role that histone methylation plays in regulation of gene expression by MYC seems to be more intricate. In *Drosophila* Myc has been found to inhibit the activity of the thriatorax protein Lid; Lid belongs to the JARID1 family, that acts as demethylases targeting MeK4-H3. Expression of dMyc abrogates Lid enzymatic activity, blocking demethylation of MeK4-H3 and maintaining an active chromatin mark (68).

MYC was also demonstrated to repress its target gene expression via direct interaction with DNMT3a and PRC2 complex (69, 70). In addition, MYC has been found to recruit the H3K4 demethylase LSD1 to target genes (71). LSD1 stimulates MYC function triggering a transient demethylation of H3K4me2 at MYC target genes. Interestingly, in this case demethylation determines activation of Myc target genes: LSD1 reaction leads to the production of hydrogen peroxide that locally induces the modification of guanines in 8-oxodG, which recruits DNA damage repair factors OGG1 and Ape1 to stimulate transcription. These findings give rise to the interest on how LSD1/MYC complex transcriptional activity could be exploited in the context of particular types of MYC-driven cancers (71).

Introduction

1.3 LSD1

LSD1/KDM1A is an amine oxidase that catalyzes lysine demethylation in a FAD-dependent reaction (72, 73). LSD1 removes mono- and dimethyl groups from lysine 4 and lysine 9 of histone H3. In this reaction, FAD oxidizes the methyl-lysine generating an imine intermediate that is subsequently hydrolyzed to form unmodified lysine and formaldehyde while the reduced FAD is oxidized by molecular oxygen, forming hydrogen peroxide as a by-product.

LSD1 is highly conserved and contains three protein domains: an N-terminal SWIRM (Swi3p/Rsc8p/Moira) structural domain, a tower domain and a C-terminal amine oxidase (AO) domain. The SWIRM and AO domains interact to form a core structure that binds FAD not-covalently and serves as the enzymatic domain; the tower domain provides a surface platform for interaction with partners (74).

LSD1 associates with different complexes. It was initially described as co-repressor of CoREST (75), but has been found to have a role in transcriptional activation as exemplified by MYC induced transcription mechanism described above. LSD1 is also part of a nucleosome remodeling and deacetylation complex, NuRD (76).

In addition to its direct activity on chromatin structure, LSD1 also regulates global or specific gene expression patterns through demethylation of non-histone targets, such as Dnmt1, the major enzyme responsible for maintaining DNA methylation during DNA replication (77).

LSD1 also inhibits DNA damage-induced cell death, through the specific demethylation of p53, which blocks the interaction between p53 and 53BP1, and then the ability of p53 in promoting apoptosis (78).

In addition, several reports strongly indicate that LSD1 is critically involved in several cell types differentiation and in the epithelial-to-mesenchymal transition (79, 80). LSD1 physically associates with Snail and is recruited to epithelial gene promoters in a-Snail mediated manner, with consequently repression of transcription via H3K4 demethylation (81, 82); moreover, LSD1 is over-expressed in several cancers, such as prostate (83), bladder (84),

Introduction

neuroblastomas (85), lung cancers sarcomas and hepatocarcinomas (86). Considering the association between high levels of LSD1 and tumorigenesis, LSD1 has been proposed as epigenetic drugs target in cancer.

1.3.1 MYCN/LSD1 complex in neuroblastoma

Neuroblastoma is the most common extra cranial solid tumour of infancy. Neuroblastomas are tumours of the sympathetic nervous system and may occur anywhere along the sympathetic ganglia (87).

Although an excellent prognosis in patients with low and intermediate risk has been registered after cure, the outcome remains very poor for relapsed high-risk disease. One of the most important biological markers is MYCN oncogene amplification, which occurs in approximately 25% of cases and correlated with poor prognosis and advanced stages of disease (89, 90).

In 2009 Schulte and co-workers addressed the functional significance of LSD1 in neuroblastoma (85). They demonstrated that LSD1 expression correlated with adverse outcome and is involved in maintaining the undifferentiated, malignant phenotype of neuroblastoma cells, highlighting its central role in the pathogenesis of the malignancy. LSD1 targeting resulted in growth inhibition of neuroblastoma cells in vitro and reduced neuroblastoma xenograft growth in vivo.

Noteworthy, Prof. Majello laboratory has recently shown that LSD1 interacts with MYCN and cooperates in repression of tumor suppressor genes involved in MYCN-driven oncogenesis in Neuroblastoma (91). They reported that MYCN interacts and recruits LSD1 on its target genes. LSD1 can form a complex with MYCN and this complex controls transcription of genes such as p21 and clusterin (CLU). Inhibition of LSD1 causes reactivation of p21, CLU and, plausibly, other potential tumor suppressor genes involved in MYCN-driven oncogenesis with therapeutic effects, suggesting that LSD1 inhibition could be therapeutically used, alone or in combination with other therapeutic tools, to counteract MYCN-amplified neuroblastomas.

CHAPTER 2

**MYC IMPAIRS RESOLUTION OF SITE-SPECIFIC DNA DOUBLE-STRAND
BREAKS REPAIR**

Susanna Ambrosio ^{a,1}, Stefano Amente ^{b,1}, Giuliana Napolitano ^a, Giacomo Di Palo ^b,
Luigi Lania ^b, Barbara Majello ^a

^a Department of Biology, University of Naples 'Federico II', Naples, Italy

^b Department of Molecular Medicine and Medical Biotechnologies, University of Naples 'Federico II', Naples, Italy

¹ These authors contributed equally to this work.

Published Mutation Research. 2015 Apr;774:6-13.

The chapter is an exact copy of the journal paper referred to above.



MYC impairs resolution of site-specific DNA double-strand breaks repair



Susanna Ambrosio^{a,1}, Stefano Amente^{b,1}, Giuliana Napolitano^a, Giacomo Di Palo^b, Luigi Lania^{b,*}, Barbara Majello^{a,**}

^a Department of Biology, University of Naples 'Federico II', Naples, Italy

^b Department of Molecular Medicine and Medical Biotechnologies, University of Naples 'Federico II', Naples, Italy

ARTICLE INFO

Article history:

Received 26 November 2014

Received in revised form 23 February 2015

Accepted 24 February 2015

Available online 4 March 2015

Keywords:

Site-specific DSBs

AsiSI restriction enzyme

MYC

MYCN

DSB repair

ABSTRACT

Although it is established that when overexpressed, the MYC family proteins can cause DNA double-strand breaks (DSBs) and genome instability, the mechanisms involved remain unclear. MYC induced genetic instability may result from increased DNA damage and/or reduced DNA repair. Here we show that when overexpressed, MYC proteins induce a sustained DNA damage response (DDR) and reduce the wave of DSBs repair. We used a cell-based DSBs system whereby, upon induction of an inducible restriction enzyme AsiSI, hundreds of site-specific DSBs are generated across the genome to investigate the role of MYC proteins on DSB. We found that high levels of MYC do not block accumulation of γ H2AX at AsiSI sites, but delay its clearance, indicating an inefficient repair, while the initial recognition of DNA damage is largely unaffected. Repair of both homologous and nonhomologous repair-prone segments, characterized by high or low levels of recruited RAD51, respectively, was delayed. Collectively, these data indicate that high levels of MYC proteins delay the resolution of DNA lesions engineered to occur in cell cultures.

© 2015 Elsevier B.V. All rights reserved.

1. Introduction

Activated oncogenes generally associate with the induction of DNA damage response (DDR) [1,2]. This phenomenon named oncogene induced DNA damage (OID) is exemplified by the c-MYC proto-oncogene. The Myc proteins (MYC, MYCN and MYCL in human) are basic helix-loop-helix leucine zipper transcription factors driving a wide range of cellular responses depending on the cellular context. In most human cancers MYC expression is deregulated and/or significantly increased [3,4]. It has been clearly demonstrated that supraphysiological levels of MYC play a causative role in the onset and progression of many types of cancers. In addition to its canonical role in transcription, MYC overexpression in mammalian cells increases genomic instability [5,6]. Although it is not clear what type of physical alterations are induced at the DNA level, recent observations propose that at least two types of DNA damage can be associated with MYC. First, MYC overexpression in mammalian cells results in loss of chromo-

somal integrity associated with chromosomal aberrations [5–9]. An additional source of MYC-induced DNA damage is replication stress, a poorly understood perturbation of DNA replication. Replication stress generates aberrant DNA replication intermediates that induce the activation of DDR at sites of active DNA replication [10–12]. Such non-transcriptional Myc effects are likely crucial to its role in tumorigenesis. However, in both cases the molecular mechanisms involved remain unclear.

It is likely that MYC-induced genomic abnormalities might be generated by defects in the repair of double-strand-breaks (DSB). DSBs are one of the most challenging forms of DNA damage, which in turn if not correctly repaired, can trigger the onset and progression of cancer cells. A number of studies have been focused on DNA-damage response (DDR) mechanisms induced by chemical compounds or radiations. A limitation of this approach is that the sites of DNA damage within the genome occur random and therefore differ from cell to cell, precluding efforts to determine co-association at specific DSBs. To overcome such limitations several systems have been developed that rely on inducible restriction enzymes capable to generate unambiguously positioned sequence-specific DSBs. However, sequence-specific DSB-inducible systems that induce either a single DSB (HO, I-SceI and FokI systems) [13,14] or several DSBs in ribosomal DNA (I-PpoI system) [15] hamper the comparison of DSB repair occurring at different locations.

* Corresponding author. Tel.: +39 081 7643029.

** Corresponding author. Tel.: +39 081 679062.

E-mail addresses: lania@unina.it (L. Lania), majello@unina.it (B. Majello).

¹ These authors contributed equally to this work.

Recently, stable human cell lines have been developed that express the 8-bp restriction enzyme (AsiSI) fused to a modified estrogen receptor ligand binding domain that induces nuclear localization of the enzyme after administration with 4-hydroxytamoxifen (4OHT) causing the rapid and reproducible induction of about 150 sequence-specific DSBs across the genome [16–19]. This system offers the opportunity to study the wave of repair events in a defined and reproducible manner.

Using defined cell systems in which site-specific DSBs were induced in the presence or absence of overexpressed MYC proteins, we found here that overexpression of MYC proteins (MYC and MYCN) does not block recruitment of H2AX at DSBs whereas induces a sustained DNA damage response (DDR) and most importantly reduce the resolution of DNA lesions engineered to occur in cell cultures.

2. Materials and methods

2.1. Cell culture, transfection and drug treatment

U2OS-AsiSI-ER and SHEP-TET-21/N cells were cultured in Dulbecco's modified Eagle's medium (DMEM) supplemented with antibiotics, 10% fetal calf serum at 37 °C in humidified atmosphere with 5% CO₂. The pBABE-HA-AsiSI-ER plasmid was stably transfected in SHEP-TET-21/N cells using a MicroPorator Digital Bio Technology, in according to the protocol described in [20] and selection was performed using 1 µg/ml puromycin for two weeks. U2OS-AsiSI-ER cells were transiently transfected with a Flag-Myc expression vector [20] by the polyethylenimine (PEI 25 kDa) method as described [21] with a 6:1 ratio of PEI (µg):total DNA (µg). Induction of HA-AsiSI-ER chimera was carried out as described [22] by treatment with 300 nM 4OHT for 4 h. MYCN expression under control of the TET-OFF system in double stable TET-21/N-AsiSI-ER cells was turned off by the addition of tetracycline 1 µg/ml for 1 week before 4OHT treatment. When indicated, 4OHT-treated cells were washed three times in prewarmed PBS and further incubated with normal medium for the indicated times.

2.2. Western blot analysis

Whole-cell extracts were obtained using buffer F (10 mM Tris-HCl pH 7.5, 150 mM NaCl, 30 mM Na₄O₇P₂, 50 mM NaF, 5 mM ZnCl₂, 0.1 mM Na₃VO₄, 1% Triton, 0.1 mM PMSF). 50 µg of protein extracts were loaded and separated by SDS-PAGE and WB was performed with following antibodies: anti-actinin (H-2, Santa Cruz, 1:1000), anti-MYCN (B8.4.B, Santa Cruz, 1:1000), anti-c-Myc (9E10, Santa Cruz, 1:500), anti-Phospho-p53 (Ser15) (#9284, Cell Signaling, 1:1000).

2.3. Immunofluorescence

Immunofluorescence of U2OS-AsiSI-ER and TET-21/N-AsiSI-ER cells was performed as previously described [22]. Briefly, cells were fixed in 4% paraformaldehyde in PBS, permeabilized in 0.1% Triton X-100 in PBS, pre-blocked in 2% BSA–3% NS-PBS for 30 min at room temperature, and then incubated for 1 h at 37 °C with mouse anti-HA (32–6700, Invitrogen, 1:50) and rabbit anti-γH2AX (Abcam, 1:70) for 30' at 37 °C. Primary antibody were detected by incubation with Cy3-conjugated anti-mouse or FITC-conjugated anti-rabbit antibody. Images were acquired using a Nikon Eclipse TE 2000-U microscope.

2.4. FACS analysis

To analyze the DNA profile cells were treated as indicated, fixed in methanol at –20 °C and stained in hypotonic solution of 0.1% Na-Citrate, 50 µg/ml propidium iodide, 50 µg/ml RNase and 0.00125% NP40 for 30' at room temperature. Cytofluorimetric acquisition and analysis were performed on a Becton Dickinson FACScalibur flow cytometer using FACSDiva, CellQuest Pro and ModFit LT 3.0 softwares.

2.5. Chromatin immunoprecipitation

ChIP experiments with chromatin extracts from U2OS-AsiSI-ER and TET-21/N-AsiSI-ER cells were performed as described [19]. IPs materials were analyzed in duplicate by quantitative PCR, using Syber Green 2X PCR Master Mix (Applied Biosystem). For qPCRs 3 µl out of 150 µl immunoprecipitated DNA was used. Primer pairs used to measure NBS1 enrichment were located proximal to AsiSI site at Chr. 1 (250 bp) and Chr. 6 (180 bp), respectively; whereas those used to assess γH2AX recruitment were located at 1200 (Chr1) and 1000 (Chr6) bp from AsiSI site, respectively. For each assay distal (D) amplicons were used as negative controls, complete list of oligos are presented in Supplementary Table S1. IP efficiency was calculated as described [19] and presented as percentage of input. All values represent the average of at least three independent experiments. The following antibodies were used: anti-γH2AX (phospho S139, Abcam); anti-p95 NBS1 (Abcam).

3. Results

3.1. AsiSI-dependent DSBs induce DDR activation followed by efficient wave of repair

Following DSBs detection DDR induces cellular DNA-repair activities with a concomitant transient arrest of cell-cycle progression (checkpoint function) until DNA damage has been removed. To analyze the transient arrest of cell-cycle progression following induction of DSBs, we designed an experimental condition in which proliferating U2OS-AsiSI-ER cells were treated for 4 h with 4OHT, then cells were allowed to recovery in the absence of 4OHT, and samples collected at 24, 48 and 72 h for cell-cycle distribution DDR, activation and accumulation of γH2AX. As expected, 4OHT induces nuclear translocation of the fused HA-AsiSI-ER protein in a large number of cells. After 24 h of recovery the nuclear localization of HA-AsiSI-ER was strongly reduced (Fig. 1A), indicating that HA-AsiSI-ER was not generating DSBs. Accordingly with previous studies [14,22], cell cycle analysis shows that AsiSI-dependent DSBs induced a significant G2 arrest, which was completely resolved after 72 h of recovery (Fig. 1B), and such effect was specific to 4OHT treatment since control untreated cells did not displayed a prominent G2 arrest (Supplementary Fig. 1). The induction of a robust DDR, measured by accumulation of phosphorylated form of p53-Ser15 (Fig. 1C), was resolved by an efficient wave of repair, which reduced p53-Ser15 levels. To evaluate DSBs formation at AsiSI sites, we performed S139-phosphorylated histone H2AX (γH2AX) ChIP. Following the robust increase of γH2AX at the AsiSI sites after 4OHT treatment we found a progressively reduction in time of the γH2AX accumulation (Fig. 1D).

Collectively, these data indicate that AsiSI-dependent DSBs in U2OS cells, induces a robust DDR activation, which is followed by efficient wave of repair leading to a progressive reduction of DDR at 48 h after DSBs onset.

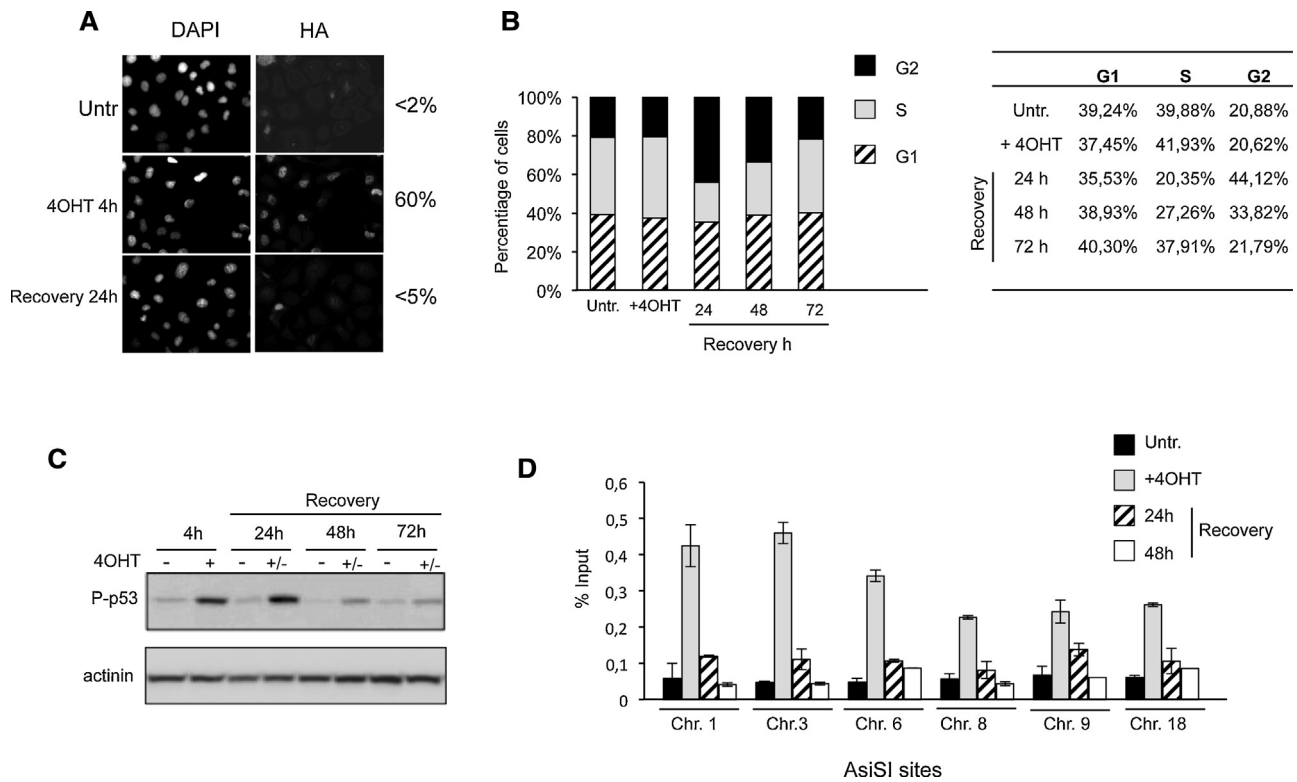


Fig. 1. AsiSI-induced DSBs trigger DDR activation followed by efficient wave of repair. (A) U2OS-AsiSI-ER cells were treated for 4 h with 4OHT or vehicle (Untr) and then released into fresh medium for 24 h (recovery 24 h). Cells were fixed and processed for anti-HA immunofluorescence and DAPI staining. Values on the right side indicate percentage of nuclear HA positively stained cells. (B) Cell-cycle distribution of U2OS-AsiSI-ER cells, treated as indicated, was measured by FACS analysis; the average values from three independent experiments are reported in the table; all standard deviations are <15%. (C) U2OS-AsiSI-ER cells were treated for 4 h with 4OHT or vehicle and then released into fresh medium for indicated times. Cellular extracts were prepared and stained with anti-phospho-p53. Actinin has been probed as loading control. (D) γ H2AX enrichment was estimated by ChIP experiments in AsiSI-ER U2OS treated as indicated above. IP materials were analyzed by q-PCR using a set of primers located about 1 kb away from the DSB at the indicated chromosomes. The values reported were calculated as percentage of input. The result is an average of three experiments with error bars showing standard deviation.

3.2. MYC overexpression affects DSBs repair in U2OS-AsiSI-ER cells

To investigate the impact of MYC overexpression in DDR, U2OS-AsiSI-ER cells were transfected with a Flag-MYC expression vector, treated 24 h later with 4OHT (4 h) and, collected at 24 h, 48 h and 72 h after treatment. Fig. 2A shows that, overexpression of MYC interferes with the timing of AsiSI-induced DSBs repair. We found that transient arrest of cell proliferation in control cells is resumed at 48 h after DSBs; in contrast, MYC expressing cells with induced DSBs show reduced cell numbers, particularly from 48 to 72 h suggesting that cell death is occurring (Fig. 2A). Damaged MYC overexpressing cells are mainly arrested in G2 even 72 h after treatment (Fig. 2C) suggesting that these cells display a longer DDR. The persistent activation of DDR is indicated by the accumulation of P-p53-Ser15 at 48 h after DSBs (compare lanes 4 and 8 of Fig. 2D). Conversely, in 4OHT-untreated cells Myc overexpression does not induce detectable increase P-p53-Ser15 (compare lanes 1 and 5 of Fig. 2D), while a small induction of γ H2AX foci was found in a fraction of cells (Supplementary Fig. 2). Consequently, DDR activation is largely due to DSBs induction rather than MYC overexpression.

DDR cascade begins with the detection of DSBs by the MRN (MRE11-RAD50-NBS1) complex, which recruits and activates PIKK kinases (ATM, ATR and DNA-PK) each capable to phosphorylate H2AX at Ser139 [23–25]. To analyze the efficiency of these steps detecting DSBs and to monitor the resolution of DNA damage-associated γ H2AX and NBS1 accumulation at defined AsiSI sites we performed ChIP with γ H2AX and NBS1 antibodies. The ChIP

samples were analyzed by quantitative qPCR with probes located in the proximal (P) and distal (D) positions of the chromosomal AsiSI site (Fig. 3A and B). As expected, we found that in control cells expressing endogenous low levels of MYC both sites accumulated γ H2AX at DSBs that disappeared by 24 h of recovery. In cells overexpressing MYC protein the levels of γ H2AX and NBS1 recruited to DSBs were largely similar to control cells, while a persistent accumulation of both γ H2AX and NBS1 at DSBs was found, indicating that high levels of MYC impairs resolution of DNA repair. Moreover, cells that cannot resolve the breaks may die.

Because DSBs accumulation of γ H2AX occurs within minutes of the DNA damage event, we determined the timing of recruitment and resolution of γ H2AX in cells exposed to AsiSI-damage for a short period of time (30'). Fig. 3 panel C, shows that MYC overexpression does not inhibit γ H2AX deposition, but its release from the damaged sites.

Collectively, our data indicate that overexpressed MYC does not significantly affect early γ H2AX recruitment, but it reduces the efficiency of repair and the release of the recruited γ H2AX and NBS1 from the damaged sites. It is likely that cells that cannot resolve DSB would eventually die.

3.3. MYCN impairs DSBs repair in Neuroblastoma cells

Because MYC and MYCN proteins share many similar sequences and functions we sought to investigate the effects of overexpressed MYCN in the repair mechanisms of AsiSI-induced DSBs. To this end, U2OS-AsiSI-ER cells were transfected with the Flag-MYCN expression vector and after 24 h cells were treated with 4OHT

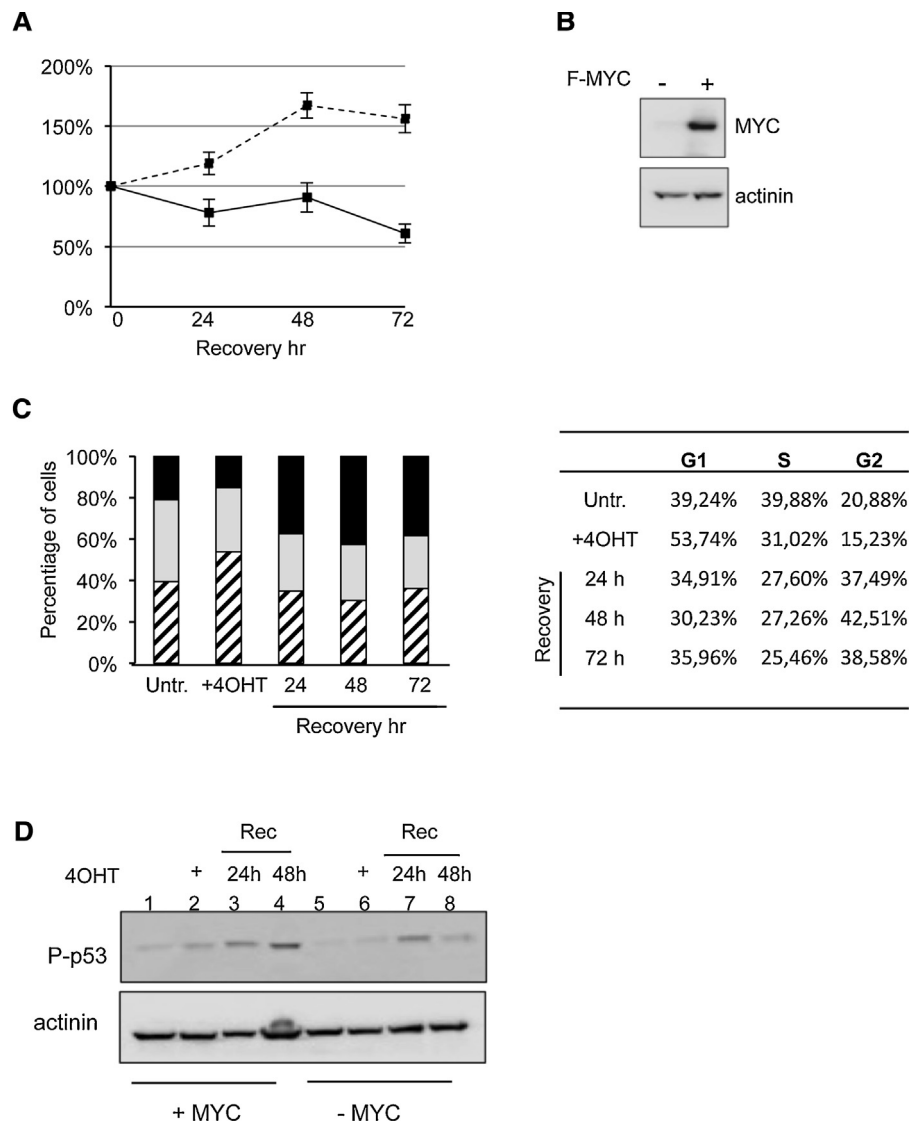


Fig. 2. MYC overexpression affects DSBs repair in U2OS-AsiSI-ER cells. (A–D) U2OS-AsiSI-ER cells were transfected with the Flag-MYC expression vector or empty vector; after 24 h cells were treated for 4 h with 4OHT or vehicle (Untr), washed three times, and allowed to recover for the indicated times before processing. (A) Direct cell count time course analysis was performed in parental U2OS-AsiSI-ER cells (dashed line) and in MYC-overexpressed cells (solid line). Values are expressed as a percentage of seeded cells number. All values represent the average of three independent experiments. Error bars indicate SD. (B) MYC protein levels in transfected U2OS-AsiSI-ER cells were determined by WB. (C) Cell-cycle distribution of MYC-overexpressed U2OS-AsiSI-ER cells treated as indicated was measured by FACS analysis; the average values from three independent experiments are reported in the table; all standard deviations are <15%. (D) Whole cell extracts from control and MYC-transfected U2OS-AsiSI-ER cells were prepared from 4OHT-treated cells for 4 h with OHT and after recovery (Rec) for the indicated times and probed with anti-phospho-p53 or anti-actinin as loading control.

(4 h) and with additional 24 h (recovery). We found that MYCN overexpression induces a persistent accumulation of γ H2AX at AsiSI DSBs, suggesting that like MYC also MYCN impairs the repair mechanisms of AsiSI-induced DSBs in U2OS-AsiSI-ER cells (Supplementary Fig. 3). Because MYCN plays a causative role in human Neuroblastoma, to further analyze the role of MYCN in DSBs repair mechanisms, we constructed an inducible AsiSI-ER derived Neuroblastoma SHEP-TET-21/N cell line (TET-21/N-AsiSI-ER). The SHEP-TET-21/N cells express MYCN under control of the TET-OFF system thus addition of tetracycline strongly reduces MYCN expression [26]. In the double stable TET-21/N-AsiSI-ER cells, MYCN can be turned off by the addition of tetracycline, while AsiSI-ER can be induced by 4OHT treatment. TET-21/N-AsiSI-ER cell populations grown in the presence or absence of tetracycline were treated with 4OHT for 4 h and the effects were analyzed by indirect immunofluorescence. Exposure to 4OHT of both high and low MYCN expressing cells, resulted in nuclear accumulation of the AsiSI fusion protein, as detected by immunofluorescence (Fig. 4A). This was accompanied

by a significant increase in the number of DNA damage γ H2AX foci. To address the role of MYCN overexpression in DDR mechanisms of site-specific DSBs, TET-21/N-AsiSI-ER cells expressing high or low MYCN levels were exposed to 4OHT and samples collected after recovery at 24 h and 48 h, and analyzed for DDR activation and accumulation of γ H2AX. A wave of DDR activation as indicated by the accumulation of P-p53, was found in both high and low-expressing MYCN cell populations, with an increase of the relative amounts of P-p53 at 24 h after recovery (compare lanes 3 and 7 of Fig. 4 panel B). In parallel, we performed CHIP with γ H2AX antibody to evaluate the efficiency of DSBs induction and the wave of repair. We found that γ H2AX accumulated at AsiSI-DSB with a similar efficiency in either high and low expressing MYCN cells. In low MYCN cells we found a progressively reduction in time of the γ H2AX deposition. Conversely, MYCN overexpression induces a persistent accumulation of γ H2AX, indicating that in analogy with MYC, overexpression of MYCN delays resolution of DNA damage-associated γ H2AX recruitment.

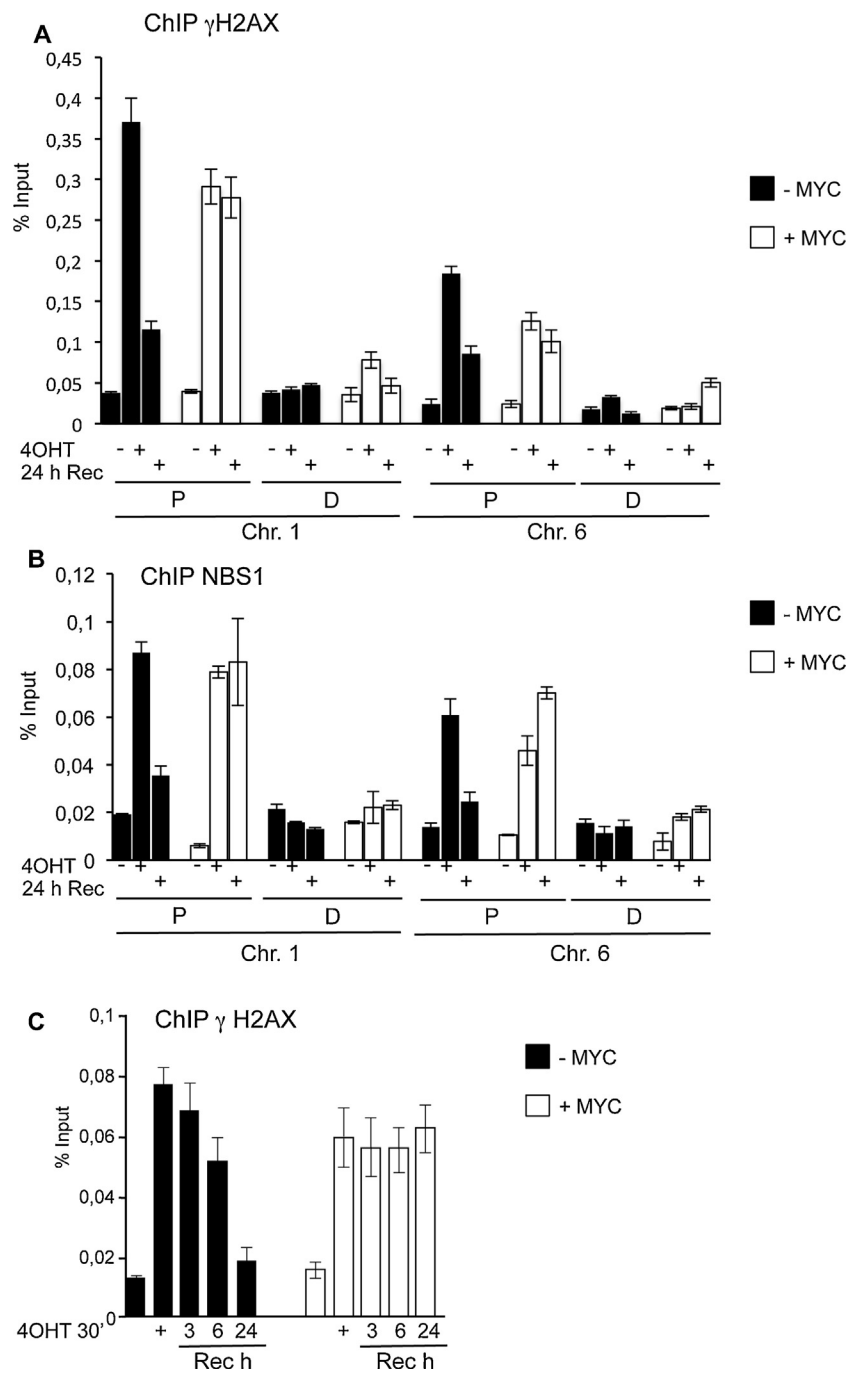


Fig. 3. MYC overexpression delays the presence of γ H2AX and NBS1 in cells following DSBs induction. Control and MYC-transfected U2OS-AsiSI-ER cells were treated as described in Fig. 2, and processed for ChIP experiments using anti- γ H2AX (A and C) and anti-NBS1 (B) antibodies. γ H2AX and NBS1 enrichment was estimated by q-PCR, using probes located in proximal (P) and distal (D) position from the AsiSI-site. Distal amplicon were used as negative control. (C) ChIP analysis with γ H2AX of control and MYC-transfected U2OS-AsiSI-ER cells after a sort pulse of 4OHT treatment (30') and wave of recovery of 3, 6 and 24 h as indicated. The values reported were calculated as percentage of input. Error bars indicate SD for three independent experiments.

3.4. MYC represses both RAD51-bound and RAD51-unbound DSBs repair

In a recent work from Legube's laboratory, [19] ChIP-seq analysis of U2OS-AsiSI-ER chromatin have been used to define and characterize two subsets (containing 20 DSBs each) of RAD51-bound and RAD51-unbound DSBs on the basis of respective enrichment of XRCC4 and RAD51 (RAD51/XRCC4 ratio). RAD51 plays a major role in homologous repair of DSB and the presence of RAD51 at chromatin sites undergoing DSB has been indicated as a signature of homologous repair. Specifically, RAD51-rich DSBs are repaired

essentially by HR, while RAD51-depleted are most likely repaired by NHEJ. To determine if MYC overexpression interferes with HR-prone sites, we investigated the timing of γ H2AX recruitment to the RAD51-rich or depleted sites in cells overexpressing MYC. U2OS-AsiSI-ER cells were transfected with the Flag-MYC expression vector and after 24 h cells were treated with 4OHT (4 h) followed by 24 h of recovery (Fig. 5). We found that recruitment and resolution of γ H2AX of either RAD51-bound or RAD51-unbound DSBs exhibited a similar accumulation and resolution of γ H2AX, suggesting that MYC overexpression abnormally delays resolution of DNA lesions occurring at both DSBs categories.

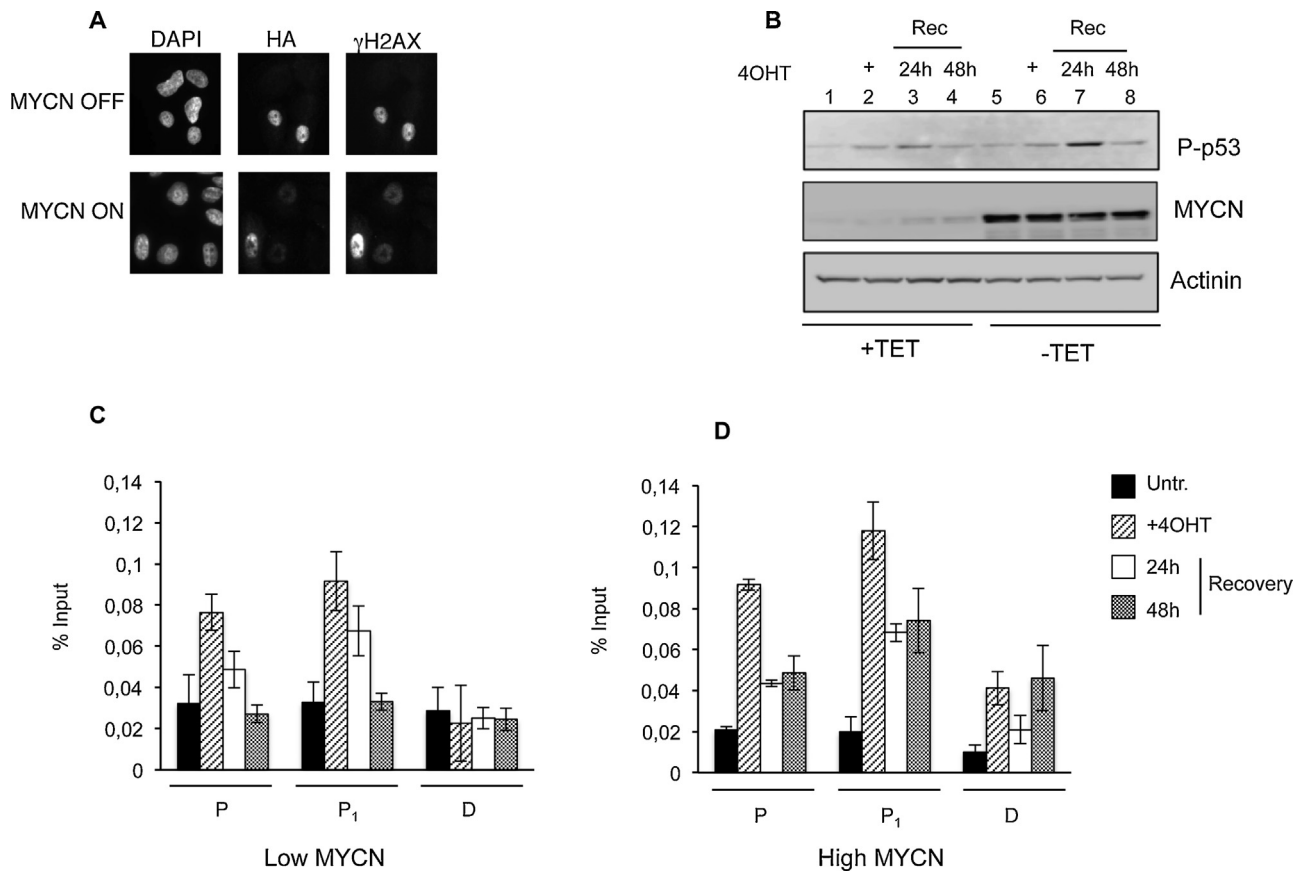


Fig. 4. MYCN impairs DSBs repair in Neuroblastoma cells. (A) TET-21/N-AsiSI-ER were grown in presence (Low MYCN) or absence (High MYCN) of tetracycline, treated for 4 h with 4OHT or vehicle (Untr) and co-stained with anti-HA and anti- γ H2AX antibodies. DAPI staining of nuclei is shown. (B) Protein extracts from TET-21/N-AsiSI-ER were prepared after 4 h of treatment with 4OHT or vehicle (Untr) and recovery for the indicated times. Immunoblots were probed with anti-MYCN, anti-Phospho-p53 and anti-actinin antibodies as indicated. (C, D) TET-21/N-AsiSI-ER expressing cells Low (C) and High (D) levels of MYCN were treated as above and ChIP experiments were performed using anti- γ H2AX antibody primers localized in proximal (P and P₁) and distal (D) position from the AsiSI-site. Data are from independent experiments with SD ($n = 3$).

4. Discussion

In this study, by using human cell lines expressing the estrogen receptor-inducible AsiSI restriction enzyme (U2OS-AsiSI-ER and TET-21/N-AsiSI-ER), we have found that overexpression of MYC proteins (MYC and MYCN) induce a sustained DDR and impair the wave of DSBs repair at the DNA lesions.

Using a ChIP approach we have addressed the influence of MYC protein levels on the DSBs recruitment and resolution of repair factors. One of the key events of DNA lesion repair is the phosphorylation and recruitment of H2AX at DSBs. There are three PIKK kinases (ATM, ATR and DNA-PK) each capable to phosphorylate H2AX at Ser139 [23–26], a modification that occurs shortly after DNA damage event. γ H2AX spreads up to a megabase from the site of the break [16], and it is thought to provide a platform for recruitment and retention of additional DDR proteins forming a focus that is detectable by immunofluorescence. We have found that MYC modestly inhibits deposition of γ H2AX and NBS1, a component of the MRN complex (MRE11-RAD50-NBS1). However, such effect was not observed in Neuroblastoma cells [26] suggesting that the modest inhibition of γ H2AX and NBS1 recruitment seen in U2OS cells is likely cell-specific. Hence, MYC does not prevent appropriate γ H2AX formation, suggesting that at least the initial recognition steps of DSBs are largely unharmed. In sharp contrast, overexpressed MYC or MYCN protein induced a persistent accumulation of γ H2AX and NBS1 at DSBs, thus, affecting resolution of DNA damage-associated γ H2AX recruitment. Based on our data it appears that MYC most likely indirectly affects gene products that

mediate DSBs repair processes rather than directly interfere with the initial steps of the DNA repair response.

DSBs are repaired mainly by two types of mechanisms: nonhomologous end-joining (NHEJ) and homologous recombination (HR). Recently, ChIP-seq analysis of induced AsiSI-DSBs in U2OS-AsiSI-ER cells with antibodies for RAD51 and XRCC4, core components of the HR and NHEJ machineries allowed the identification of an HR-prone subset that recruit the HR protein RAD51 [19]. Using specific probes for these DSBs categories we found that MYC impairs repair of both RAD1-bound as well as RAD1-unbound DSBs suggesting that either HR or NHEJ repair mechanisms are negatively regulated by MYC.

The mechanism by which MYC impairs DSBs repair is not clear. MYC does not block activation of H2AX; thus, initial recognition of DNA damage is unlikely to be affected. However, MYC overexpression activates DDR that results in cell cycle arrest, senescence, or apoptosis [7–9,27,28]. A well described model linking MYC overexpression to p53 pathway is via transcription induction of ARF by MYC, which in turn inhibits MDM2 (a key negative regulator of p53)[29]. However, in U2OS the ARF locus (p14 and 16) expression is undetectable, hence the sustained activation of p53 mainly relays on MYC-dependent inhibition of DSBs repair.

DNA repair pathways involve a large number of factors, thus MYC may affect proper DNA repair at several different layers. Intriguingly, MYC binds to and regulates expression of several repair factors such as TIP60, MRE11, ATM. On the other end, it has been shown that MYC can interact with several DNA repair factors

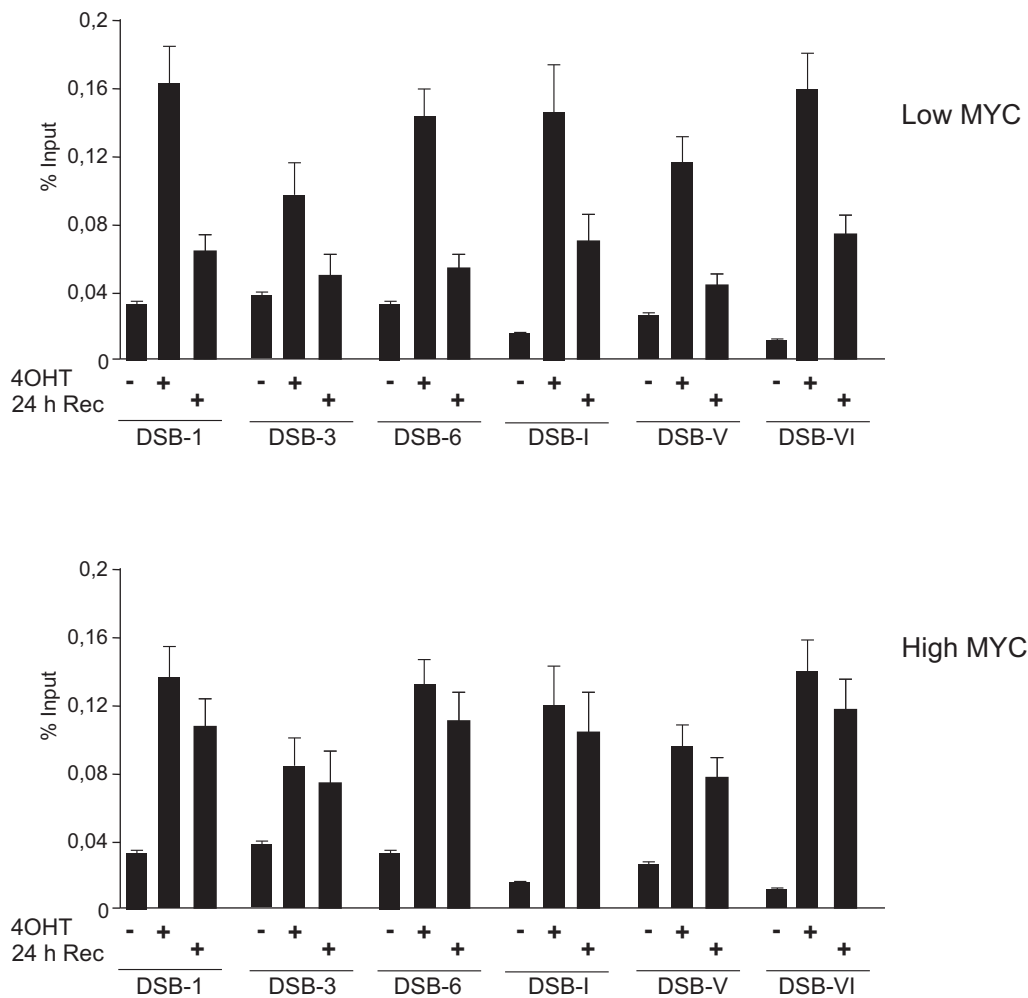


Fig. 5. MYC represses both RAD51-bound and RAD51-unbound DSBs. ChIP was carried out using anti- γ H2AX antibody in untransfected (–MYC) and Flag-Myc (+MYC) transfected U2OS-AsiSI-ER cells treated as described in Fig. 2. γ H2AX enrichment was analyzed by qPCR, using probes located at 800 bp from selected DSBs (DSBs-1, -3 and -6 are RAD51-unbound; DSBs-I, -V and -VI are RAD51-bound). Oligo primers were as described [19]. The values reported were calculated as percentage of input. Error bars indicate SD ($n = 3$).

such as TIP60, DNA-PK and MRE11 [31,32]; however the functional consequences of such interactions remain elusive.

Recent studies have clearly highlighted the role of chromatin structure in the control of DSBs repair mechanisms [30–36]. MYC binds thousands of genomic loci inducing robust chromatin changes. Using the same cell line employed in this work (U2OS cells), ChIP-sequencing identified 20,014 peaks for endogenous low-levels of MYC, while in cells overexpression MYC the number of MYC-bound loci increase to 45,645, of which 14,903 were localized in promoters [37]. It is possible that high levels of MYC protein may influence DNA repair by altering chromatin structure surrounding DSBs.

In conclusion, we have reported here for the first time that MYC does not affect the initial stages of DNA repair, but it inhibits resolution of DSBs. We suggest that the use of dedicated cell lines in which inducible specific DSBs may occur, could be instrumental for future characterization of the molecular events underlying MYC's ability to suppress DNA repair.

Conflict of interest

The authors declare no conflict of interest.

Acknowledgements

We are grateful to Gaëlle Legube for providing the HA-AsiSI-ER vector and U2OS-AsiSI-ER cell line and E.V. Avvedimento for helpful discussion. S.A. has been supported by fellowship from P.O.R. Campania FSE 2007–2013 Project CREMe. This work was supported by grants AIRC (IG 13173) and MIUR to B.M. and from Epigenomics Flagship Project – EPIGEN, C.N.R.

Appendix A. Supplementary data

Supplementary data associated with this article can be found, in the online version, at <http://dx.doi.org/10.1016/j.mrfmmm.2015.02.005>.

References

- [1] T.D. Halazonetis, V.G. Gorgoulis, J. Bartek, An oncogene-induced DNA damage model for cancer development, *Science* 319 (2008) 1352–1355.
- [2] S.P. Jackson, J. Bartek, The DNA-damage response in human biology and disease, *Nature* 461 (2009) 1071–1078.
- [3] M. Eilers, R.N. Eisenman, Myc's broad reach, *Genes Dev.* 22 (2008) 2755–2766.
- [4] C.V. Dang, MYC on the path to cancer, *Cell* 149 (2012) 22–35.
- [5] S.F. Louis, B.J. Vermolen, Y. Garini, I.T. Young, A. Guffei, Z. Lichtensztejn, F. Kuttler, T.C. Chuang, S. Moshir, V. Mougey, A.Y. Chuang, P.D. Kerr, T. Fest,

- P. Boukamp, S. Mai, c-Myc induces chromosomal rearrangements through telomere and chromosome remodeling in the interphase nucleus, *Proc. Natl. Acad. Sci. U. S. A.* 102 (2005) 9613–9618.
- [6] D.J. Murphy, M.R. Junttila, L. Pouyet, A. Karnezis, K. Shchors, D.A. Bui, L. Brown-Swigart, L. Johnson, G.I. Evan, Distinct thresholds govern Myc's biological output in vivo, *Cancer Cell* 14 (2008) 447–457.
- [7] A. Karlsson, D. Deb-Basu, A. Cherry, S. Turner, J. Ford, D.W. Felsner, Defective double-strand DNA break repair and chromosomal translocations by MYC overexpression, *Proc. Natl. Acad. Sci. U. S. A.* 100 (2003) 9974–9979.
- [8] S. Ray, K.R. Atkuri, D. Deb-Basu, A.S. Adler, H.Y. Chang, L.A. Herzenberg, D.W. Felsner, MYC can induce DNA breaks in vivo and in vitro independent of reactive oxygen species, *Cancer Res.* 66 (2006) 6598–6605.
- [9] O. Vafa, M. Wade, S. Kern, M. Beeche, T.K. Pandita, G.M. Hampton, G.M. Wahl, c-Myc can induce DNA damage, increase reactive oxygen species, and mitigate p53 function: a mechanism for oncogene-induced genetic instability, *Mol. Cell* 9 (2002) 1031–1044.
- [10] S. Herold, B. Herkert, M. Eilers, Facilitating replication under stress: an oncogenic function of MYC? *Nat. Rev. Cancer* 9 (2009) 441–444.
- [11] T. Aparicio, R. Baer, J. Gautier, DNA double-strand break repair pathway choice and cancer, *DNA Repair* 19 (2014) 169–175.
- [12] S. Rohban, S. Campaner, Myc induced replicative stress response: how to cope with it and exploit it, *Biochim. Biophys. Acta* (2014), <http://dx.doi.org/10.1016/j.bbarm.2014.04.008>.
- [13] P. Rouet, F. Smih, M. Jasin, Expression of a site-specific endonuclease stimulates homologous recombination in mammalian cells, *Proc. Natl. Acad. Sci. U. S. A.* 91 (1994) 6064–6068.
- [14] B. Wolner, S. van Komen, P. Sung, C.L. Peterson, Recruitment of the recombinational repair machinery to a DNA double-strand break in yeast, *Mol. Cell* 12 (2003) 221–232.
- [15] N.M. Shanbhag, I.U. Rafalska-Metcalf, C. Balane-Bolivar, S.M. Janicki, R.A. Greenberg, ATM-dependent chromatin changes silence transcription in cis to DNA double-strand breaks, *Cell* 141 (2010) 970–981.
- [16] J.S. Iacovoni, P. Caron, I. Lassadi, E. Nicolas, L. Massip, D. Trouche, G. Legube, High-resolution profiling of gammaH2AX around DNA double strand breaks in the mammalian genome, *EMBO J.* 29 (2010) 1446–1457.
- [17] L. Massip, P. Caron, J.S. Iacovoni, D. Trouche, G. Legube, Deciphering the chromatin landscape induced around DNA double strand breaks, *Cell cycle* 9 (2010) 2963–2972.
- [18] P. Caron, F. Aymard, J.S. Iacovoni, S. Briois, Y. Canitrot, B. Bugler, L. Massip, A. Losada, G. Legube, Cohesin protects genes against gammaH2AX induced by DNA double-strand breaks, *PLoS Genet.* 8 (2012) e1002460.
- [19] F. Aymard, B. Bugler, C.K. Schmidt, E. Guillou, P. Caron, S. Briois, J.S. Iacovoni, V. Daburon, K.M. Miller, S.P. Jackson, G. Legube, Transcriptionally active chromatin recruits homologous recombination at DNA double-strand breaks, *Nat. Struct. Mol. Biol.* 21 (2014) 366–374.
- [20] S. Amente, A. Bertoni, A. Morano, L. Lania, E.V. Avvedimento, B. Majello, LSD1-mediated demethylation of histone H3 lysine 4 triggers Myc-induced transcription, *Oncogene* 29 (2010) 3691–3702.
- [21] S.E. Reed, E.M. Staley, J.P. Mayginnes, D.J. Pintel, G.E. Tullis, Transfection of mammalian cells using linear polyethylenimine is a simple and effective means of producing recombinant adeno-associated virus vectors, *J. Virol. Methods* 138 (2006) 85–98.
- [22] G. Napolitano, S. Amente, M.L. Lavadera, G. Di Palo, S. Ambrosio, L. Lania, G.I. Dellino, P.G. Pelicci, B. Majello, Sequence-specific double strand breaks trigger P-TEFb-dependent Rpb1-CTD hyperphosphorylation, *Mutat. Res.* 749 (2013) 21–27.
- [23] C. Kuhne, M.L. Tjornhammar, S. Pongor, L. Banks, A. Simoncsits, Repair of a minimal DNA double-strand break by NHEJ requires DNA-PKcs and is controlled by the ATM/ATR checkpoint, *Nucleic Acids Res.* 31 (2003) 7227–7237.
- [24] S. Matsuoka, B.A. Ballif, A. Smogorzewska, E.R. McDonald 3rd, K.E. Hurov, J. Luo, C.E. Bakalarski, Z. Zhao, N. Solimini, Y. Lerenthal, Y. Shiloh, S.P. Gygi, S.J. Elledge, ATM and ATR substrate analysis reveals extensive protein networks responsive to DNA damage, *Science* 316 (2007) 1160–1166.
- [25] E.P. Rogakou, D.R. Pilch, A.H. Orr, V.S. Ivanova, W.M. Bonner, DNA double-stranded breaks induce histone H2AX phosphorylation on serine 139, *J. Biol. Chem.* 273 (1998) 5858–5868.
- [26] W. Lutz, M. Stohr, J. Schurmann, A. Wenzel, A. Lohr, A. Schwab, Conditional expression of N-myc in human neuroblastoma cells increases expression of alpha-prothymosin and ornithine decarboxylase and accelerates progression into S-phase early after mitogenic stimulation of quiescent cells, *Oncogene* 13 (1996) 803–812.
- [27] Z. Li, T.K. Owonikoko, S.Y. Sun, S.S. Ramalingam, P.W. Doetsch, Z.Q. Xiao, F.R. Khuri, W.J. Curran, X. Deng, c-Myc suppression of DNA double-strand break repair, *Neoplasia* 14 (2012) 1190–1202.
- [28] T.J. Pehesse, K.B. Myant, A.M. Cole, R.A. Ridgway, H. Pearson, V. Muncan, G.R. van den Brink, K.H. Vousden, R. Sears, L.T. Vassilev, A.R. Clarke, O.J. Sansom, Endogenous c-Myc is essential for p53-induced apoptosis in response to DNA damage in vivo, *Cell Death Differ.* 21 (2014) 956–966.
- [29] C.A. Schmitt, M.E. McCurrach, E. de Stanchina, R.R. Wallace-Brodeur, S.W. Lowe, INK4a/ARF mutations accelerate lymphomagenesis and promote chemoresistance by disabling p53, *Genes Dev.* 13 (1999) 2670–2677.
- [30] P. Agrawal, K. Yu, A.R. Salomon, J.M. Sedivy, Proteomic profiling of Myc-associated proteins, *Cell Cycle* 9 (2010) 4908–4921.
- [31] H.B. Koch, R. Zhang, B. Verdoodt, A. Bailey, C.D. Zhang, J.R. Yates 3rd, A. Menssen, H. Hermeking, Large-scale identification of c-MYC-associated proteins using a combined TAP/MudPIT approach, *Cell Cycle* 6 (2007) 205–217.
- [32] A. Gospodinov, Z. Herceg, Chromatin structure in double strand break repair, *DNA Repair* 12 (2013) 800–810.
- [33] A. Gospodinov, Z. Herceg, Shaping chromatin for repair, *Mutat. Res.* 752 (2013) 45–60.
- [34] K.M. Miller, S.P. Jackson, Histone marks: repairing DNA breaks within the context of chromatin, *Biochem. Soc. Trans.* 40 (2012) 370–376.
- [35] G. Soria, S.E. Polo, G. Almouzni, Prime, repair, restore: the active role of chromatin in the DNA damage response, *Mol. Cell* 46 (2012) 722–734.
- [36] H. Chandler, H. Patel, R. Palermo, S. Brookes, N. Matthews, G. Peters, Role of polycomb group proteins in the DNA damage response – a reassessment, *PLOS ONE* 9 (2014) e102968.
- [37] S. Walz, F. Lorenzin, J. Morton, K.E. Wiese, B. von Eyss, S. Herold, L. Rycak, H. Dumay-Odelot, S. Karim, M. Bartkuhn, F. Roels, T. Wustefeld, M. Fischer, M. Teichmann, L. Zender, C.L. Wei, O. Sansom, E. Wolf, M. Eilers, Activation and repression by oncogenic MYC shape tumour-specific gene expression profiles, *Nature* 511 (2014) 483–487.

CHAPTER 3

CELL CYCLE-DEPENDENT RESOLUTION OF DNA DOUBLE-STRAND BREAKS

Susanna Ambrosio¹, Giacomo Di Palo², Giuliana Napolitano¹, Stefano Amente², Gaetano Ivan Dellino^{3,4},
Mario Faretta³, Pier Giuseppe Pelicci^{3,4}, Luigi Lania², Barbara Majello¹

¹Department of Biology, University of Naples 'Federico II', Naples, Italy

²Department of Molecular Medicine and Medical Biotechnologies, University of Naples 'Federico II', Naples, Italy

³Department of Experimental Oncology, European Institute of Oncology, Milan, Italy

⁴Department of Oncology and Haemato-oncology, University of Milan, Italy

Published Oncotarget. 2016 Jan 26;7(4):4949-60.

The chapter is an exact copy of the journal paper referred to above.

Cell cycle-dependent resolution of DNA double-strand breaks

Susanna Ambrosio¹, Giacomo Di Palo², Giuliana Napolitano¹, Stefano Amente², Gaetano Ivan Dellino^{3,4}, Mario Faretta³, Pier Giuseppe Pelicci^{3,4}, Luigi Lania², Barbara Majello¹

¹Department of Biology, University of Naples 'Federico II', Naples, Italy

²Department of Molecular Medicine and Medical Biotechnologies, University of Naples 'Federico II', Naples, Italy

³Department of Experimental Oncology, European Institute of Oncology, Milan, Italy

⁴Department of Oncology and Haemato-oncology, University of Milan, Italy

Correspondence to: Luigi Lania, **e-mail:** lania@unina.it
Barbara Majello, **e-mail:** majello@unina.it

Keywords: cell-cycle, DSB repair, site-specific DSBs, AsiSI restriction enzyme

Received: November 05, 2015

Accepted: November 27, 2015

Published: December 17, 2015

ABSTRACT

DNA double strand breaks (DSBs) elicit prompt activation of DNA damage response (DDR), which arrests cell-cycle either in G₁/S or G₂/M in order to avoid entering S and M phase with damaged DNAs. Since mammalian tissues contain both proliferating and quiescent cells, there might be fundamental difference in DDR between proliferating and quiescent cells (or G₀-arrested). To investigate these differences, we studied recruitment of DSB repair factors and resolution of DNA lesions induced at site-specific DSBs in asynchronously proliferating, G₀-, or G₁-arrested cells. Strikingly, DSBs occurring in G₀ quiescent cells are not repaired and maintain a sustained activation of the p53-pathway. Conversely, re-entry into cell cycle of damaged G₀-arrested cells, occurs with a delayed clearance of DNA repair factors initially recruited to DSBs, indicating an inefficient repair when compared to DSBs induced in asynchronously proliferating or G₁-synchronized cells. Moreover, we found that initial recognition of DSBs and assembly of DSB factors is largely similar in asynchronously proliferating, G₀-, or G₁-synchronized cells. Our study thereby demonstrates that repair and resolution of DSBs is strongly dependent on the cell-cycle state.

INTRODUCTION

Eukaryotic genome is constantly being challenged by various endogenous and exogenous insults. These damaging events include crosslinks, base modifications, base mismatches, stalled replication forks, single-strand breaks (SSBs), and particularly dangerous double-strand breaks (DSBs). To deal with such dangerous insults, eukaryotes possess an array of distinct pathways to monitor and repair damaged DNA.

The initial phases of DSB recognition and recruitment of repair factors are now quite elucidated. Following DSB the MRE11/RAD50/NBS1 complex senses a DSB within seconds and then activates PI3K-like kinases ATM (ataxia-telangiectasia mutated) protein kinase, a large Ser/Thr kinase of the PI3K-

like kinase family, which also includes DNA-PKcs (DNA-dependent protein kinase catalytic subunit), and ATR [1–4]. ATM then phosphorylates histone H2AX on Ser139 (named γ H2AX when phosphorylated) in DSB adjacent chromatin. The primary function of γ H2AX is to recruit its decoder, MDC1 (mediator of DNA damage checkpoint protein 1), which recognizes the phosphorylated Ser139 epitope on γ H2AX. γ H2AX-bound MDC1 recruits in turn more MRN complexes (via an interaction with NBS1) and thus initiates a positive ATM feedback loop that leads to the amplification of the γ H2AX chromatin domain [5–8]. Concomitant with the assembly of DNA repair factors at DNA lesion, DSB response activates DNA-damage checkpoints (DDR), and diffusible signaling events that can arrest cell cycle progression either in G₁ or G₂ to allow for DNA repair

and prevent transmission of damaged DNA to daughter cells (9,10). However, it must be emphasized that the tissue and organs of mammals consist of different cell types, including dividing, non-dividing and stem cells that coexist in several tissues, in separate yet adjoining locations [11]. Normal mammalian cells possess unique regulatory mechanisms to shift from a quiescent state to a proliferative state and dysregulation of these mechanisms might result in malignant transformation. Cellular quiescence and the capacity to enter the proliferation cycle are critical for maintaining tissue homeostasis [12, 13].

During interphase, DSB can be repaired in a cell-cycle dependent manner by two major mechanisms: classical non-homologous end joining (NHEJ, during G₁ phase) or homologous recombination repair (HR, mainly in S-G₂ phases) [14–16]. Several studies unveiled cell cycle-regulated circuits that govern DSB repair pathway choice to ensure that NHEJ dominates in G₁ and HR is favored from S phase onward [17–21]. Although cell-cycle phase contributes to this choice, these pathways coexist in S- and G₂-phases, thus implying that other factors participate in this decision such as chromatin context in which DSB occurs [22–24].

It is now well established that DDR differs in mitotic and interphase cells [25, 26]. It has been shown that DDR is dampened during mitosis. Cells have evolved mechanisms to suppress DSB repair during M phase to prevent genome instability [27, 28]. Clearly, different molecular mechanisms involved in DNA repair occurring at specific cell cycle phases have been evolved, and recruitment of DSB repair factors and resolution of DNA lesions induced at site-specific DSBs occurring during different phases of the cell cycle could be instrumental to investigate these differences.

To avoid potential anomalies associated with transformed cell lines, we produced a cellular system suitable to the induction of specific DSBs in the immortalized non-tumorigenic epithelial cell line MCF10A. We stably transfected these cells with a well-documented AsiSI-inducible vector that express the 8-base restriction endonuclease AsiSI fused to a modified oestrogen receptor ligand binding domain that induces nuclear localization of the enzyme after administration with 4-hydroxytamoxifen (4OHT) causing the rapid and reproducible induction of about 150 sequence-specific DSBs across the genome [23, 29–31]. This system (MCF10A-AsiSI-ER) offers the opportunity to study the wave of repair events occurring at defined stages of the cell cycle in a defined and reproducible manner.

We found the DSBs occurring in G₀ quiescent cells are irreparable with a sustained activation of the p53-pathway. Conversely, re-entry into cell cycle of damaged G₀-arrested cells shows a delayed clearance of recruited DNA repair factors bound at DSBs, indicating inefficient repair. This study thereby demonstrates the crucial role of cell cycle phases in repair and resolution of DSBs.

RESULTS

Induction of specific DSBs in non-tumorigenic epithelial MCF10A cells

To investigate DSB damage and avoid potential anomalies associated with transformed cell lines, we sought to produce a cellular system suitable to the induction of specific DSBs in the immortalized non-tumorigenic epithelial cell line MCF10A. To this end MCF10A cells were transduced with a retroviral vector expressing the fusion protein between the HA-tagged AsiSI restriction enzyme and a modified hormone-binding domain from the estrogen receptor. Following drug selection, one cell clone was isolated (named MCF10-AsiSIER) and the effects of 4OHT administration at different time points were analyzed by indirect immunofluorescence. Exposure to 4OHT for 2 hours resulted in nuclear accumulation of the AsiSI fusion protein, as detected by anti-HA-tag antibodies (Figure 1A). This was accompanied by a significant increase in the number of DNA damaged foci, visualized with antibodies against S139-phosphorylated histone γ H2AX (Figure 1B). 4OHT was removed from the medium after 2 hours and cells cultivated for additional 4 and 8 hours (Recovery). As shown in Figure 1A, the nuclear localization of HA-AsiSI-ER was strongly reduced after 4 hours of recovery, and barely detectable after 8 hours, indicating that the HA-AsiSI-ER endonuclease was not active anymore (Figure 1A). The generation of the MCF10-AsiER clone enabled us to investigate recruitment of DNA damaging factors at specific DSBs by using ChIP-based approaches. As initial test we focused on the AsiSI sites on chromosomes 1 and 6 at which γ H2AX recruitment had been observed and documented by treatment of U2OS AsiSI cells [29]. We conducted ChIP assays with antibodies against some of the DDR components and we used sequences of published primer sets (listed in Table S2). As illustrated in Figure 1C, we observed increased enrichment of γ H2AX, NBS1, and XRCC4 at the Chr1 and Chr6 AsiSI sites. These results confirm that recruitment of these factors in MCF10-AsiER paralleled the effects observed in previously described clonal population of U2OS-AsiER cells.

DSBs induce DDR activation followed by efficient repair in MCF10A proliferating cells

Following the generation of DSBs, DDR promotes cellular DNA-repair activities with a concomitant transient arrest of cell-cycle progression (checkpoint function) until DNA damage has been removed. To analyze the transient arrest of cell-cycle progression following induction of DSBs, proliferating MCF10-AsiSIER cells were treated for 2 hours with 4OHT and then allowed to recover in

the absence of 4OHT for 24, 48 and 72 hours. Samples were analyzed for cell-cycle distribution, DDR activation, and ChIP accumulation of γ H2AX and NBS1 at specific AsiSI sites. Cell cycle analysis showed that AsiSI-dependent DSBs induced a significant G2 arrest, which was completely resolved after 72hr of Recovery (Figure 2A). As shown in Figure 2B, p53-Ser15 phosphorylation increased after 4OHT treatment and its levels decreased 3 days after the removal of the DNA damage insult.

DDR cascade begins with the detection of DSBs by the MRN (MRE11-RAD50-NBS1) complex, which recruits and activates different PIKK kinases (ATM, ATR and DNA-PK), each capable to phosphorylate H2AX at Ser139 [3–5]. To analyze the efficiency of these steps detecting DSBs and to monitor the resolution of DNA damage-associated γ H2AX and NBS1 accumulation at defined AsiSI sites we performed ChIP with anti- γ H2AX and -NBS1 antibodies. Following the robust increase of γ H2AX and NBS1 signals at the AsiSI sites after 4OHT treatment, we observed their progressive reduction within 24 hours (Figure 2C and Supplementary Figure 1).

Collectively, these data indicate that induction of DSBs in asynchronously proliferating MCF10 cells promotes a robust DDR activation, which is followed by an efficient wave of repair leading to a progressive reduction of DDR after DSBs onset.

DSBs in quiescent MCF10 cells are irreparable and cause a sustained activation of the p53-pathway

In mammalian tissues, cells are in both proliferating and quiescent states depending on the given tissue and these two different populations may also coexist in several tissues, in separate yet adjoining locations. However, comparative study of these two distinct cell cycle states regarding the capability to sense and resolve DNA DSB damaging insults has been poorly characterized. To address this issue and investigate if quiescent or proliferating cells equally sense and resolve DSBs over time, we took advantage of the MCF10AsiER cells which can be induced in a quiescent state by growth factors deprivation for 2 days (referred to as G_0 cells). G_0 cells were then treated or not with 4OHT for 2 hours to induce DSBs. The efficiency of DSB induction at each AsiSI site was measured in these two conditions by ChIP-sequencing of proliferating and G_0 -arrested cells using the anti- γ H2AX antibody. Similarly to ChIP data already available for U2OS cells [22], γ H2AX showed a typical pattern with signals encompassing the DSBs for 1-2Mb around the AsiSI sites, with the typical signal drop occurring exactly at the restricted AsiSI sites (Figure 3, and Supplementary Figure 2).

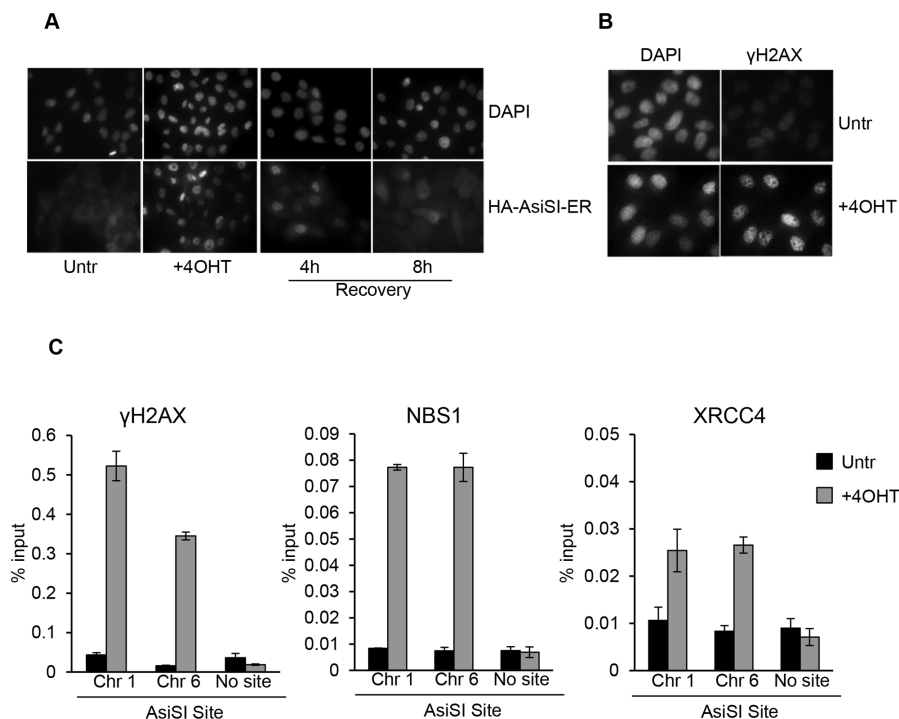


Figure 1: 4OHT treatment triggers DSBs formation at AsiSI sites in MCF10A. **A.** MCF10A-AsiSI-ER cells were treated for 2 h with 4OHT or vehicle (Untr) and then released into fresh medium for 4 and 8 h (Recovery). Cells were fixed and processed for anti-HA immunofluorescence and DAPI staining. **B.** MCF10A-AsiSI-ER cells were treated for 2 h with 4OHT and stained with anti- γ H2AX antibody. DAPI staining of nuclei is shown. **C.** MCF10A-AsiSI-ER cells were treated as above and ChIP experiments were performed using antibodies against γ H2AX, NBS1 and XRCC4. Real-time qPCR was done on ChIP materials using primers listed in Supplementary Table 2. Amplicon far from any AsiSI site was analyzed as negative control. Data are from independent experiments with SD ($n = 3$).

Most importantly, we confirmed the results by analyzing 150 γ H2AX peaks and found that γ H2AX mapped with similar efficiency in both G_0 and proliferating cells (Figure 3 and Supplementary Figure 2 and Table 3). From these observations we assessed that the efficiency of DSBs induced in either proliferating or G_0 -arrested cells is largely similar. Next, we followed γ H2AX and 53BP1 foci formation by immunofluorescence in damaged G_0 -arrested cells. We found that, similarly to proliferating cells, G_0 -arrested cells exposed to 4OHT for 2 hours showed a drastic induction of γ H2AX and 53BP1 foci. However, we found that DSB in G_0 -arrested cells were not repaired, with a persistent accumulation of γ H2AX and 53BP1 foci up to 5 days after DSB induction, thus suggesting an impaired repair proficiency (Figure 4A). Accordingly, γ H2AX ChIP data showed a sustained accumulation of γ H2AX signal at the AsiSI sites (Figure 4B). We cannot exclude that DSBs might normally repaired in quiescent cells but fail to recover normal chromatin arrangement after repair. However, sustained expression of the P-p53-p21 axis was observed, suggesting that the DDR p53 pathway

operates in G_0 -damaged cell. Interestingly, p21, which was present at high levels in quiescent cells, was further up-regulated after damage (Figure 4C). Moreover we found that damaged G_0 -arrested cells underwent to apoptosis after 3 days of OHT treatment, as documented by a robust increase of the cleaved PARP1 protein in damaged cells. PARP1 cleavage was not observed in vehicle treated undamaged cells (Veh) that could be kept in culture up to 10 days (Figure 4D and data not shown).

Next we investigated whether the lack of DNA repair efficiency was a consequence of different expression levels of DDR genes in G_0 -arrested cells compared to proliferating cells. We comparatively quantified expression levels of DDR genes in G_0 -arrested versus asynchronous proliferating cells by qRT-PCR and Western blot analysis. As shown in Figure 4E and 4F, G_0 -arrested cells expressed the analyzed DDR factors at comparable levels with proliferating cells except for RAD51 and ATR. The low expression levels of RAD51 and ATR are consistent with their role in G_1/S phases. Data obtained showed that no significant differences were seen between G_1/S and asynchronous proliferating cells.

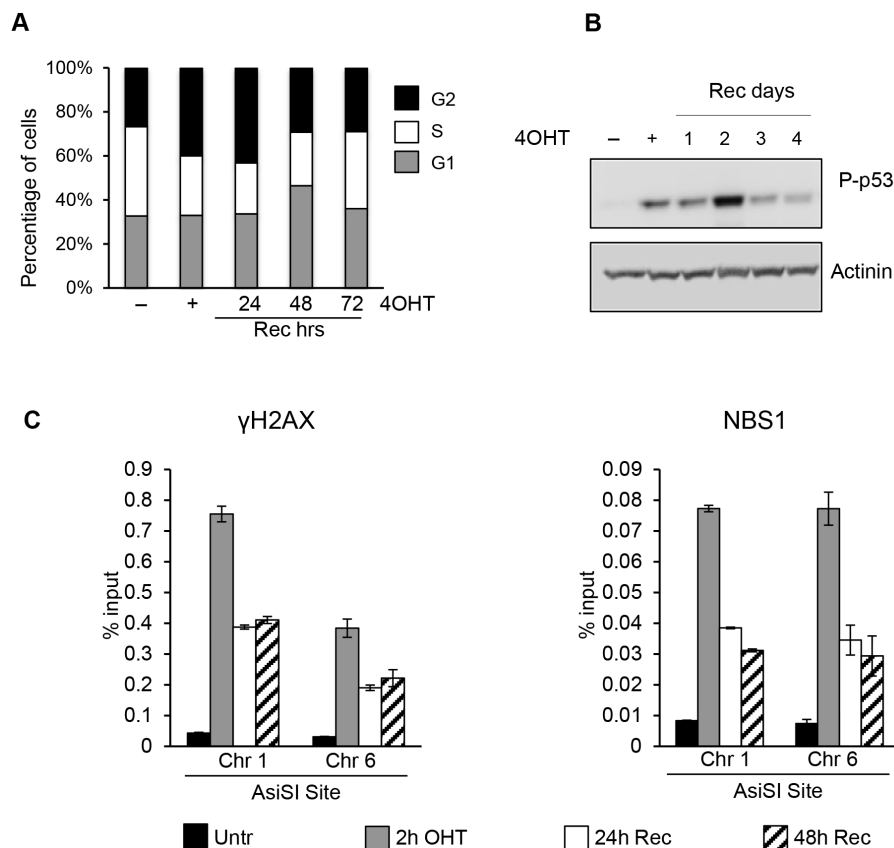


Figure 2: AsiSI-induced DSBs trigger DDR activation followed by efficient wave of repair. **A.** Cell cycle distribution of asynchronously growing MCF10A-AsiSI-ER treated for 2h with 4OHT then released into fresh medium and collected as indicated. DNA content of propidium iodide stained cells was determined by flow cytometry. **B.** Total cell extracts from proliferating MCF10A-AsiSI before and at the indicated times after 4OHT removal were probed with anti-phospho-p53 and normalized for actinin. **C.** ChIP against γ H2AX and NBS1 in MCF10A-AsiSI-ER treated for 2h with 4OHT then released into fresh medium, collected as indicated and analyzed by qPCR. Data are from independent experiments with SD ($n = 3$).

From these findings we concluded that G_0 -arrested cells lack DNA repair proficiency, but retain the capability to activate DNA damage response.

Cell-cycle reentry induces a delayed resolution of DSBs

Our findings demonstrated that DSB occurring in G_0 -arrested cells are not repaired. We then sought to determine whether reentry of G_0 -damaged cells

in cell cycle progression might recover DNA repair proficiency. First, we monitored the cell cycle re-entry of MCF10AsiER cells upon 2 days of starvation. Cells were grown in minimal medium for 2 days and then cell cycle re-entry was induced by addition of medium containing growth factors (hydrocortisone, EGF, insulin, cholera toxin). Flow cytometry analysis revealed an increase of S phase cells 8 hours after growth factors addition, with a concomitant increase of Ki67 levels compared to starved cells; moreover after 24 h, percentages of cell cycle phases

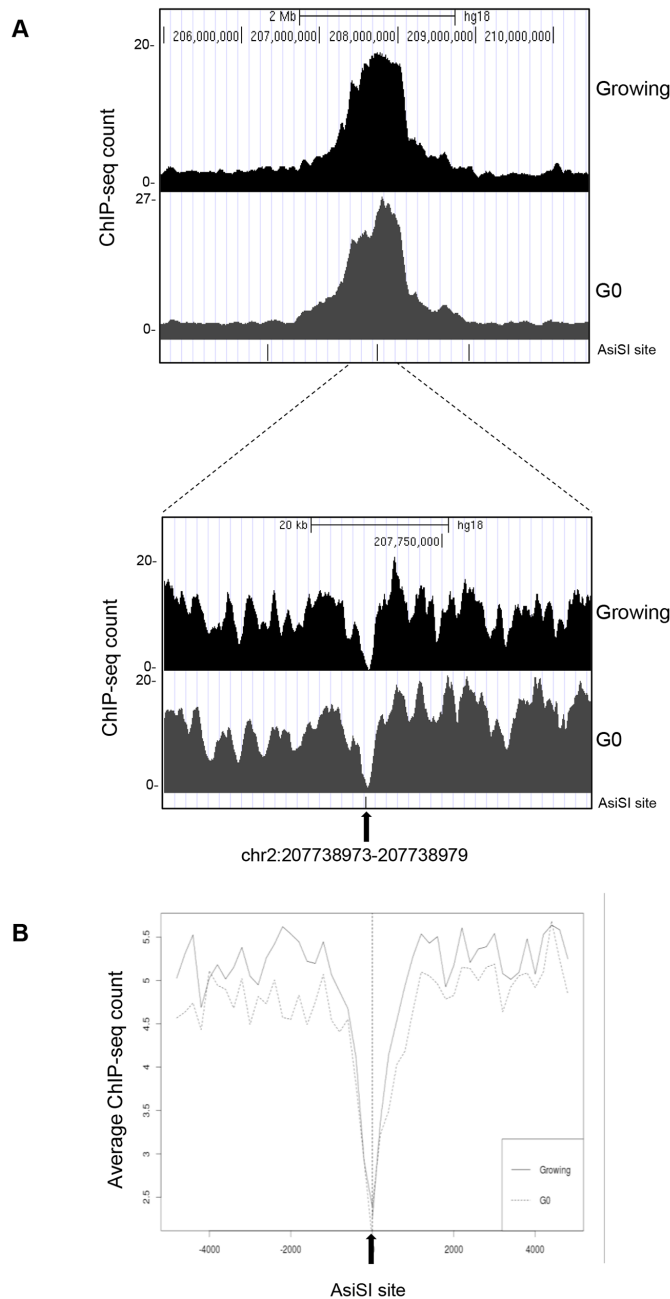


Figure 3: ChIP-seq analyses in proliferating and G_0 -arrested MCF10A-AsiSI-ER cells after 4OHT treatment (2 h), using anti- γ H2AX antibody. Panel A. show the profiles of γ H2AX around a selected AsiSI site in both proliferating and G_0 -arrested cells. B. Averaged γ H2AX signals of proliferating and G_0 cells over a 10-kb windows and centered at the AsiSI site.

and Ki67 levels were largely similar to growing control cells (Figure 5A and 5B).

Damaged G_0 -arrested cells showed an accumulation in G_2 phase with a delayed cell-cycle re-entry (Figure 5C) with abnormal accumulation on both G_1 and G_2 phases. As shown in Figure 5D, P-p53 levels increased after DNA damage and accumulation of P-p53-Ser15 was detected up to 2 days after DSBs followed by a sharp decline at 3 and 5 days after recovery, suggesting resolution of induced damage.

Finally we monitored accumulation of the DNA repair factors γ H2AX and NBS1 at specific AsiSI sites at different time-points after cell-cycle reentry. ChIP data demonstrated that γ H2AX and NBS1 factors were rapidly recruited to the AsiSI sites. However, compared to DNA damage in proliferating cells, in damaged G_0 -arrested cells we found a persistent accumulation of both γ H2AX and NBS1 at DSBs (Figure 5E).

Collectively, these data clearly indicate that cell cycle re-entry of damaged G_0 -arrested cells induces

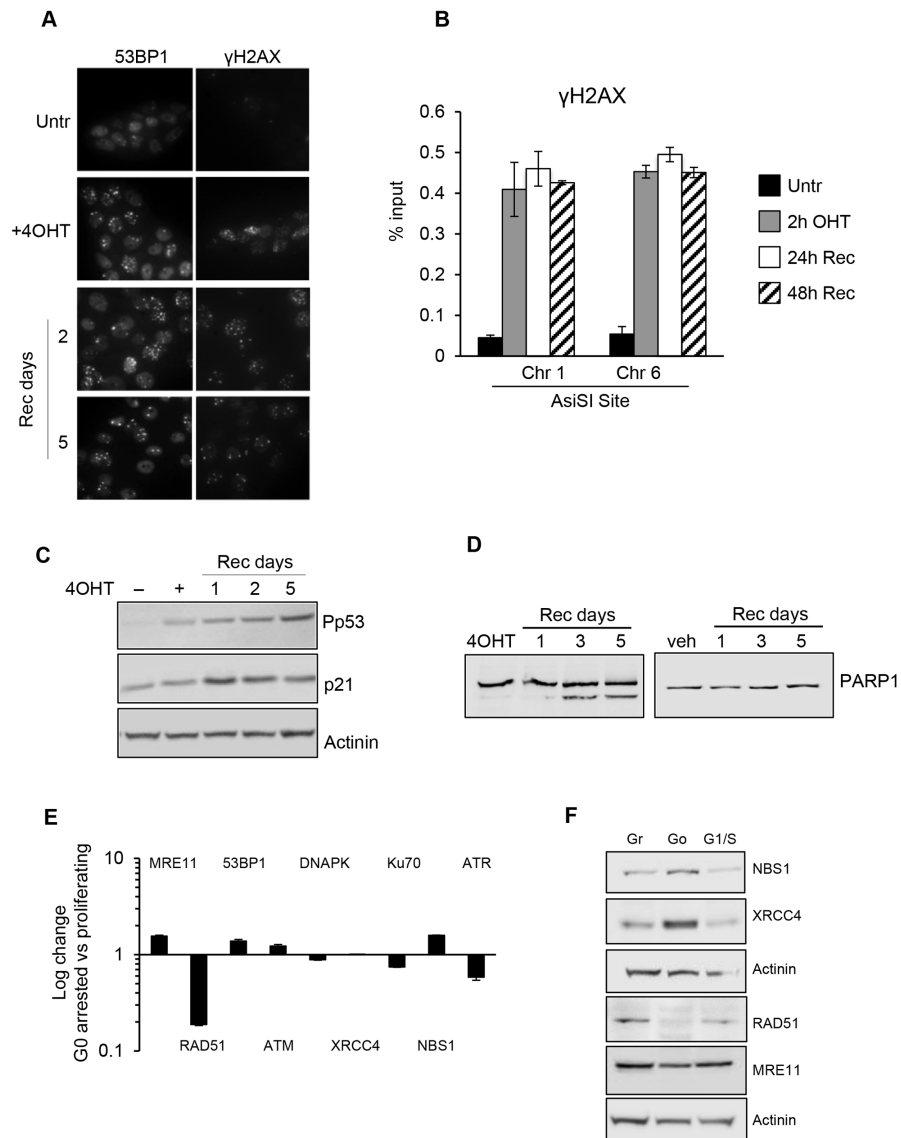


Figure 4: G_0 -arrested MCF10-AsiSIER cells lack DNA repair proficiency. **A.** MCF10A-AsiSIER cells were arrested in G_0 phase through growth factors deprivation for 40h, treated with 4OHT for 2h then kept in medium without growth factors, and analyzed at the indicated times after 4OHT removal by immunofluorescence with anti-53BP1 and anti- γ H2AX antibodies, respectively. **B.** Recruitment of γ H2AX at AsiSI sites (Chr. 1 and 6) was determined by ChIP assays. **C.** Western blotting was performed using phospho-p53 antibodies and p21. **D.** PARP1 detection of both full-length and cleaved protein fragments; western blotting of G_0 -arrested MCF10-AsiSI-ER treated with 4OHT or vehicle, collected at the indicated time points after 4OHT removal. **E.** DDR factors mRNAs expression analysis of G_0 -arrested MCF10-AsiSI-ER through quantitative RT-PCR. Expression profiles were normalized against proliferating cells. **F.** Western blot of protein extracts of Growing, G_0 and G1/S MCF10-AsiSI-ER cells using the indicated antibodies. Actinin has been probed as loading control for different blots.

delayed resolution of DSBs compared to proliferating damaged cells; following recruitment of repair factors, the progressive reduction in time of accumulation of these factors in G_0 -damaged cells was clearly delayed compared to what observed in asynchronously proliferating MCF10 cells.

Efficient resolution of DSB induced at G_1/S phase

Our findings demonstrated that cell cycle reentry of G_0 -damaged cells allows resolution of DSBs albeit with a delayed efficiency compared to proliferating cells, suggesting that transition to G_1/S phases might be required

for DSB resolution. We then sought to determine repair proficiency in synchronized G_1/S -damaged cells. As shown by FACS data, 8 hours after cell cycle re-entry, G_0 -arrested MCF10-AsiER cells were synchronized in late G_1/S phase (Figure 5A). Synchronized cells were exposed for 2 hours to 4OHT treatment and then allowed to recover: cell samples were collected at different times after the 4OHT pulse and analyzed for p53 activation and accumulation of DSB factors at specific AsiSI sites. G_1 -damaged cells exhibited a robust p53 activation (Figure 6A), and accumulation of the DNA repair factors (γ H2AX and NBS1) at specific AsiSI sites at different time-points following DNA damage. CHIP data showed

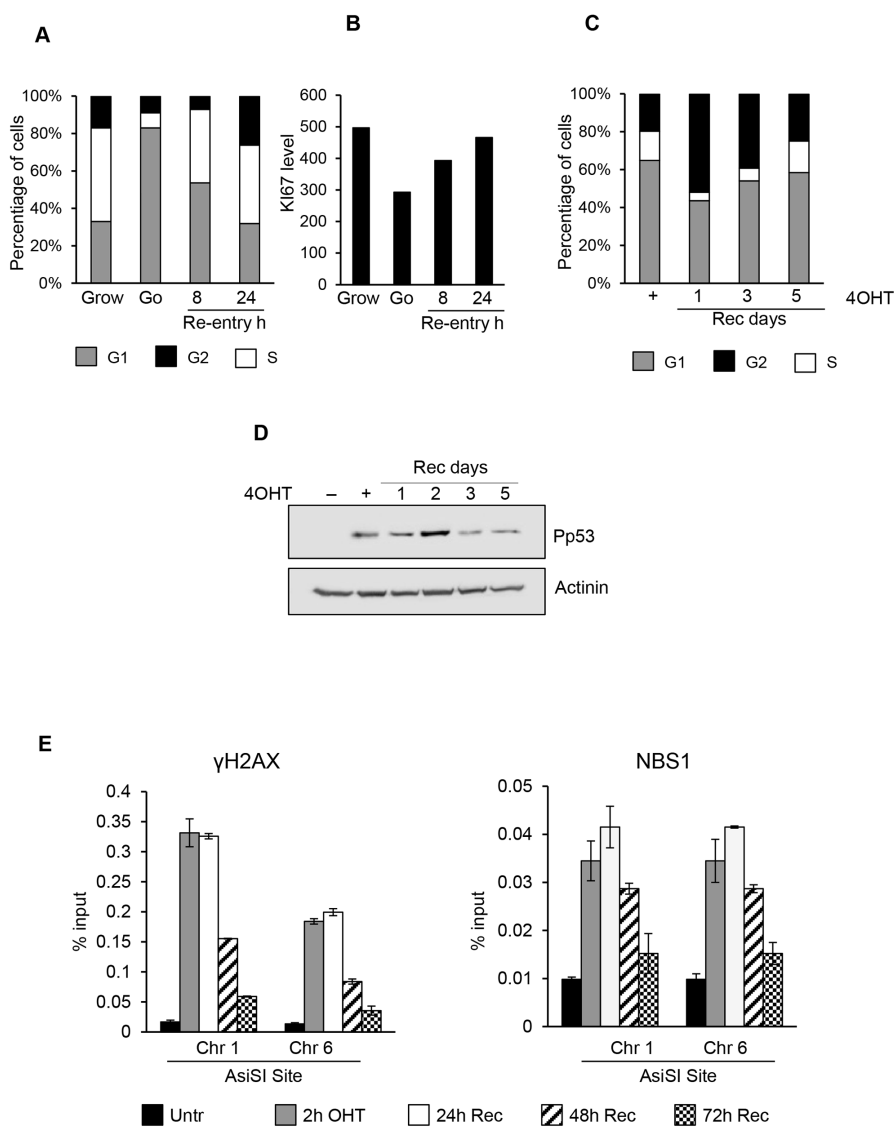


Figure 5: Cell-cycle re-entry induces a delayed resolution of DSBs. In panel **A** and **B**, cell cycle profiles and Ki67 levels detected by flow cytometry of G_0 MCF10-AsiSI-ER released into fresh medium and collected as indicated. **C**, Cell cycle distribution of G_0 -arrested MCF10A-AsiSI-ER cells treated for 2h with 4OHT, then released into fresh medium and collected as indicated. DNA content of propidium iodide stained cells was determined by flow cytometry. **D**, Western blotting of MCF10A-AsiSI-ER cells treated as above. **E**, ChIP against γ H2AX and NBS1 in MCF10A-AsiSI-ER treated for 2h with 4OHT, then released into fresh medium, collected as indicated and analyzed by qPCR. Data are from independent experiments with SD ($n = 3$).

that γ H2AX and NBS1 were rapidly recruited to the AsiSI sites and, most importantly, reduction of these DSBs factors followed a kinetics similar to that observed in asynchronously proliferating cells (compare Figure 6B and Figure 2C). The data demonstrated that, unlike damaged G_0 -arrested cells, G_1 -damaged cells exhibit efficient resolution of DSBs.

Because DSBs assembly of DDR repair factors occurs within minutes following the DNA damage event,

we comparatively determined the timing of γ H2AX, NBS1 and XRCC4 recruitment in cells exposed to AsiSI-damage for a short period of time (20') in asynchronously proliferating, G_0 -, or G_1 -arrested cells. Figure 7 shows that early recruitment of these factors is largely similar in all the three cell populations analyzed. Thus, the initial recognition of DSBs and assembly of DSB factors is largely similar regardless of the cell cycle phase during which the DSB is produced.

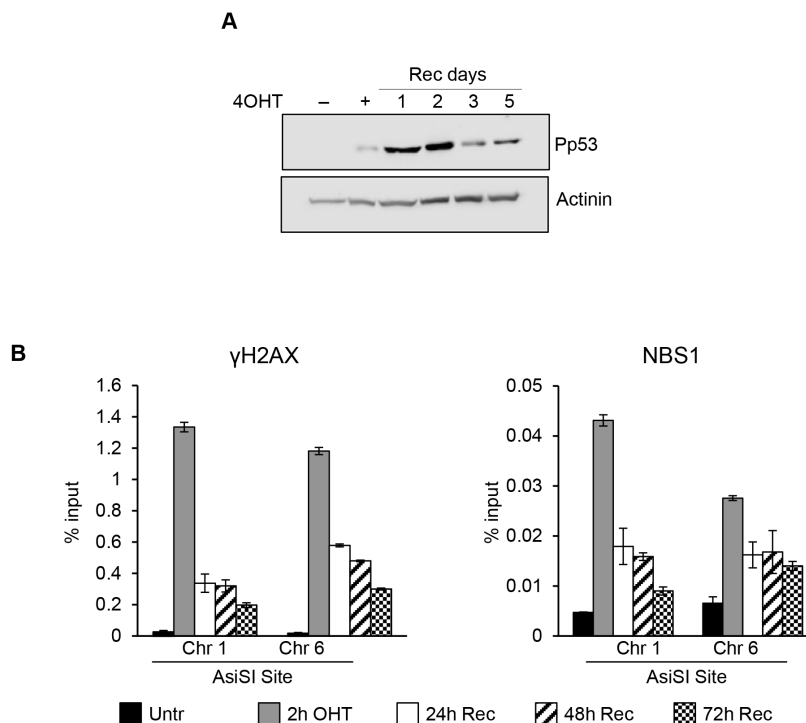


Figure 6: DSBs induced at G1/S phase. Synchronized cells were exposed for 2 hr to 4OHT and then allowed to recovery for the indicated times. **A.** total cell extracts from G1/S phase MCF10A-AsiSI before and at the indicated times after 4OHT removal were probed with anti-phospho-p53 and actinin as loading control. Panel **B.** ChIP against γ H2AX and NBS1 in MCF10-AsiSI-ER analyzed by qPCR. Data are from independent experiments with SD ($n = 3$).

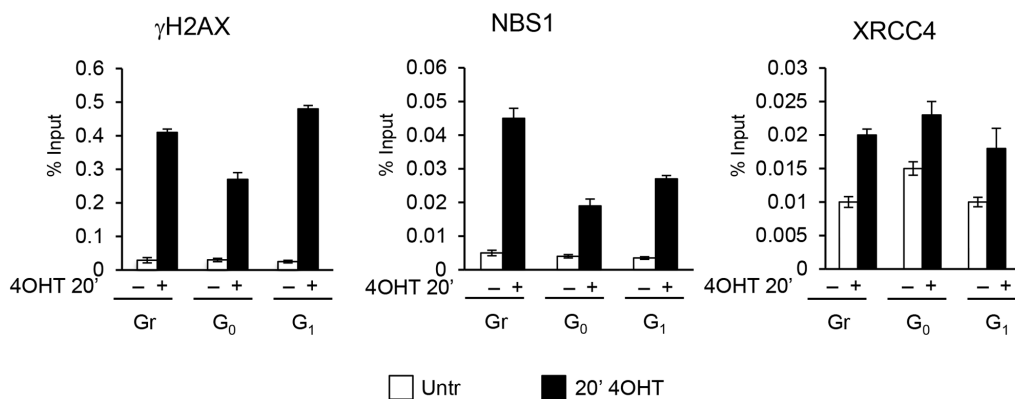


Figure 7: ChIP analysis with γ H2AX, NBS1 and XRCC4 antibodies in MFC10AsiSI-ER cells after a short pulse of 4OHT treatment (20'). The values reported were calculated as percentage of input. Error bars indicate SD for three independent experiments.

DISCUSSION

Here we report a comparative study of DSB response occurring at specific stages of the cell cycle. We generated a human normal non-tumorigenic epithelial MCF10A cell line expressing the estrogen receptor-inducible AsiSI restriction enzyme, which allows the study of the wave of repair events occurring during specific stages of the cell cycle. We found that DSBs occurring in G_0 cells are irreparable and G_1/S transition is required for complete DNA damage resolution. We demonstrated that the G_0 cells retain a functional DDR but, lacking DNA repair competence, they may accumulate DNA damage, which could reach critical levels and triggers the apoptotic cascade.

In agreement with previous studies in U2OS [22, 30–33], AsiSI dependent DSBs in proliferating MCF10A induce canonical DDR activation, which is followed by progressive resolution of DSBs. Conversely, we found that DSB induction in G_0 -arrested cells leads to efficient γ H2AX and 53BP1 foci formation, but differently from asynchronous cells, damage is never repaired. Damaged G_0 -arrested cells show a robust and irreversible activation of the phospho-p53/p21 axis, and undergo apoptosis one week after DSBs induction. Through CHIP-sequencing we found that proliferating and G_0 damaged cells showed the same number of DSB domains with similar enrichment of γ H2AX, demonstrating that the efficiency of DSBs induced in either proliferating or G_0 -arrested cells is largely similar. Moreover, CHIP experiments revealed that in G_0 damaged cells the levels of γ H2AX, NBS1 and XRCC4 recruited to DSBs were largely similar to synchronous proliferating cells; thus, the cell cycle phase does not interfere with the initial steps of DNA damage response. However, the persistent accumulation of repair factors at DSBs indicates that DNA repair resolution is compromised in G_0 cells. The inability of G_0 cells to repair damage was not due to altered expression of DDR genes, since G_0 -arrested cells show similar expression levels of different repair factors when compared to proliferating cells, with the exception of RAD51 expression. Lack of RAD51 expression in G_0 cells is consistent with the notion that HR, which relays on RAD51 activity is efficient in S and G_2 cell cycle phase, but limited in G_0/G_1 [14–16].

Most notably, we find that cell cycle re-entry of G_0 damaged cells restored DNA repair competence, but led to delayed resolution of DSBs compared to proliferating cells, suggesting that G_0 -damaged cells required G_1/S transition to complete DSBs repair. Accordingly, resolution of DSBs induced in synchronized G_1/S cells occurred with kinetic similar to that observed in proliferating cells.

Here we demonstrated that DDR activation does not depend on the phase of the cell cycle in which the DSB is generated. Similarly, a recent work reported that in IR-exposed fibroblasts, quiescence does not affect the DNA damage response, and activation of p53

and phosphorylation of γ H2AX are similar between proliferating and quiescent cells [34].

Our data reveal that in G_0 most of examined DDR factors are expressed at levels comparable to those observed in proliferating cells, and NHEJ is the main repair pathway since RAD51, a critical component of HR, is undetectable in G_0 . However, the G_1/S transition is required to complete resolution of DSBs induced in G_0 cells. A possible explanation is that some DSBs induced in G_1 are repaired by HR as cells progress to S phase [35]. Clearly, different molecular mechanisms involved in DNA repair occurring at specific cell cycle phases have been evolved, and the DDR differs in mitotic and interphase cells. It has been shown that DDR is dampened during mitosis. During mitosis DDR is inhibited to prevent telomere fusion and entry into mitosis in the presence of unrepaired DNA can lead to cell death, thus DDR clearly differs in mitotic and interphase cells [25–28].

Mammalian tissues and organs consist of different cell types, including dividing, non-dividing and stem cells. Terminally differentiated cells are permanently withdrawn from the cell cycle and partly resistant to apoptosis [36, 37]. d'Adda di Fagagna and collaborators showed that terminally differentiated astrocytes exhibit radio-resistance and strongly attenuated expression of most of DDR genes compared to undifferentiated progenitors [38]. It has been shown that in IR-exposed quiescent myoblast the ATM-p53 axis operates normally, while it is compromised in differentiated myotubes [39], indicating that the lack of a robust DDR and radio-resistance can be linked to the terminal differentiation and irreversible exit from the cell cycle. We cannot exclude, however, that differences in DNA damage response in cultured G_0 -arrested cells and in terminally differentiated non-proliferating cells are strictly cell type-specific and depend on the physiological context.

Our findings also help to dispel the dogma that completion of DNA damage repair is the essential condition for entry in the next phase of the cell cycle and stresses the notion the cell cycle position of a damage cell affects the repair competence. Further investigations are needed to understand mechanisms that coordinate repair in proliferating, quiescent and terminally differentiated cells to preserve genome integrity.

MATERIALS AND METHODS

Cell cultures and retroviral infection

MCF10A were cultured in 1:1 mixture DMEM-F12 supplemented with 5% horse serum, 10 μ g/ml insulin, 0,5 μ g/ml hydrocortisone, 100 ng/ml cholera enterotoxin, and 20 ng/ml epidermal growth factor, and incubated at 37°C in humidified atmosphere with 5% CO₂. To generate MCF10Asi-ER cells the pBABE-HA-AsiSI-ER plasmid was transfected into

293T cells expressing the structural components for retrovirus packaging, medium was harvested after 36 h, filtered and used to infect MFC10 cells and selection performed using 1 µg/ml puromycin; single cell clones were isolated and analyzed.

Cell cycle synchronization

MCF10A-AsiSI cells were arrested in G₀ by growth in minimal medium (1:1 mixture DMEM-F12 supplemented with 5% horse serum) for two days. To induce re-entry into cell cycle, the G₀ arrested cells were cultured in complete medium and cell cycle re-entry was monitored by flow cytometry analysis and Ki67 content.

Antibodies

The antibodies used for different applications in this study are listed in Supplementary Table S1.

Flow cytometry analysis

To analyze the DNA profile, cells were fixed in methanol at -20°C and stained in hypotonic solution of 0,1% Na-Citrate, 50 µg/ml propidium iodide, 50 µg/ml RNase and 0,00125% NP40 for 30' at room temperature. For Ki67 quantification cells were permeabilized with 0,1% Triton X-100/PBS, blocked in 5% Bovine Serum Albumin/PBS and stained with the primary antibody anti-Ki67; then, cells were incubated with the secondary antibody Alexa647 Donkey anti-goat (Invitrogen) before propidium iodide staining. Cytofluorimetric acquisition and analysis were performed on a Becton Dickinson FACScalibur flow cytometer using FACSDiva, CellQuest Pro and ModFit LT 3.0 software.

Western blot analysis

Whole-cell extracts were obtained using buffer F (10 mM TrisHCl pH 7.5, 150 mM NaCl, 30 mM Na4O7P2, 50 mM NaF, 5 mM ZnCl2, 0.1 mM Na3VO4, 1% Triton, 0.1mM PMSF). 50 µg of protein extracts were loaded and separated by SDS-PAGE and WB was performed with indicated antibodies.

Immunofluorescence

Immunofluorescences of MFC10AsiSI-ER cells were performed as previously described. Briefly, cells were fixed in 4% paraformaldehyde in PBS, permeabilized in 0.1% Triton X-100 in PBS, pre-blocked in 2% BSA–3%NS-PBS for 30 min at room temperature, and then incubated for 1 h at 37° C with mouse anti-HA and rabbit anti-γH2AX for 30' at 37°C anti-53BP1. Primary antibodies were detected by incubation with Cy3-coniugated anti-mouse or FITC-conjugated anti-rabbit antibody. Images were acquired using a Nikon Eclipse TE 2000-U microscope.

Chromatin immunoprecipitation assays

ChIP experiments with chromatin extracts from MCF10-AsiSIER cells were performed as described [32]. IPs materials were analyzed in duplicate by quantitative PCR, using Syber Green 2X PCR Master Mix (Applied Biosystem). For qPCRs 3 µl out of 150µl immunoprecipitated DNA was used. The antibodies are listed in Table S1. After reversal of the crosslinks, the immunoprecipitated DNA was quantified by qPCR with the primer sets described in Table S2. For each ChIP assay a control amplicon from Chromosome X (Table S2) was used.

Chip-sequencing, mapping and peak analysis

ChIP-seq libraries were prepared from 10 ng of ChIP (or Input) DNA with TruSeq ChIP Sample Prep Kit (Illumina) according to the manufacturer's instructions. Prior to sequencing, libraries were quantified using Qubit (Invitrogen) and quality-controlled using Agilent's Bioanalyzer. 50bp single-end sequencing was performed using Illumina HiSeq 2000 platform (Genomix4life S.R.L., Baronissi, Salerno, Italy) according to standard operating procedures. Alignments were performed with BWA [40] to hg18 using default parameters. SAMtools [41] and BEDtools [42] were used for filtering steps and file formats conversion. The peaks were identified from uniquely mapped reads without duplicates using MACS and the p-value cutoff used for peak detection was 1e-5. DNA Input was used as control. UCSC genome browser was used for data visualization. To plot data of average profiles around DSBs, AsiSI site positions were retrieved from the human genome (hg18). ChIP-seq counts were retrieved for 10 kb around each of these DSBs and averaged with a 200-bp window using a custom R-script [43]. ChIP-seq data were deposited to NCBI GEO and are available under accession number GSE71447

RNA extraction and qRT-PCR quantification

RNA was extracted from MCF10A-AsiSIER cells using EuroGold Trifast (EuroClone). cDNA was generated using Quantitec Reverse Transcription Kit (Qiagen), according to manufacturer's protocol. Quantitative analysis was performed using SYBR Green 2X PCR Master Mix (Applied Biosystem). Each sample was run in triplicate and normalized to the expression of housekeeping beta-glucuronidase (GUS) gene as previously described [44]. Primers are presented in Supplementary Table S2.

ACKNOWLEDGMENTS

We are grateful to Gaele Legube from providing the HA-AsiSI-ER vector. This work was supported by grants

AIRC (IG 13173) to B.M., from Epigenomics Flagship Project—EPIGEN, C.N.R. and P.O.R. Campania FSE 2007–2013 Project MoVIE to L.L.

CONFLICTS OF INTEREST

The authors declare no conflicts of interest.

REFERENCES

1. Berkovich E, Monnat RJ, Jr., Kastan MB. Roles of ATM and NBS1 in chromatin structure modulation and DNA double-strand break repair. *Nature Cell Biology*. 2007; 9:683–690.
2. Matsuoka S, Ballif BA, Smogorzewska A, McDonald ER, 3rd, Hurov KE, Luo J, Bakalarski CE, Zhao Z, Solimini N, Lerenthal Y, Shiloh Y, Gygi SP, Elledge SJ. ATM and ATR substrate analysis reveals extensive protein networks responsive to DNA damage. *Science*. 2007; 316:1160–1166.
3. Thompson LH. Recognition, signaling, and repair of DNA double-strand breaks produced by ionizing radiation in mammalian cells: the molecular choreography. *Mutation Research*. 2012; 751:158–246.
4. Price BD, D'Andrea AD. Chromatin remodeling at DNA double-strand breaks. *Cell*. 2013; 152:1344–1354.
5. Rogakou EP, Pilch DR, Orr AH, Ivanova VS, Bonner WM. DNA double-stranded breaks induce histone H2AX phosphorylation on serine 139. *The Journal of Biological Chemistry*. 1998; 273:5858–5868.
6. Gospodinov A, Herceg Z. Chromatin structure in double strand break repair. *DNA Repair*. 2013; 12:800–810.
7. Gospodinov A, Herceg Z. Shaping chromatin for repair. *Mutation Research*. 2013; 752:45–60.
8. Fradet-Turcotte A, Canny MD, Escibano-Diaz C, Orthwein A, Leung CCY, Huang H, Landry M-C, Kitevski-LeBlanc J, Noordermeer SM, Sicheri F, Durocher D. 53BP1 is a reader of the DNA-damage-induced H2A Lys 15 ubiquitin mark. *Nature*. 2013; 499:50–54.
9. Bartek J, Lukas J. DNA damage checkpoints: from initiation to recovery or adaptation. *Curr. Opin. Cell Biol*. 2007; 19:238–245
10. Jackson SP, Bartek J. The DNA-damage response in human biology and disease. *Nature*. 2009; 461:1071–1078.
11. Li L, Clevers H. Coexistence of quiescent and active adult stem cells in mammals. *Science*. 2010; 327:542–545.
12. Cheung TH, Rando TA. Molecular regulation of stem cell quiescence. *Nat. Rev. Mol. Cell. Biol*. 2013; 14:329–340.
13. Coller HA, Sang L, Roberts JM. a new description of cellular quiescence. *PLoS Biol*. 2006; 4:e83
14. Iyama T, Wilson DM, 3rd. DNA repair mechanisms in dividing and non-dividing cells. *DNA Repair*. 2013; 12:620–636.
15. Aparicio T, Baer R, Gautier J. DNA double-strand break repair pathway choice and cancer. *DNA Repair*. 2014; 19:169–175.
16. Branzei D, Folani M. Regulation of DNA repair throughout the cell cycle. *Nat. Rev. Mol. Cell. Biol*. 2008; 9:297–308.
17. Escibano-Diaz C, Durocher D. DNA repair pathway choice—a PTIP of the hat to 53BP1. *EMBO Rep*. 2013; 14:665–666.
18. Escibano-Diaz C, Orthwein A, Fradet-Turcotte A, Xing M, Young JTF, Tkac J, Cook MA, Rosebrock AP, Munro M, Canny MD, Xu D, Durocher D. A cell cycle-dependent regulatory circuit composed of 53BP1-RIF1 and BRCA1-CtIP controls DNA repair pathway choice. *Molecular cell*. 2013; 49:872–883.
19. Radhakrishnan SK, Jette N, Lees-Miller SP. Non-homologous end joining: emerging themes and unanswered questions. *DNA Repair*. 2014; 17:2–8.
20. Shibata A, Moiani D, Arvai AS, Perry J, Harding SM, Genois MM, Maity R, van Rossum-Fikkert S, Kertokallio A, Romoli F, Ismail A, Ismalaj E, Petricci E, et al. DNA double-strand break repair pathway choice is directed by distinct MRE11 nuclease activities. *Molecular Cell*. 2014; 53:7–18.
21. Panier S, Durocher D. Push back to respond better: regulatory inhibition of the DNA double-strand break response. *Nat Rev Mol Cell Biol*. 2013; 14:661–672.
22. Aymard F, Bugler B, Schmidt CK, Guillou E, Caron P, Briois S, Iacovoni JS, Daburon V, Miller KM, Jackson SP, Legube G. Transcriptionally active chromatin recruits homologous recombination at DNA double-strand breaks. *Nature Structural & Molecular Biology*. 2014; 21:366–374.
23. Miller KM, Jackson SP. Histone marks: repairing DNA breaks within the context of chromatin. *Biochemical Society transactions*. 2012; 40:370–376.
24. Soria G, Polo SE, Almouzni G. Prime, repair, restore: the active role of chromatin in the DNA damage response. *Molecular Cell*. 2012; 46:722–734.
25. Terasawa M, Shinohara A, Shinohara M. Canonical non-homologous end joining in mitosis induces genome instability and is suppressed by M-phase-specific phosphorylation of XRCC4. *Plos Genetics*. 2014; 10:e104563.
26. Orthwein A, Fradet-Turcotte A, Noordermeer SM, Canny MD, Brun CM, Strecker J, Escibano-Diaz C, Durocher D. Mitosis Inhibits DNA Double-Strand Break Repair to Guard Against Telomere Fusions. *Science*. 2014; 344:189–193.
27. Lees-Miller SP. DNA double strand break repair in mitosis is suppressed by phosphorylation of XRCC4. *PLoS Genetics*. 2014; 10:e1004598.
28. Cesare AJ. Mitosis, double strand break repair, and telomeres: a view from the end: how telomeres and the DNA damage response cooperate during mitosis to maintain genome stability. *BioEssays: news and reviews in molecular, cellular and developmental biology*. 2014; 36:1054-1061

29. Caron P, Aymard F, Iacovoni JS, Briois S, Canitrot Y, Bugler B, Massip L, Losada A, Legube G. Cohesin protects genes against gammaH2AX Induced by DNA double-strand breaks. *PLoS Genetics*. 2012; e1002460.
30. Iacovoni JS, Caron P, Lassadi I, Nicolas E, Massip L, Trouche D, Legube G. High-resolution profiling of gammaH2AX around DNA double strand breaks in the mammalian genome. *The EMBO Journal*. 2010; 29:1446–1457.
31. Massip L, Caron P, Iacovoni JS, Trouche D, Legube G. Deciphering the chromatin landscape induced around DNA double strand breaks. *Cell cycle*. 2010; 9:2963–2972.
32. Ambrosio S, Amente S, Napolitano G, Di Palo G, Lania L, Majello B. MYC impairs resolution of site-specific DNA double-strand breaks repair. *Mutation research*. 2015; 774:6–13.
33. Napolitano G, Amente S, Lavadera ML, Di Palo G, Ambrosio S, Lania L, Dellino GI, Pelicci PG, Majello B. Sequence-specific double strand breaks trigger P-TEFb-dependent Rpb1-CTD hyperphosphorylation. *Mutation Research*. 2013; 749:21–27.
34. Dai J, Itahana K, Baskar R. Quiescence does not affect p53 and stress response by irradiation in human lung fibroblasts. *Biochemical and Biophysical Research Communications*. 2015; 458:104–109.
35. Karanam K, Kafri R, Loewer A, Lahav G. Quantitative live cell imaging reveals a gradual shift between DNA repair mechanisms and a maximal use of HR in mid-S phase. *Mol. Cell*. 2012; 47: 320–329.
36. Buttitta LA, Edgar BA. Mechanisms controlling cell cycle exit upon terminal differentiation. *Curr Opin Cell Biol*. 2007; 19: 697–704.
37. Fortini P, Dogliotti E. Mechanisms of dealing with DNA damage in terminally differentiated cells. *Mutation Research*. 2010; 685:38–44.
38. Schneider L, Fumagalli M, d'Adda di Fagagna F. Terminally differentiated astrocytes lack DNA damage response signaling and are radioresistant but retain DNA repair proficiency. *Cell Death and Differentiation*. 2012; 19:582–591.
39. Latella L, Lukas J, Simone C, Puri PL, Bartek J. Differentiation-Induced Radioresistance in Muscle Cells. *Molecular and Cellular Biology*. 2004; 24:6350–636.
40. Li H, Durbin R. Fast and accurate short read alignment with Burrows-Wheeler transform. *Bioinformatics*. 2009; 25:1754–1760.
41. Li H, Handsaker B, Wysoker A, Fennell T, Ruan J, Homer N, Marth G, Abecasis G, Durbin R, Genome Project Data Processing S. The Sequence Alignment/Map format and SAMtools. *Bioinformatics*. 2009; 25:2078–2079.
42. Quinlan AR, Hall IM. BEDTools: a flexible suite of utilities for comparing genomic features. *Bioinformatics*. 2010; 26:841–842.
43. Scala G, Affinito O, Miele G, Monticelli A, Coccozza S. Evidence for evolutionary and nonevolutionary forces shaping the distribution of human genetic variants near transcription start sites. *PloS one*. 2014; 9:e114432.
44. Amente S, Bertoni A, Morano A, Lania L, Avvedimento EV, Majello B. LSD1-mediated demethylation of histone H3 lysine 4 triggers Myc-induced transcription. *Oncogene*. 2010; 29:3691–3702.

CHAPTER 4

**LSD1 MEDIATES MYCN CONTROL OF EPITHELIAL-MESENCHYMAL
TRANSITION THROUGH SILENCING OF METASTATIC SUPPRESSOR NDRG1
GENE**

Susanna Ambrosio¹, Stefano Amente², Carmen D. Saccà¹, Mario Capasso^{2,3}, Raffaele A. Calogero⁴, Luigi Lania² and Barbara Majello¹

¹ Department of Biology, University of Naples 'Federico II', Naples, Italy

² Department of Molecular Medicine and Medical Biotechnologies, University of Naples, 'Federico II', Naples, Italy

³ CEINGE Biotechnologie Avanzate, Napoli, Italy

⁴ Molecular Biotechnology Center, Department of Molecular Biotechnology and Health Sciences, University of Torino, Turin, Italy

Published Oncotarget. 2017 Jan 17;8(3):3854-3869.

The chapter is an exact copy of the journal paper referred to above.

LSD1 mediates MYCN control of epithelial-mesenchymal transition through silencing of metastatic suppressor NDRG1 gene

Susanna Ambrosio¹, Stefano Amente², Carmen D. Saccà¹, Mario Capasso^{2,3}, Raffaele A. Calogero⁴, Luigi Lania² and Barbara Majello¹

¹ Department of Biology, University of Naples 'Federico II', Naples, Italy

² Department of Molecular Medicine and Medical Biotechnologies, University of Naples, 'Federico II', Naples, Italy

³ CEINGE Biotechnologie Avanzate, Napoli, Italy

⁴ Molecular Biotechnology Center, Department of Molecular Biotechnology and Health Sciences, University of Torino, Turin, Italy

Correspondence to: Barbara Majello, email: majello@unina.it

Keywords: MYCN; LSD1; NDRG1; EMT; neuroblastoma

Received: July 20, 2016

Accepted: October 14, 2016

Published: November 22, 2016

ABSTRACT

Neuroblastoma (NB) with MYCN amplification is a highly aggressive and metastatic tumor in children. The high recurrence rate and resistance of NB cells to drugs urgently demands a better therapy for this disease. We have recently found that MYCN interacts with the lysine-specific demethylase 1 (LSD1), a histone modifier that participates in key aspects of gene transcription. In cancer cells, LSD1 contributes to the genetic reprogramming that underlies to Epithelial-Mesenchymal Transition (EMT) and tumor metastasis. Here, we show that LSD1 affects motility and invasiveness of NB cells by modulating the transcription of the metastasis suppressor NDRG1 (N-Myc Downstream-Regulated Gene 1). At mechanistic level, we found that LSD1 co-localizes with MYCN at the promoter region of the NDRG1 gene and inhibits its expression. Pharmacological inhibition of LSD1 relieves repression of NDRG1 by MYCN and affects motility and invasiveness of NB cells. These effects were reversed by overexpressing NDRG1. In NB tissues, high levels of LSD1 correlate with low levels of NDRG1 and reduced patients survival. Collectively, our findings elucidate a mechanism of how MYCN/LSD1 control motility and invasiveness of NB cells through transcription regulation of NDRG1 expression and suggest that pharmacological targeting of LSD1 represents a valuable approach for NB therapy.

INTRODUCTION

Neuroblastoma (NB), a disease of the sympathetic nervous system, is the most common solid tumor of infancy. Despite significant advances in the treatment of pediatric cancer over the past two decades, NB remains a highly refractory malignancy, with less than 50% 5-year survival rates for the majority of patients who are diagnosed with high-risk disease. One of the most powerful independent prognostic indicators for this disease is the amplification of the MYCN oncogene, which occurs at high levels in approximately 25% of NBs [1-3]. High-risk NBs often present hematogenous metastasis indicating that MYCN amplification control epithelial-mesenchymal transition (EMT) through which NB cells lose homotypic

adhesion and acquire migratory capacity [4]. High level of MYCN expression has a great impact on global gene expression. [5]. Despite this richness of information, the entire and precise network of interactions that MYCN establishes within cancer cells remains elusive. Recently, we have demonstrated that MYCN interacts with LSD1/KDM1A, a monoamine oxidase that function as master epigenetic regulator in NB cell lines and that the MYCN/LSD1 complex is involved either in activation or repression of MYCN target genes in NB cell lines [6]. Importantly, the inhibition of LSD1 activity reduces neuroblastoma cell viability and induces differentiation. These findings suggest that LSD1 inhibition may have strong therapeutic relevance to counteract MYCN-driven oncogenesis.

LSD1 is an amine oxidase that catalyzes lysine demethylation in a flavin adenine dinucleotide (FAD)-dependent oxidative reaction. LSD1 removes mono- and dimethyl groups from lysine 4 (H3K4) and lysine 9 (H3K9) of histone H3, and can also target non-histone proteins such as p53, E2F1, and DNMT1 [7-9]. LSD1 was initially described as a cofactor of the REST/CoREST complex. Although LSD1 can function as a co-repressor of transcription factors as REST, it also has been reported to function as a coactivator of specific transcription factors by removing H3K9 methylation, suggesting that its substrate specificity defines its biological outcome [10-12]. LSD1 is overexpressed in a variety of cancers and tends to correlate with more aggressive cancers with poor prognosis. There is a large body of evidence that LSD1 is involved in maintaining the undifferentiated, malignant phenotype of neuroblastoma cells and that its overexpression correlates with aggressive disease, poor differentiation and infaust outcome [13, 14].

To address the functional significance of LSD1 inhibition in NB we performed global transcriptome analysis (RNA-seq) in LSD1-deficient NB cells. Analysis of differentially expressed gene (DEG) highlighted the biological relevance of co-target genes indicating that epithelial-mesenchymal transition pathway was significantly affected. Among genes positively affected by LSD1 inhibition we focused our attention on the metastatic tumor suppressor gene N-myc downstream regulated1, NDRG1. In fact, we find that NDRG1 is inhibited by LSD1. NDRG1 is one of the four members of the human NDRG family, and its designation comes from its expression being repressed by MYC and MYCN [15, 16] and its expression is negatively correlated with tumor progression in multiple neoplasms. NDRG1 is a potent metastatic suppressor that has been shown to restrain TGF- β -induced EMT in prostate and colon cancer cells, while its reduction induces EMT [17-22]. Collectively these studies demonstrated that NDRG1 functions as a metastatic suppressor that inhibits EMT in human cancer a key initial step in metastasis.

We found that LSD1 inhibition suffices to repress NDRG1 expression even in the presence of MYCN amplification. Expression of NDRG1 suppresses motility and invasiveness of NB cells. *In silico* studies of neuroblastoma tumor samples revealed that low expression of NDRG1 was associated with poor survival. Low NDRG1 and high LSD1 levels were mutually exclusive in MYCN-amplified NB samples, corroborating the *in vitro* results. Taken together, our findings provide a previously unidentified model to control of EMT in NB, suggesting that LSD1 represents a novel and promising target for selective inhibition of cell migration and invasiveness in neuroblastoma cells.

RESULTS

LSD1 depletion selectively affects EMT pathway

LSD1 is highly expressed in undifferentiated Neuroblastoma and its high expression correlates with adverse outcome [13, 14]. We recently showed that MYCN interacts with LSD1 and that the LSD1/MYCN complex controls transcription of tumor suppressor genes such as p21 and CLU [6]. Moreover LSD1 inhibition results in cell growth arrest of cultured NB cells. To address in more details the role of LSD1 function in NB cells, we performed global transcriptome analysis (RNA-seq) of Tet-21/N cells treated with tranlycypromine (TCP) a potent inhibitor of LSD1. In parallel, we performed RNA-seq from Tet-21/N cells treated with siRNA targeting LSD1 (LSD1-KD). RNA-seq data from duplicate biological replicas were then analyzed for differentially expressed gene (DEG). Statistical analysis allows us to screen out 661 DEGs in TCP sample ($\log_2FC \geq 1$; $FDR \leq 0.1$) and 526 DEGs in LSD1-KD ($\log_2FC \geq 1$; $FDR \leq 0.1$). 125 were commonly present in both treatments (Figure 1A, B and Supplementary Table 3). To clarify the biological relevance of co-target genes we used Gene set enrichment analysis. GSEA revealed that among top scoring pathways the gene set of Epithelial-Mesenchymal Transition, EMT, was ranked as significantly affected in both TCP and LSD1-KD samples (Figure 1C). We quantified expression levels of EMT marker genes in TCP treated or LSD1-KD Tet-21/N cells *versus* control cells by qRT-PCR. As shown in Figure Supplementary 1, LSD1 inhibition increased the levels of the epithelial markers, E-cadherin, occludin and desmoplakin, and reduced the expression mesenchymal markers, Vimentin and α -SMA, whereas no significant differences were detected in N-cadherin expression.

Previous studies have shown that LSD1 is indeed involved in the control of EMT, through interaction with the SNAG domain of SNAI1, a master EMT regulator [23, 24]. Among the several genes that were affected in TCP-treated and LSD1-KD cells related to EMT (SAT1, PLAUR, TNFRSF12A, RGS4, BDNF, MPP3, NDRG1 and SGK1) we focused our attention on the MYCN regulated gene, the metastasis suppressor gene NDRG1 (N-myc downstream regulated gene 1). NDRG1 was first isolated as a gene up-regulated in N-Myc knockout mouse embryos [25] and directly repressed by MYCN and c-MYC through binding to the NDRG1 core promoter [26]. The metastasis suppressor NDRG1 is negatively correlated with tumor progression of several types of cancer, and most importantly down-regulation of NDRG1 expression enhances cell proliferation and invasiveness. In contrast, its up-regulation reduces cell proliferation and invasiveness [27-29].

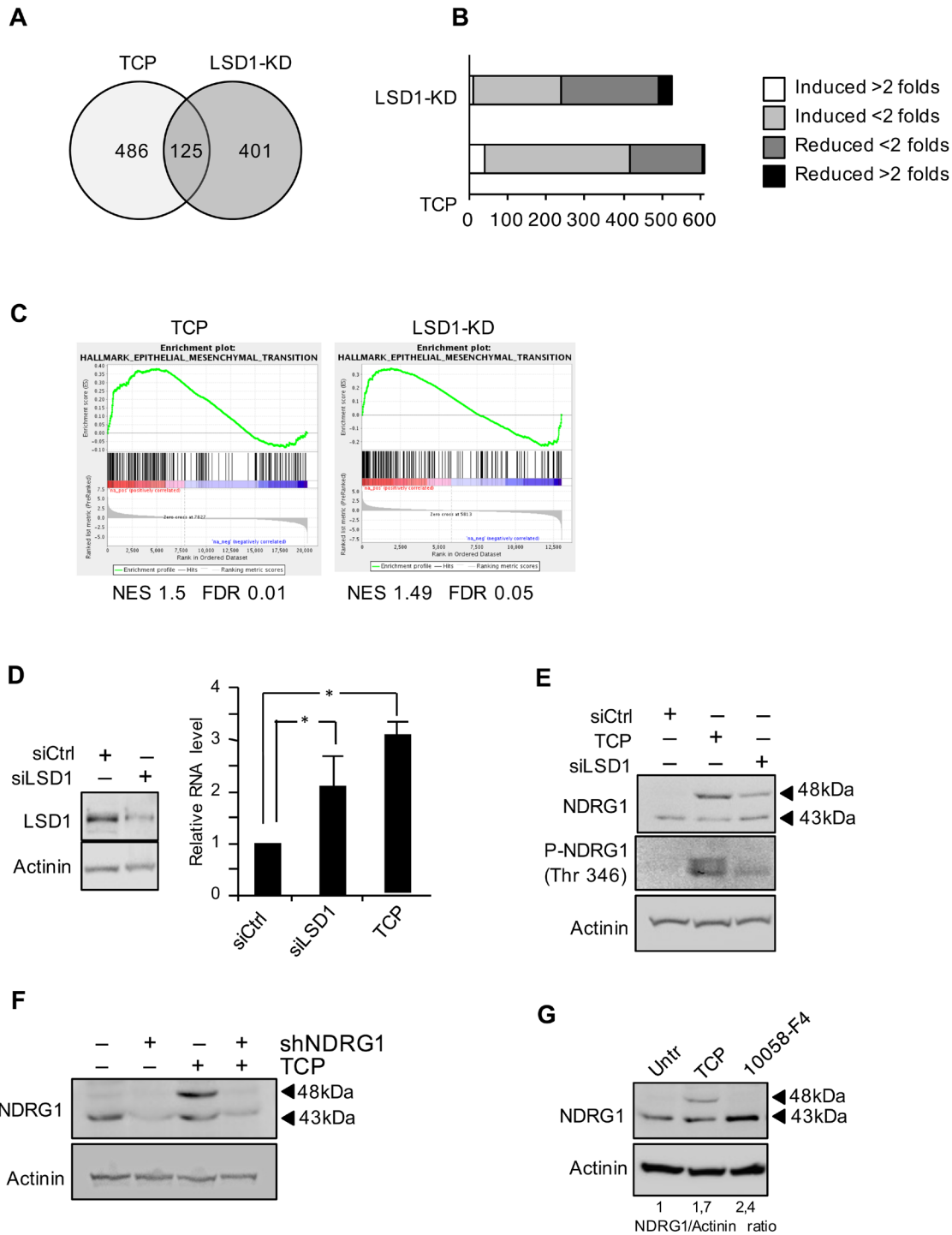


Figure 1: A. Venn diagram of the DEG present in both LSD1-knockdown (LSD1-KD) and TCP treatment. **B.** Gene set of regulated genes by TCP treatment and LSD1-KD. **C.** Gene set enrichment analysis (GESA) plots show enrichment of gene sets regulated by LSD1-KD and TCP treatment. In each panel, nominal NES and false discovery rates (FDRs) are indicated. **D.** NDRG1 gene expression was analyzed by qRT-PCR, using samples prepared from Tet-21/N cells and treated with TCP or siRNA-LSD1 and siRNA-control as indicated. LSD1 protein level in Tet-21/N cells transfected with siRNA-LSD1 or control was determined by western blot. *, statistical significance ($P < 0.01$; Student t test). **E.** Western blotting of protein extracts from Tet-21/N cells prepared as described in D, using NDRG1 and phospho-NDRG1 (Thr 346) antibodies. **F.** NDRG1 silencing using sh-NDRG1 in Tet-21/N cells treated with TCP or vehicle, was assayed by western blot. **G.** Western blotting of protein extract from Tet-21/N treated with vehicle, TCP or 10058-F4 for 48 hrs, using NDRG1 antibody. Actinin has been probed as loading control.

To validate the role of LSD1 in NDRG1 expression we inhibited LSD1 in Tet-21/N cells with TCP or siRNA-targeted knockdown and measured NDRG1 mRNA and protein expression levels. We found that TCP treatment or LSD1 silencing stimulates NDRG1 expression (Figure 1D and 1E). Previously immunoblotting studies revealed that NDRG1 might appear as multiple protein bands depending from the cellular context likely due to different isoforms and/or post-translational modifications such as phosphorylation and glycosylation [27, 30, 31]. It has been shown that the signal cascade mTORC2/serum glucocorticoid induced protein kinase1 (SGK1) phosphorylates NDRG1 at T346 and this modification is essential to suppress tumor growth [20, 32]. Tet-21/N cells treated with TCP or siLSD1 were probed with an antibody that specifically recognize NDRG1 phosphorylated at T346 demonstrating that LSD1 inhibition induces NDRG1 phosphorylation, Figure 1E. Finally shRNA-targeted NDRG1 knockdown demonstrates specificity of NDRG1 bands (Figure 1F). To address the contribution of MYC and LSD1 to NDRG1 expression, Tet-21/N cells were treated with 10058-F4, a small molecule inhibitor of MYC/MAX dimerization [6] that has effect on either cMYC then MYCN. Following 10058-F4 treatment we found an increase of the 43kDa NDRG1 band, while TCP activates the 48kDa (Figure 1G). These findings suggest that inhibition of either MYCN or LSD1 de-repress NDRG1 expression. However, while MYCN inhibition activates NDRG1, LSD1-KD also induces NDRG1 phosphorylation.

MYCN and LSD1 co-localize at NDRG1 promoter and repress its expression

To determine whether LSD1 is directly involved in transcriptional control of NDRG1 we inhibited LSD1 in Tet-21/N cells with TCP or with siRNA against LSD1 and assessed the relative binding of MYCN and LSD1 to the NDRG1 gene by chromatin immune-precipitation (ChIP) assays. The immunoprecipitated chromatin samples were subjected to qPCR using primers corresponding to the transcriptional start site (TSS) of the NDRG1 gene, Figure 2A. As shown in Figure 2B and 2C, MYCN and LSD1 were both recruited selectively at the transcriptional start site (TSS) of the NDRG1 gene but not at distal sites (-10kb), indicating that the MYCN/LSD1 complex binds to the NDRG1 promoter. We find also that MYCN binding was unaffected by TCP or LSD1 depletion implying that MYCN binding does not require LSD1 while, in contrast, LSD1 binding was reduced in TCP-treated and LSD1-KD samples, suggesting that the binding of LSD1 require the catalytic activity of the enzyme. Next, we monitored the histone modifications occurring at NDRG1 promoter (Figure 2D, 2E). Depletion of LSD1 enhances H3-acetylation whereas it reduces the repressive

mark H3K27me3, consistent with the induction of NDRG1 expression in these cells. Overall, our findings demonstrate that: 1) both LSD1 and MYCN are recruited to the NDRG1 promoter chromatin to repress NDRG1 expression; 2) LSD1 inhibition is sufficient to relieve MYCN-driven NDRG1 repression.

Effects of TCP and SP2509 inhibitors on LSD1/MYCN-mediated regulation of NDRG1

During last years several small molecular inhibitors of LSD1 based on different molecular mechanisms have been developed [33]. SP2509 is a reversible inhibitor of LSD1 and differently from TCP does not target the catalytic activity of the enzyme. SP2509 attenuates the binding of LSD1 to CoREST and it has been found to be effective in inhibition of cultured and primary AML blasts [34]. To further substantiate the role of LSD1 in the suppression of NDRG1 we analyzed the effects of treatment of NB cells on NDRG1 expression by treatment with this different LSD1 inhibitor. As shown in Figure 3A, SP2509 treatment enhances NDRG1 mRNA expression and increases the NDRG1 48kDa protein levels in a dose dependent manner. Thus, both TCP and SP2509 enhance NDRG1 expression albeit these drugs inhibit LSD1 through different mechanisms. Because LSD1/MYCN negatively controls NDRG1 transcription we assessed whether TCP or SP2509 may interfere with the LSD1/MYCN interaction. To this end, HEK293T cells co-transfected with expression vectors encoding LSD1 and MYCN were exposed to TCP and the complex between MYCN and LSD1 was analyzed by immunoprecipitation. As shown in Figure 3B, LSD1 and MYCN readily interact in the absence of TCP but their association was impaired in presence of the drug. This inhibitory effect of TCP is specific to LSD1-MYCN complex since it did not interfere with the interaction of MYCN with its endogenous partner MAX (Figure 3B). In contrast, SP2509 did not inhibit the interaction between LSD1 and MYCN. Also LSD1/CoREST association was inhibited by SP2509, not by TCP (Figure 3C). Collectively these results demonstrate that LSD1 activity is necessary for the interaction with MYCN, not with CoREST. Thus, inhibition by TCP or SP2509, de-represses NDRG1 expression, albeit the two drugs have a marked different mode of action.

Since SP2509 is a reversible inhibitor of LSD1, we tested whether re-activation of NDRG1 by SP2509 treatment was reversible. Tet-21/N cells were treated with SP2509 for 48 hrs and then cells were washed, fed with normal medium and collected at 12, 24 and 48 hrs thereafter SP2509 wash out. Results in Figure 3D shows that NDRG1 expression decreases in a time dependent manner following removal of the SP2509, demonstrating that NDRG1 activation is directly dependent upon LSD1 inhibition.

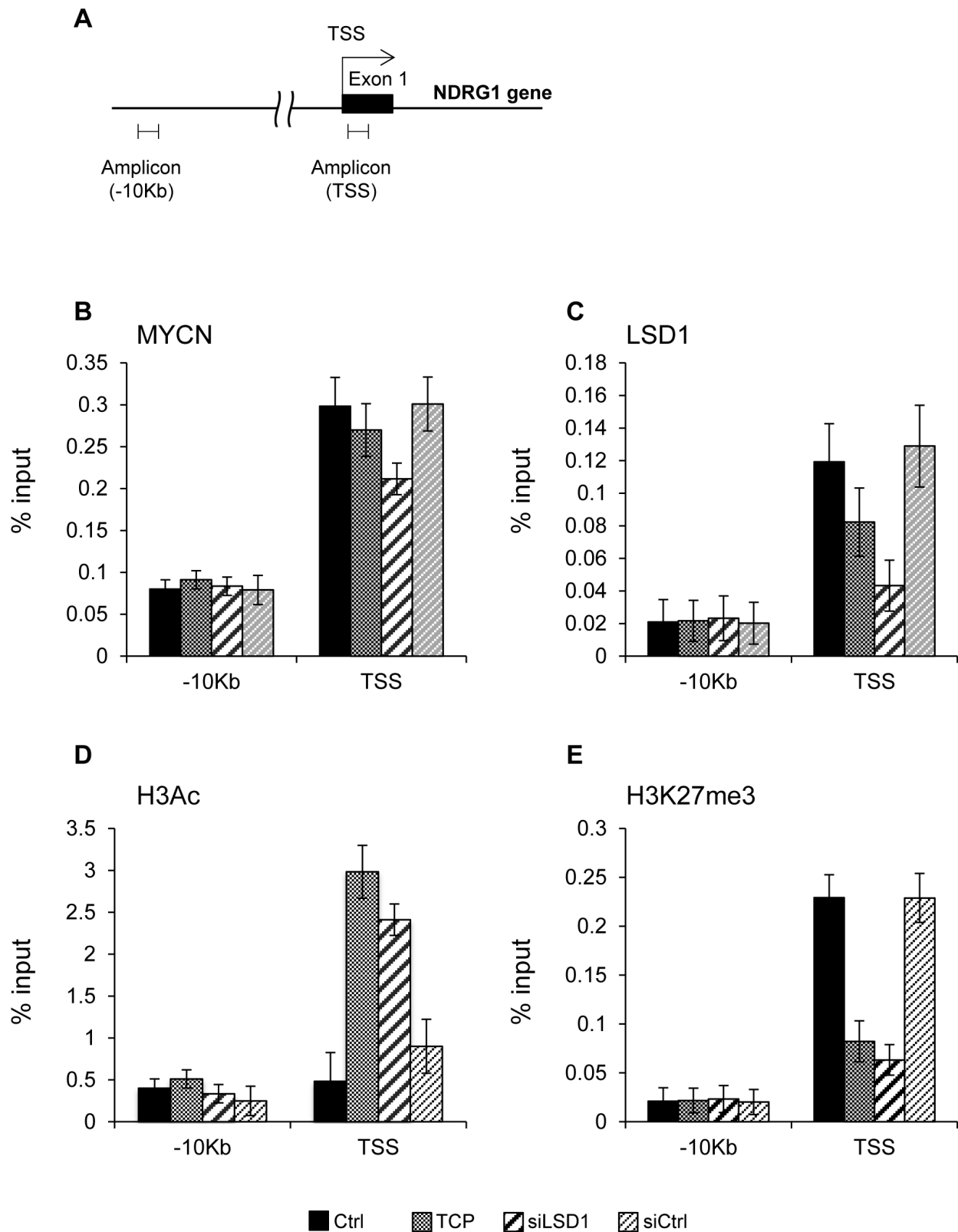


Figure 2: A. Schematic representation of the NDRG1 promoter. B. and C. MYCN and LSD1 binding to NDRG1 chromatin. Cell treatments are indicated at the bottom of the figure. qPCR was performed with primers for NDRG1 TSS, and -10kb. D. and E. Histone modifications at NDRG1 chromatin; ChIPs were carried out using the indicated antibodies and analyzed with primers encompassing the TSS region and -10kb from TSS. Values from three independent ChIP assays are presented along with standard deviations, $n = 3$. Changes in % input are shown normalized over IgG controls and are all statistically significant ($P < 0,05$; Student t test).

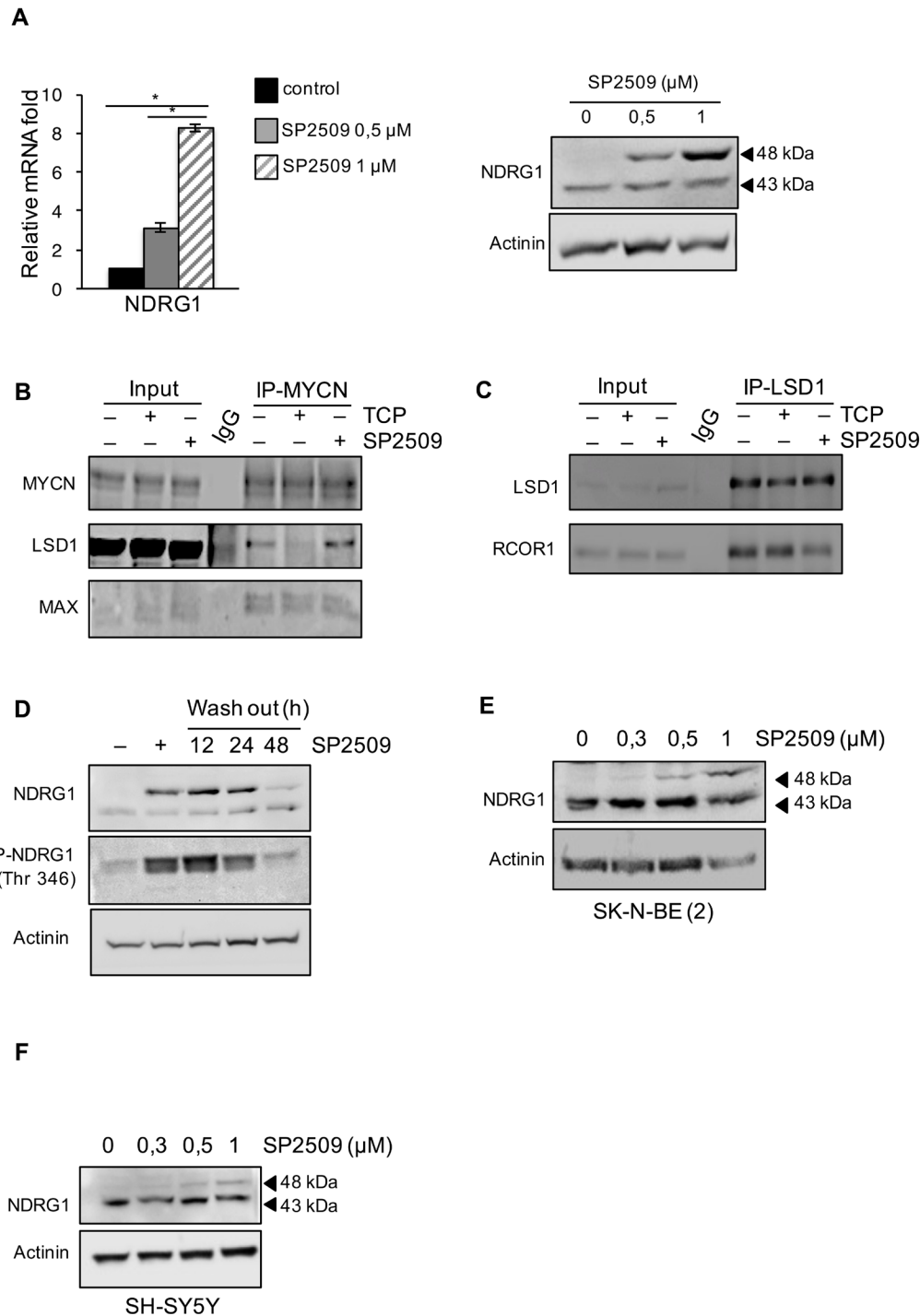


Figure 3: A. NDRG1 gene expression was determined by qRT-PCR or by western blot in Tet-21/N cells treated with SP2509 at different concentrations, as indicated. *, statistical significance ($P < 0.01$; Student t test). B. Co-Immunoprecipitation with MYCN antibody was performed in 293T cells co-transfected with LSD1 and MYCN expression vectors and treated with TCP, SP2509 or vehicle. Extract were analyzed by western blotting with MYCN, LSD1 and MAX antibodies as indicated. C. Interaction between endogenous LSD1 and MYCN in Tet-21/N cells, treated with TCP, SP2509 or vehicle, was assessed by co-Immunoprecipitation. Cell lysates were immune-precipitated with a LSD1 antibody Western blot analysis was performed on immuno-precipitated extracts with LSD1 and RCOR1 antibodies. IgG-sample was used as negative control. D. Tet-21/N cells were treated for 48 h with SP2509 or vehicle and then released into fresh medium for the indicated times. Cellular extracts were prepared and stained with anti-NDRG1 and phospho-NDRG1 (Thr 346). E. and F. Cell extracts from SK-N-BE (2) and SH-SY5Y cells treated with SP2509 at the indicated concentrations were prepared and probed with NDRG1 antibody. Actinin was probed as loading control.

To address if LSD1 inhibition affects NDRG1 expression in the context of MYCN amplification, we analyzed the effect of SP2509 in a non-amplified MYCN SH-SY5Y cell line. Moreover, since activation of NDRG1 may also occur as result of p53 binding in colon cancer cell lines [35] we also used the p53 mutated, MYCN-amplified NB cell line SK-N-BE (2) to address the relative contribution of p53 in NDRG1 activation. The SH-SY5Y (MYCN non-amplified) and MYCN-amplified p53 mutated SK-N-BE (2) cells were treated with SP2509 at different concentration for 48 hrs and western blot was performed using the NDRG1 antibody. Results reported in Figure 3E, 3F show that up regulation of the 48 kDa NDRG1 band is observed in both cell lines demonstrating that NDRG1 activation by LSD1 inhibition is not due to p53 activity and is not cell specific.

Collectively our results demonstrate that NDRG1 expression is modulated by LSD1 and that pharmacological LSD1 inhibition in NB cells up-regulates NDRG1 expression.

Effect of LSD1 inhibition on migration and invasion of NB cells

NDRG1 over-expression promotes formation of adherent junctions and inhibits cell migration and invasion in several types of tumors cells indicating that NDRG1 inhibits the establishment of the epithelial-mesenchymal transition (EMT) program [18, 36]. Our findings suggest that LSD1 pharmacological silencing might control EMT in NB tumor cell lines by upregulating NDRG1 expression.

LSD1 was demonstrated to activate the Wnt/ β -catenin signaling pathway by down-regulating the pathway antagonist DKK1 in colorectal cancer cells [37]. In different studies NDRG1 overexpression has been

shown to inhibit β -catenin phosphorylation inducing its accumulation at cell membranes [21]. We examined if NDRG1 activation mediated by pharmacological inhibition of LSD1 affected β -catenin subcellular localization. To this end we performed immunofluorescence to detect β -catenin in Tet-21/N cells untreated (Ctrl) or treated with SP2509. As shown in Figure 4A, SP2509 enhanced β -catenin accumulation on cellular membrane. A modest increase of β -catenin protein levels was detected in Tet-21N and SH-SY5Y cells by immuno-blotting, Figure 4B, suggesting that SP2509 treatment enhanced β -catenin accumulation on cellular membrane. Consistent with such effect, expression of the β -catenin downstream target, Cyclin D1 was down-regulated in LSD1 inhibited cells. These results indicate that pharmacological treatment of NB cells with LSD1 inhibitor results in NDRG1 activation and suggest that the anti-metastatic activity of NDRG1 in NB occurs at least in part through accumulation of β -catenin at cell membrane.

We then asked whether treatment with LSD1 inhibitors and over-expression of NDRG1 might impair the migration and invasion of tumor NB cell lines. Untreated Tet-21/N (High MYCN), tetracycline-treated (Low MYCN) and the SH-SY5Y cells were used in wound-healing assays in presence or absence of TCP or SP2509. Both Tet-21/N (High MYCN) and SH-SY5Y cells filled almost completely the wounded area 24hrs after scratching the cell monolayer, while Tet-21/N (Low MYCN) showed impaired migration efficiency (Figure 5A and 5B). TCP or SP2509 treatment markedly suppressed repair of the wound area. Such inhibitory effect was enhanced in Low-MYCN cells suggesting that reduction of MYCN levels cooperates with LSD1 in blocking the migration of LSD1-KD cells. Next, we tested the effect of NDRG1 over-expression on cell invasiveness of Tet-21/N and SH-SY5Y cells. Both cell lines were transfected with a human expression vector for NDRG1, whose expression

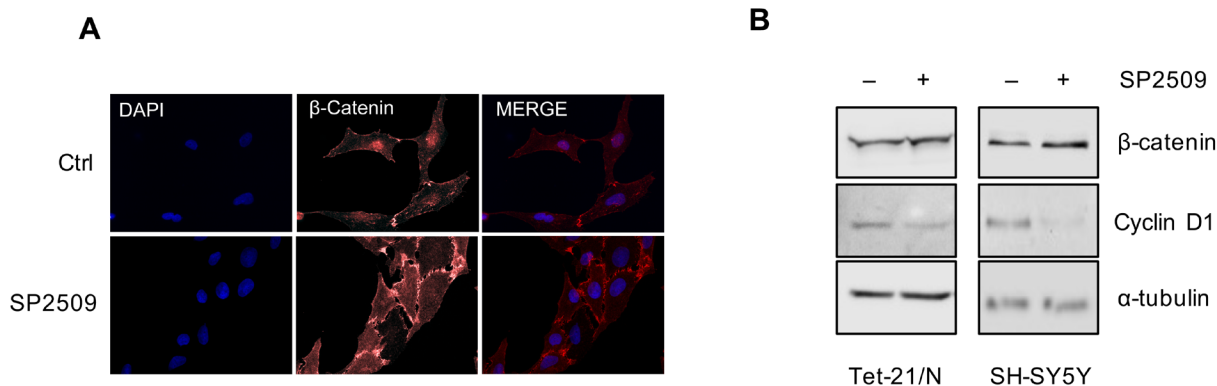


Figure 4: A. Tet-21/N cells were treated with SP2509 or vehicle, fixed and processed for anti- β -catenin immunofluorescence and DAPI staining. B. Western blot assay of protein extracts of Tet-21/N and SH-SY5Y cells treated as indicated using β -catenin and Cyclin D1 antibodies. α -tubulin has been probed as loading control. *, $P < 0,01$.

was assayed by Western blots, Figure 5C. We determined that overexpression of NDRG1 recapitulates the inhibitory effects exerted by LSD1 inhibitors. Next, we determined the effect of LSD1 inhibition and NDRG1 over-expression on cell invasion (Figure 6). Using the trans-well migration assay, we showed that NDRG1 overexpression as well as

LSD1 pharmacological inhibition in both Tet-21/N and SH-SY5Y cells resulted in a significant reduction ($\geq 25\%$) of migratory capacity compared with control cells.

These findings demonstrated that pharmacological inhibition of LSD1 blocks migration and invasion of neuroblastoma cells and most importantly overexpression

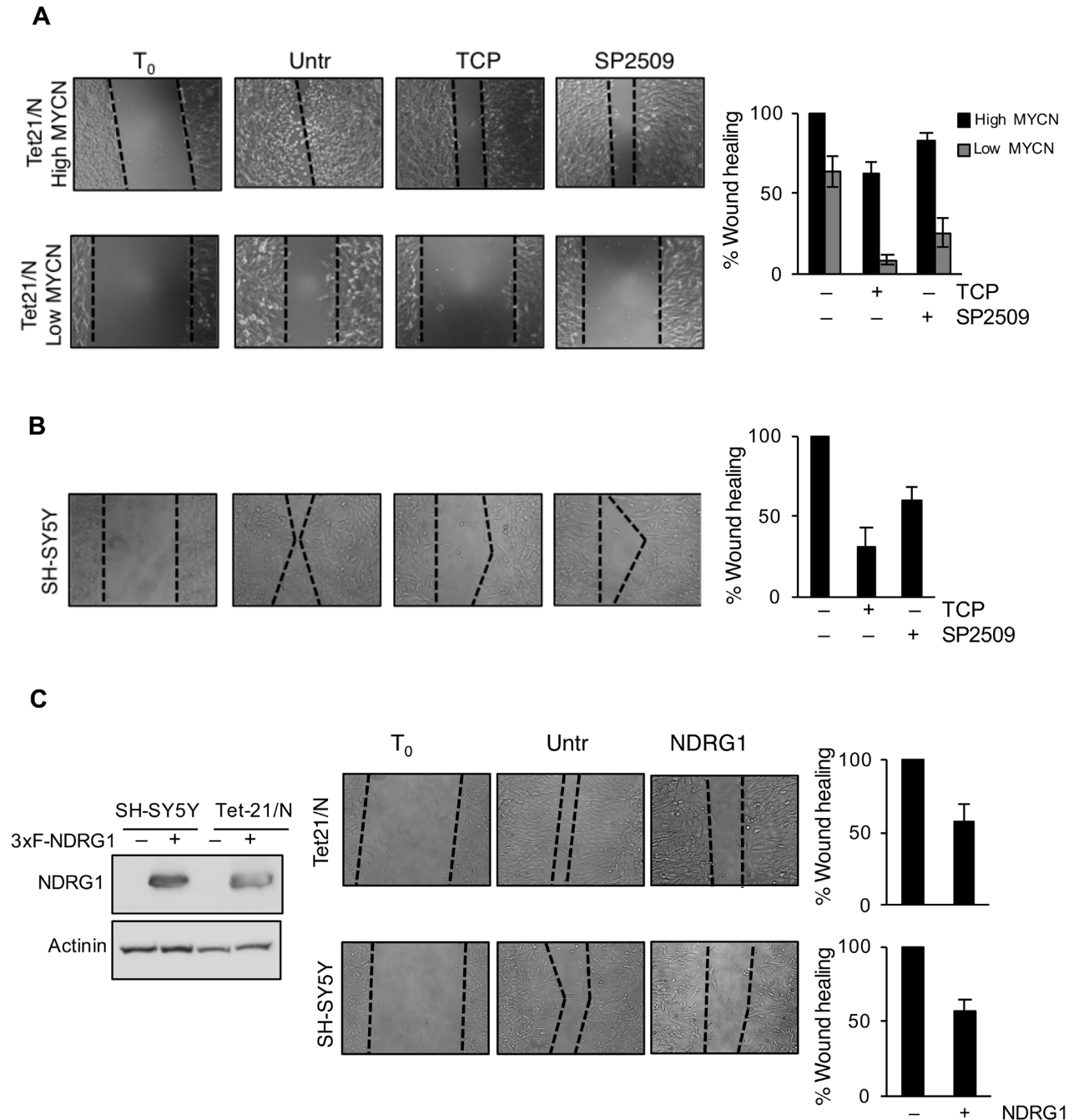


Figure 5: LSD1 inhibition reduces migration of Neuroblastoma cells. A. Wound healing of Tet-21/N (High MYCN), Tetracycline-treated Tet-21/N (Low MYCN) and **B.** SH-SY5Y cells treated with vehicle, TCP or SP2509. **C.** Wound healing was performed in Tet-21/N and SH-SY5Y cells 3XFlag-NDRG1 or mock transfected. Migration was assessed under treatment conditions at several time points using a scratch wound assay. Representative phase contrast images were shown acquired at 24hrs after scratch. Western blot shows NDRG1 protein levels in 3xFlag-NDRG1 or mock transfected Tet-21/N and SH-SY5Y cells. Actinin was used as loading control. Graphs showing the results represent the mean \pm SD of three independent experiments carried out in duplicate. Statistical significance $P < 0,01$.

of NDRG1 recapitulate these effects. Collectively, these findings demonstrated that pharmacological inhibition of LSD1 suppresses the mobility and invasiveness of cancer cells through up-regulation of NDRG1.

NDRG1 expression during differentiation and in NB tumors

It had been shown that LSD1 expression is reduced following *in vitro* induced differentiation of neuroblastoma cells [14, 38]. The findings reported above indicated that high levels of LSD1 inversely correlate to NDRG1 expression. To address the relative expression levels of MYCN, LSD1 and NDRG1 during differentiation, SK-N-

BE(2) cells were induced to differentiate by treatment with RA. Cell samples were collected at different time points after treatment and analyzed for LSD1 and NDRG1 and MYCN expression levels. As shown in Figure 7A, *in vitro* induced differentiation results in reduction of LSD1 and MYCN expression along to a concomitant up-regulation of NDRG1 levels. These results further confirm the role of LSD1 on NDRG1 expression and highlight their antagonism during differentiation of NB cells. Moreover these data strongly suggest that NDRG1 can be used as marker of neuroblastoma differentiation *in vivo*.

To further corroborate the mutually exclusive expression of NDRG1 and LSD1 we examined the relevance of NDRG1 in neuroblastoma patients. Independent studies have shown that low NDRG1 levels

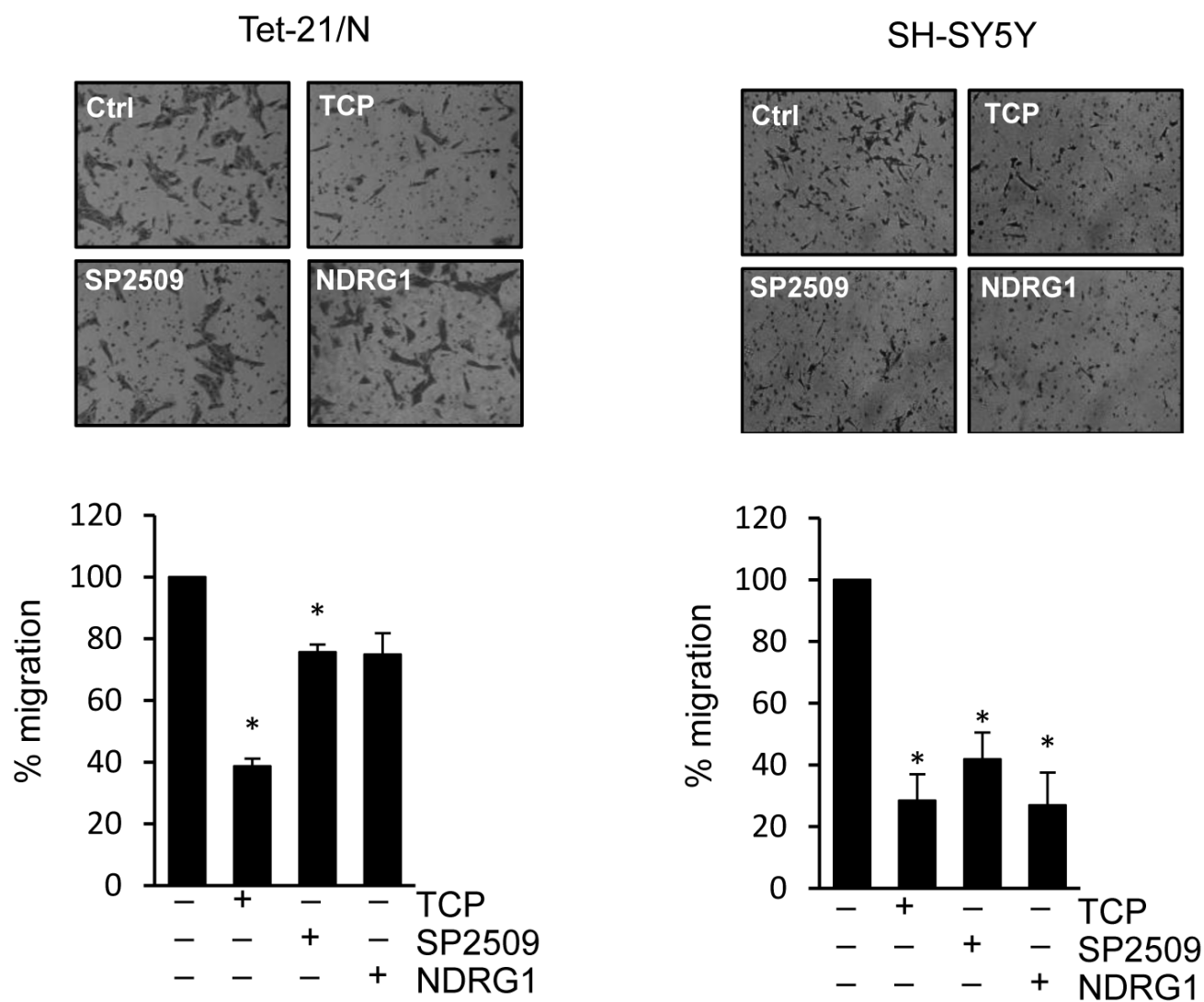


Figure 6: Trans-membrane migration assay of Tet-21/N and SH-SY5Y cells treated with vehicle, TCP or SP2509, or NDRG1-transfected. Graphs showing the results represent the mean \pm SD of three independent experiments carried out in duplicate. *, $P < 0,05$.

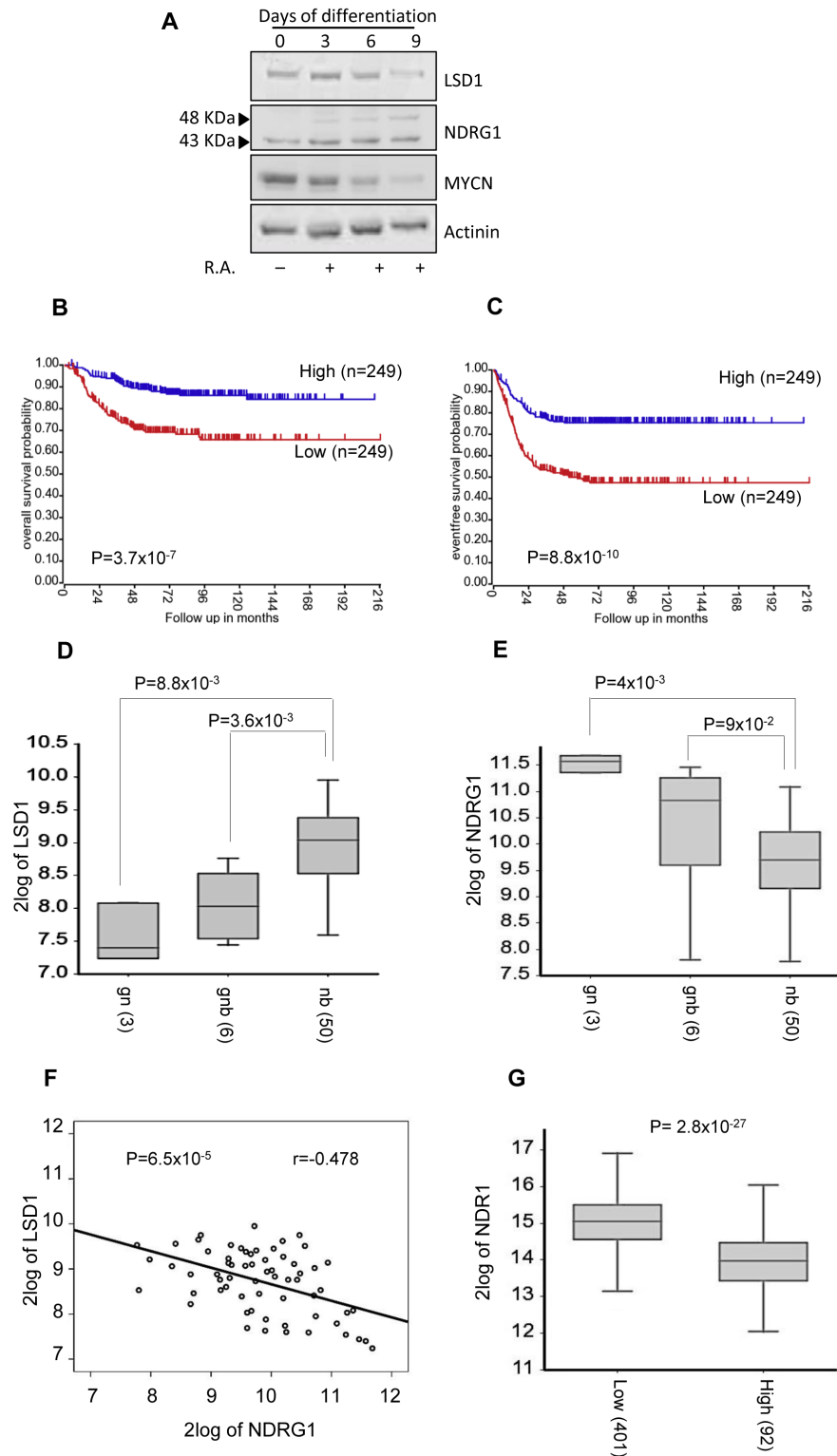


Figure 7: A. SK-N-BE (2) cells were treated with RA up to 9 days. LSD1, NDRG1 and MYCN protein levels were detected in differentiated SK-N-BE (2) cells at the indicated days by western blotting. NDRG1 expression is associated with good outcome and differentiated tumors. B. and C. Low NDRG1 expression is associated with negative prognosis. The number of tumors is indicated in parentheses. Kaplan-Meier analysis is shown, with individuals grouped by median of expression of NDRG1. Log-rank P values are shown. Changes in expression for LSD1 D. and NDRG1 E. in ganglioneuroblastoma (GNB), ganglioneuroma (GN) and neuroblastoma (NB). F. Inverse correlation between the expression values of NDRG1 and LSD1 in NB tumors (Pearson's correlation coefficient is shown). G. Box plot showing differential NDRG1 expression in NB tumors without (Low) or with (High) MYCN amplification.

are associated with worse prognosis for patients with breast, glioma, colorectal, esophageal squamous cell carcinoma, and prostate cancer [19]. More recently, it has been reported that low levels of NDRG1 is associated with poor prognosis in neuroblastoma patients [39]. In sharp contrast, LSD1 expression inversely correlates with differentiation and adverse outcome [14, 38] of neuroblastoma. Our *in vitro* findings imply that also in patients high LSD1 and low NDRG1 levels should be inversely correlated in metastatic Neuroblastomas. To this end we analyzed available RNAseq data of 498 NBs and we found that high NDRG1 expression correlates with better overall and event-free survival (Figure 7B and 7C, Mann-Whitney test, $P = 3.7 \times 10^{-7}$ and $P = 8.8 \times 10^{-10}$). Next, we analyzed LSD1 and NDRG1 expression in a microarray gene expression data of 59 NBs, of which 50 were neuroblastoma and 9 were ganglioblastoma and ganglioneuromas. LSD1 expression was considerably higher in neuroblastoma than in ganglioblastomas and ganglioneuromas (Figure 7D). In contrast, NDRG1 expression was higher in well-differentiated tumors (Figure 7E). Thus, LSD1 and NDRG1 appear to be expressed in opposite fashion in NB. Accordingly, we found that the expression of NDRG1 is inversely correlated with the expression of LSD1 (Figure 7F, $P = 6.5 \times 10^{-5}$). Finally, we determined that NDRG1 expression levels were appreciably lower in MYCN-amplified NB samples (Figure 7G). Collectively, these findings demonstrated that high levels of LSD1 and NDRG1 expression are mutually exclusive in neuroblastoma, and the expression levels of NDRG1 are significantly lower in MYCN-amplified tumors.

DISCUSSION

In the current study, we demonstrated that LSD1 in cooperation with MYCN controls cell migration and invasiveness of neuroblastoma cells through transcription regulation of the metastatic suppressor NDRG1. Our findings support a previously unidentified model to control EMT in neuroblastoma, proposing that epigenetics changes caused by LSD1 inhibition lead to up-regulation of NDRG1 thereby inducing an NDRG1-dependent inhibitory effect on cell migration and invasiveness of neuroblastoma cells

We found that in neuroblastoma cells the MYCN/LSD1 complex binds and represses NDRG1 expression. Following LSD1 inhibition epigenetics changes occur on the chromatin region surrounding the transcriptional start site of NDRG1 leading to transcription activation of NDRG1 gene expression. In a recent study it has been shown that the signal cascade mTORC2/serum glucocorticoid induced protein kinase1 (SGK1) phosphorylates NDRG1 [20]. It is likely that LSD1-KD may also affect mTORC2/GSK1 pathway, clearly further

investigations are required to clarify the role of LSD1 in the phosphorylation of NDRG1.

LSD1 inhibition suppresses motility and invasiveness of NB cells and ectopic over expression of NDRG1 phenocopy the pharmacological treatments with LSD1 inhibitors, suggesting that de-repression of NDRG1 expression plays a causative role in blocking cell migration and invasiveness. Moreover, lowering MYCN expression we observed a cooperative inhibition with TCP to restrain cell mobility, suggesting that MYCN and LSD1 cooperatively control EMT.

High-risk neuroblastoma (NB) with MYCN amplification is a highly metastatic tumor in children. NB presenting with hematogenesis metastasis is one of the most difficult cancers to cure [1, 40]. EMT is an important process that contributes to tumor invasion and dissemination [41]. How MYC control EMT is largely unknown [42]. EMT process requires extensive reorganization of the epigenetic information of the cells. Previous works showed that SNAIL represses transcription of epithelial genes such as E-cadherin, by recruiting repressive chromatin-modifying factors including Polycomb repressive complex 2 and LSD1-CoREST complex [41]. Our findings of targeting NDRG1 expression through LSD1 inhibitors add new insight on how MYCN may control EMT. Thus, LSD1 controls EMT through at least two different mechanisms, as co-factors of SNAIL function and in association with MYCN as a direct epigenetic regulator of NDRG1 expression. Previous work showed that blocking interactions of LSD1 with SNAIL blocks NB cell invasion [43]. The findings reported here add further support to the critical role of LSD1 in EMT and most importantly highlight an additional mechanism through which LSD1 inhibition affects cell migration and invasiveness of NB cancer cells. Clearly multiple signaling pathways cooperate in the initiation and progression of EMT and cooperation between different pathways likely occurs in a synergistic manner and in a cell-type specific fashion.

Therapy for high-risk patients includes differentiating agents. Previous studies showed that NDRG1 expression is regulated by differentiation-related environments [19]. We determined that during RA-mediated *in vitro* differentiation of NB cells the NDRG1 protein increases during time and inversely correlates with LSD1 and MYCN protein expression. Thus, these data address that NDRG1 is a biologically important MYCN/LSD1 target, and it is inversely expressed in relation to MYCN and LSD1 during NB differentiation.

The relative expression levels of NDRG1, LSD1 and MYCN were further analyzed in neuroblastoma patients. Analysis of publicly available expression data of large number of NBs highlighted that high NDRG1 expression correlates with better overall and event-free survival. Interestingly, high levels of LSD1 and NDRG1

expression are mutually exclusive in neuroblastoma tumors and NDRG1 expression levels are significantly lower in MYCN-amplified NB samples. Collectively, these findings support and corroborate the broad significance of our *in vitro* results, and suggest that NDRG1 and LSD1 expressions can be considered as valuable biomarkers to monitor NB development in humans.

In summary, our findings uncover a previously unidentified model in the control of EMT, suggesting that MYCN/LSD1 inhibition de-represses NDRG1 expression, thereby inducing an NDRG1-dependent inhibitory effect on cell migration and invasiveness of neuroblastoma cells. These findings raise the possibility that improved approaches aimed to target the epigenetic control of NDRG1 expression may lead to development of novel strategies to inhibit the invasive potential of neuroblastoma cells.

MATERIALS AND METHODS

Cell culture and treatments

Human HEK 293T, SH-SY5Y and SHEP Tet-21/N cells were cultured in Dulbecco's modified Eagle's Medium (DMEM) supplemented with antibiotics, 10% fetal calf serum. SK-N-BE (2) was cultured in 1:1 mixture DMEM/F-12 containing 10% FBS. All cell lines were incubated at 37°C in humidified atmosphere with 5% CO₂. Tet-21/N cells are cultivated with (Low MYCN) or without (High MYCN) tetracycline (6 days). When indicated, cells were treated with TCP (1mM, Enzo Life Sciences), SP2509 (0,3/0,5/1 μM, Cayman Chemical Company) or 10054-F4 (75 μM, Sigma) for 24 or 48 hrs. To induce differentiation in SK-N-BE (2) cells were exposed to 10 μM all-*trans* Retinoic Acid for 9 days.

LSD1 Knock-Down

100 nM siRNA targeting LSD1 (GE Dharmacon) or scramble were transfected in Tet-21/N cells using a MicroPorator Digital Bio Technology, according to the recently described protocol [6]. Briefly, 2x10⁶ cells were collected by trypsin/EDTA digestion, washed once with calcium and magnesium-free PBS and resuspended in 100μl of resuspension buffer, mixed with siRNA or scramble and electroporated according to the manufacturer's protocol. Transfected cells were seeded in a 100 mm dish in antibiotic-free DMEM supplemented with 10% FBS. The efficiency of siRNA to knockdown LSD1 protein expression was assayed 48h after transfection by western blot.

RNA sequencing

RNA was prepared from Tet-21N cells treated with TCP or with siLSD1 and control untreated cells. RNA-seq libraries (two biological replicas for each sample) were generated using TruSeq RNA Sample Prep Kit v2 (Illumina) according to the manufacturer's recommendation. All the high-throughput sequencing experiments were run on a NexSeq 500 (Illumina) sequencer at the Genomix4life S.R.L., Baronissi, Salerno, Italy, according to standard operating procedures. Raw sequences files (-fastq files) were aligned to the human genome (h19 version), gene-level quantification was performed using R-SEM and UCSC annotation [44]. Subsequently, data were normalized with VOOM method [45] and differential expression evaluated with limma Bioconductor packages. Differential expressed genes were detected applying the following cutoff: log₂ Fold Change ≥ 1 and FDR ≤ 0.1. RNA-seq data were deposited to NCBI GEO and are available under accession number GSE80753.

RNA extraction and qRT-PCR

RNA was extracted from NB cells using EuroGold Trifast (EuroClone). cDNA was generated using Quantitec Reverse Transcription Kit (Qiagen), according to manufacturer's protocol. Quantitative analysis was performed using SYBR Green 2X PCR Master Mix (Applied Biosystem). Each sample was run in triplicate and normalized to the expression of housekeeping beta-glucuronidase (GUSb) gene as previously described [6]. Primers are presented in Supplementary Table S1.

Protein extraction and western blot

Whole-cell extracts were obtained using buffer F (10 mM TrisHCl pH 7.5, 150 mM NaCl, 30 mM Na₄O₇P₂, 50 mM NaF, 5 mM ZnCl₂, 0.1 mM Na₃VO₄, 1% Triton, 0.1mM PMSF). 50 μg of protein extracts were loaded and separated by SDS-PAGE and WB was performed with indicated antibodies. For NDRG1 silencing in Tet-21/N cells, 3 μg/10⁶ cells of shRNA plasmid (Santa Cruz) targeting NDRG1 was used with the protocol described above.

Chromatin immunoprecipitation assay

Chromatin immunoprecipitation assays were performed as recently described [6]. Briefly 1x10⁷ cells were cross-linked using formaldehyde to a final concentration of 1% and reaction was stopped using 0.125M Glycine. Cell pellet was resuspended in Cell Lysis Buffer and after 6000 rpm centrifugation RIPA buffer

were added to perform nuclei lysis. DNA shearing was conducted by sonication using Bioruptor (Diagenode). A small aliquot of sonicated material was put aside and remaining sample immunoprecipitated using 5 micrograms of ChIP-grade antibodies. Rec-sepharose Protein A or G beads (Invitrogen) were used to immobilize immunocomplexes and after RNase-A treatment (37°C 1 hour) reverse cross-linking were performed using Proteinase K (Roche) for 6 hours at 65°C. Immunoprecipitated DNA was purified using Phenol/Chloroform and Ethanol precipitation techniques. The antibodies used are listed in Table S2. The immunoprecipitated DNA was quantified by qPCR with the primer sets described in Table S1.

Migration assays

In migration experiments, 2,5 $\mu\text{g}/10^6$ cells of 3xFLAG-NDRG1 or empty vector were transiently transfected into Tet-21/N by electroporation, by protocol as described previously. For transient transfections of SH-SY5Y, cells cultured on 100 mm dishes were transfected with 3xFLAG-NDRG1 plasmid or empty vector using Lipofectamine 2000 according to manufacturer's protocol. The expression of protein was determined by western blot. For the wound-healing assay, NDRG1-transfected or control cells were plated to confluence in a 12-well plate and scraped with a p200 pipet tip to create a scratch of the cell monolayer; when indicated cells were treated with TCP or SP2509 for an overnight before scratch and during the whole experiment. Cells were then allowed to fill the wounded area for 2 days and images were acquired using a Nikon Eclipse TE 2000-U microscope. Percentage of wound healing was measured as following: $[(\text{empty area at } T_0) - (\text{empty area at 24hrs})] / (\text{empty area at } T_0) \times 100$. For trans-membrane migration assay, cells were NDRG1-transfected or pre-treated with TCP or SP2509 for an overnight, before plating (150000 cells/chamber) in free serum medium in the upper side of chambers (BD Falcon Cell Culture Inserts). In the wells 20% of FBS was used as chemo-attractant. After 24 h, non-migrating cells were scraped-off, whereas migrating cells were stained with a 20% ethanol-1% crystal violet solution for 10', washed thrice with water and counted at least in ten fields with a 10x objective. For each assay three independent experiments were carried out in duplicate.

Co-immunoprecipitation

Co-immunoprecipitation assays were performed using Tet-21/N and HEK 293T cells. 293T cells were transiently co-transfected with 3xFLAG-LSD1, 3xFLAG-MYCN or scramble by the polyethylenimine (PEI 25 K) method. 1 mg of protein extract from Tet-21/N cells or 0,3 mg from HEK 293T cells, treated with TCP, SP2509 or vehicle, were incubated respectively with LSD1 or MYCN

antibody and processed as previously described [6, 46]. Protein interactions were assessed by immunoblotting using the indicated antibodies.

Immunofluorescence

For immunofluorescence assay Tet-21/N were seeded on coverslips and treated as indicated. Cells were then fixed in 4% paraformaldehyde in PBS, permeabilized in 0.1% Triton X-100 in PBS, pre-blocked in 2% BSA-3%NS-PBS for 30 min at room temperature, and then incubated for 1 h at 37° C with mouse anti- β -catenin. Primary antibodies were detected by incubation with Cy3-conjugated anti-mouse. Images were acquired using a Nikon Eclipse TE 2000-U microscope.

Gene expression data for survival analysis and association with neuroblastoma stages

Normalized gene expression data from RNA sequencing of 498 tumors were downloaded from "R2: Genomics Analysis and Visualization Platform" (GEO ID: GSE62564). To test association of gene expression levels with overall survival and event free survival, individual gene expression profiles were dichotomized by median split into 'high' or 'low' expression groups, and Kaplan-Meier survival curves were plotted for each group. Long rank test was used to evaluate the significant difference between the two groups. Another set of gene expression data of 64 tumors (GEO ID: GSE12460) including 50 NB, 6 ganglioneuroblastoma and 3 ganglioneuroma was downloaded. Mann-Whitney test was used to test the significant different gene expression among groups. The correlation between the gene expression between NDRG1 and KDM1A was evaluated by Pearson correlation in 64 NBs. The gene expression data for Low and High MYCN expression (493 samples) were generate by customized 4x44K oligonucleotide microarrays produced by Agilent Technologies and analyzed as previously reported [47].

Statistical analysis

All experiments were repeated two or three times. Graphs representing data express mean \pm SD. Statistical significance was obtained by unpaired, two-tailed Student *t* test. $P < 0,05$ was considered statistically significant.

ACKNOWLEDGMENTS

We thank Drs. Enrico Vittoria Avvedimento and Antonio Feliciello for their critical reading of the manuscript. We thank Dr. W. Wick for the NDRG1 expression vector.

CONFLICT OF INTEREST

The authors declare no conflict of interest.

GRANT SUPPORT

This work was supported by following grants: AIRC (IG13173 to B.M.), Epigenomics Flagship Project—EPIGEN, C.N.R. and from Grant MOVIE of the Rete delle Biotecnologie in Campania.

Editorial note

This paper has been accepted based in part on peer-review conducted by another journal and the authors' response and revisions as well as expedited peer-review in *Oncotarget*.

REFERENCES

1. Huang M, Weiss WA. Neuroblastoma and MYCN. *Cold Spring Harbor perspectives in medicine* 2013;3:a014415.
2. Irwin MS, Park JR. Neuroblastoma: paradigm for precision medicine. *Pediatric Clinics of North America* 2015;62:225-256
3. Dang CV. MYC on the path to cancer. *Cell* 2012;149:22–35.
4. Maris JM, Hogarty MD, Bagatell R, Cohn SL. Neuroblastoma. *Lancet* 2007;369:2106-2120
5. Schwab M. MYCN in neuronal tumours. *Cancer letters* 2004;204:179–187.
6. Amente S, Milazzo G, Sorrentino MC, Ambrosio S, Di Palo G, Lania L, Perini G, Majello B. Lysine-specific demethylase (LSD1/KDM1A) and MYCN cooperatively repress tumor suppressor genes in neuroblastoma. *Oncotarget* 2015;6:14572-14783. doi: 10.18632/oncotarget.3990.
7. Shi Y, Lan F, Matson C, Mulligan P, Whetstone JR, Cole PA, Casero RA, Shi Y. Histone demethylation mediated by the nuclear amine oxidase homolog LSD1. *Cell* 2004;119(7):941-53.
8. Lan F, Nottke AC, Shi Y. Mechanisms involved in the regulation of histone lysine demethylases. *Current opinion in cell biology* 2008;20:316-325.
9. Nicholson TB, Chen T. LSD1 demethylates histone and non-histone proteins. *Epigenetics* 2009;4:129-132.
10. Kahl P, Gullotti L, Heukamp LC, Wolf S, Friedrichs N, Vorreuther R, Solleder G, Bastian PJ, Ellinger J, Metzger E, Schüle R, Buettner R. Androgen receptor coactivators lysine-specific histone demethylase 1 and four and a half LIM domain protein 2 predict risk of prostate cancer recurrence. *Cancer Research* 2006;66:11341-11347.
11. Metzger E, Wissmann M, Yin N, Muller JM, Schneider R, Peters AH, Gunther T, Buettner R, Schule R. LSD1 demethylates repressive histone marks to promote androgen-receptor-dependent transcription. *Nature* 2005;437:436-439.
12. Wang J, Scully K, Zhu X, Cai L, Zhang J, Prefontaine GG, Kronen A, Ohgi KA, Zhu P, Garcia-Bassets I, Liu F, Taylor H, Lozach J, et al. Opposing LSD1 complexes function in developmental gene activation and repression programmes. *Nature* 2007;446:882-887.
13. Amente S, Lania L, Majello B. The histone LSD1 demethylase in stemness and cancer transcription programs. *Biochimica et biophysica acta* 2013;1829:981-986.
14. Schulte JH, Lim S, Schramm A, Friedrichs N, Koster J, Versteeg R, Ora I, Pajtler K, Klein-Hitpass L, Kuhfittig-Kulle S, Metzger E, Schüle R, et al. Lysine-specific demethylase 1 is strongly expressed in poorly differentiated neuroblastoma: implications for therapy. *Cancer Research* 2009;69:2065-2071.
15. Shimono A, Okuda T, Kondoh H. N-myc-dependent repression of *ndr1*, a gene identified by direct subtraction of whole mouse embryo cDNAs between wild type and N-myc mutant. *Mechanisms of development* 1999;83:39-52.
16. Zhang J, Chen S, Zhang W, Zhang J, Liu X, Shi H, Che H, Wang W, Li F, Yao L. Human differentiation-related gene *NDRG1* is a Myc downstream-regulated gene that is repressed by Myc on the core promoter region. *Gene* 2008;417:5-12.
17. Sun J, Zhang D, Bae DH, Sahni S, Jansson P, Zheng Y, Zhao Q, Yue F, Zheng M, Kovacevic Z, Richardson DR. Metastasis suppressor, *NDRG1*, mediates its activity through signaling pathways and molecular motors. *Carcinogenesis* 2013;34:1943-54.
18. Chen Z, Zhang D, Yue F, Zheng M, Kovacevic Z, Richardson DR. The iron chelators *Dp44mT* and *DFO* inhibit TGF-beta-induced epithelial-mesenchymal transition via up-regulation of N-Myc downstream-regulated gene 1 (*NDRG1*). *The Journal of biological chemistry* 2012;287:17016-17028.
19. Bae DH, Jansson PJ, Huang ML, Kovacevic Z, Kalinowski D, Lee CS, Sahni S, Richardson DR. The role of *NDRG1* in the pathology and potential treatment of human cancers. *Journal of clinical pathology* 2013;66:911-917.
20. Weiler M, Blaes J, Pusch S, Sahm F, Czabanka M, Luger S, Bunse L, Solecki G, Eichwald V, Jugold M, Hodecker S, Osswald M, Meisner C. et al. mTOR target *NDRG1* confers *MGMT*-dependent resistance to alkylating chemotherapy. *Proceedings of the National Academy of Sciences of the United States of America* 2014;111:409-414.
21. Jin R, Liu W, Menezes S, Yue F, Zheng M, Kovacevic Z, Richardson DR. The metastasis suppressor *NDRG1* modulates the phosphorylation and nuclear translocation of beta-catenin through mechanisms involving *FRAT1* and *PAK4*. *Journal of cell science* 2014;127:3116-3130.
22. Sahni S, Krishan S, Richardson DR. *NDRG1* as a molecular

- target to inhibit the epithelial-mesenchymal transition: the case for developing inhibitors of metastasis. *Future medicinal chemistry* 2014;6:1241-124.
23. Lin Y, Wu Y, Li J, Dong C, Ye X, Chi YI, Evers BM, Zhou BP. The SNAG domain of Snail1 functions as a molecular hook for recruiting lysine-specific demethylase 1. *The EMBO journal* 2010;29:1803-18016.
 24. Lin T, Ponn A, Hu X, Law BK, Lu J. Requirement of the histone demethylase LSD1 in Snail-mediated transcriptional repression during epithelial-mesenchymal transition. *Oncogene* 2010;29:4896-4904.
 25. Shimono A, Okuda T, Kondoh H. N-myc-dependent repression of ndr1, a gene identified by direct subtraction of whole mouse embryo cDNAs between wild type and N-myc mutant. *Mechanisms of development* 1999;83:39-52.
 26. Zhang J, Chen S, Zhang W, Zhang J, Liu X, Shi H, Che H, Wang W, Li F, Yao L. Human differentiation-related gene NDRG1 is a Myc downstream-regulated gene that is repressed by Myc on the core promoter region. *Gene* 2008;417:5-12.
 27. Fang BA, Kovacevic Z, Park KC, Kalinowski DS, Jansson PJ, Lane DJ, Sahni S, Richardson DR. Molecular functions of the iron-regulated metastasis suppressor, NDRG1, and its potential as a molecular target for cancer therapy. *Biochimica et biophysica acta* 2014;1845:1-19.
 28. Guan RJ, Ford HL, Fu Y, Li Y, Shaw LM, Pardee AB. Drg-1 as a differentiation-related, putative metastatic suppressor gene in human colon cancer. *Cancer Research* 2000;60:749-755.
 29. Bandyopadhyay S, Pai SK, Gross SC, Hirota S, Hosobe S, Miura K, Saito K, Commes T, Hayashi S, Watabe M, Watabe K. The Drg-1 gene suppresses tumor metastasis in prostate cancer. *Cancer Research* 2003;63:1731-1736.
 30. Banz VM, Medová M, Keogh A, Furer C, Zimmer Y, Candinas D, Stroka D. Hsp90 transcriptionally and post-translationally regulates the expression of NDRG1 and maintains the stability of its modifying kinase GSK3beta. *Biochimica et biophysica acta* 2009;1793:1597-1603.
 31. Kovacevic Z, Sivagurunathan S, Mangs H, Chikhani S, Zhang D, Richardson DR. The metastasis suppressor, N-myc downstream regulated gene 1 (NDRG1), upregulates p21 via p53-independent mechanisms. *Carcinogenesis* 2011;32:732-740.
 32. Murray JT, Campbell DG, Morrice N, Auld GC, Shpiro N, Marquez R, Peggie M, Bain J, Bloomberg GB, Grahammer F, Lang F, Wulff P, Kuhl D, et al. Exploitation of KESTREL to identify NDRG family members as physiological substrates for SGK1 and GSK3. *Biochemical Journal* 2004 Dec 15; 384: 477-488.
 33. Zheng Y, Ma J, Wang Z, Li J, Jiang B, Zhou W, Shi X, Wang X, Zhao W, Liu HM. A systematic review of histone lysine-specific demethylase 1 and its inhibitors. *Medicinal Research Reviews* 2015;35:1032-1071.
 34. Fiskus W, Sharma S, Shah B, Portier BP, Devaraj SG, Liu K, Iyer SP, Bearss D, Bhalla KN. Highly effective combination of LSD1 (KDM1A) antagonist and pan-histone deacetylase inhibitor against human AML cells. *Leukemia* 2014;28:2155-2164.
 35. Stein S, Thomas EK, Herzog B, Westfall MD, Rocheleau JV, Jackson RS 2nd, Wang M, Liang P. NDRG1 is necessary for p53-dependent apoptosis. *The Journal of Biological Chemistry* 2004;279:48930-48940.
 36. Liu W, Xing F, Iizumi-Gairani M, Okuda H, Watabe M, Pai SK, Pandey PR, Hirota S, Kobayashi A, Mo YY, Fukuda K, Li Y, Watabe K. N-myc downstream regulated gene 1 modulates Wnt- β -catenin signalling and pleiotropically suppresses metastasis. *EMBO Molecular Medicine* 2012;4:93-108.
 37. Huang Z, Li S, Song W, Li X, Li Q, Zhang Z, Han Y, Zhang X, Miao S, Du R, Wang L. Lysine-specific demethylase 1 (LSD1/KDM1A) contributes to colorectal tumorigenesis via activation of the Wnt/ β -catenin pathway by down-regulating Dickkopf-1 (DKK1). *PLoS One* 2013;8:e70077
 38. Han X, Gui B, Xiong C, Zhao L, Liang J, Sun L1, Yang X1, Yu W1, Si W1, Yan R1, Yi X1, Zhang D1, Li W1, et al. Destabilizing LSD1 by Jade-2 promotes neurogenesis: an antibraking system in neural development. *Molecular Cell* 2014;55:482-494.
 39. Matsushita K, Uchida K, Saigusa S, Ide S, Hashimoto K, Koike Y, Otake K, Inoue M, Tanaka K, Kusunoki M. Low NDRG1 mRNA expression predicts a poor prognosis in neuroblastoma patients. *Pediatric Surgery International* 2013;29:363-368.
 40. Majello B, Perini G. Myc proteins in cell biology and pathology. *Biochimica et biophysica acta* 2015;1849:467-468.
 41. Lamouille S, Xu J, Derynck R. Molecular mechanisms of epithelial-mesenchymal transition. *Nature reviews Molecular cell biology* 2014;15:178-196.
 42. Wolfer A, Ramaswamy S. MYC and metastasis. *Cancer Research* 2011;71:2034-2037.
 43. Ferrari-Amorotti G, Fragliasso V, Esteki R, Prudente Z, Soliera AR, Cattelani S, Manzotti G, Grisendi G, Dominici M, Pieraccioli M, Raschella G, Chiodoni C, Colombo MP, et al. Inhibiting interactions of lysine demethylase LSD1 with snail/slugs blocks cancer cell invasion. *Cancer Research* 2013;73:235-245.
 44. Li B, Fillmore N, Bai Y, Collins M, Thomson JA, Stewart R, Dewey CN. Evaluation of de novo transcriptome assemblies from RNA-Seq data. *Genome biology* 2014;15:553.
 45. Law CW, Chen Y, Shi W, Smyth GK. voom: Precision weights unlock linear model analysis tools for RNA-seq read counts. *Genome biology* 2014;15:R29.
 46. Amente S, Bertoni A, Morano A, Lania L, Avvedimento EV, Majello B. LSD1-mediated demethylation of histone H3 lysine 4 triggers Myc-induced transcription. *Oncogene*

47. Lasorsa VA, Formicola D, Pignataro P, Cimmino F, Calabrese FM, Mora J, Esposito MR, Pantile M, Zanon C, De Mariano M, Longo L, Hogarty MD, de Torres C, et al. Exome and deep sequencing of clinically aggressive neuroblastoma reveal somatic mutations that affect key pathways involved in cancer progression. *Oncotarget* 2016, doi: 10.18632/oncotarget.8187.

CHAPTER 5

**LYSINE-SPECIFIC DEMETHYLASE LSD1 REGULATES AUTOPHAGY IN
NEUROBLASTOMA THROUGH SESN2-DEPENDENT PATHWAY**

Susanna Ambrosio ^a, Carmen D. Saccà ^a, Stefano Amente ^b, Simona Paladino ^{b,c}, Luigi Lania ^b and Barbara Majello ^a

^a Department of Biology, University of Naples 'Federico II', Naples, Italy.

^b Department of Molecular Medicine and Medical Biotechnologies, University of Naples, 'Federico II', Naples, Italy.

^c Ceinge Biotechnologie Avanzate s.c.a.r.l., Naples, Italy.

Submitted Oncogene. 2017, Mar

**Lysine-specific demethylase LSD1 regulates autophagy in Neuroblastoma through
SESN2-dependent pathway**

Susanna Ambrosio¹, Carmen D. Saccà¹, Stefano Amente², Simona Paladino^{2,3}, Luigi Lania² and
Barbara Majello¹

¹ Department of Biology, University of Naples 'Federico II', Naples, Italy.

² Department of Molecular Medicine and Medical Biotechnologies, University of Naples, 'Federico II', Naples, Italy.

³ Ceinge Biotechnologie Avanzate s.c.a.r.l., Naples, Italy.

To whom correspondence should be addressed:

Barbara Majello
Professor of Genetics
Department of Biology
University of Naples 'Federico II'
via Cinthia, Edificio 7
80126, Naples ITALY
tel +39-081679061
Email: majello@unina.it

ABSTRACT

Autophagy is a physiological process, important for recycling of macromolecules and maintenance of cellular homeostasis. Defective autophagy is associated with tumorigenesis and plays a causative role in chemotherapy resistance in leukemia and in solid cancers. Here, we report that autophagy is regulated by the Lysine-specific demethylase LSD1/KDM1A, an epigenetic marker whose overexpression is a feature of malignant neoplasia with an instrumental role in cancer development. In the present study we determine that two different LSD1 inhibitors (TCP and SP2509) as well as selective ablation of LSD1 expression, promote autophagy in Neuroblastoma cells. At mechanistic level we show that LSD1 binds to the promoter region of Sestrin2 (SESN2), a critical regulator of mTORC1 activity. Pharmacological inhibition of LSD1 triggers SESN2 expression that hampers mTORC1 activity leading to enhanced autophagy. SESN2 overexpression suffices to promote autophagy in Neuroblastoma cells while loss of SESN2 expression reduces autophagy induced by LSD1-inhibition. Our findings elucidate a mechanism whereby LSD1 control autophagy in Neuroblastoma cells through transcription regulation of SESN2 expression and we suggest that pharmacological targeting of LSD1 may have effective therapeutic relevance in the control of autophagy in Neuroblastoma.

INTRODUCTION

Cancerous cells must deal with effective mechanisms of cell death, thereby reducing activation of defense pathways in response to oncogenic insults.^{1, 2} The induction of apoptosis is the major route of cell death yet multiple cellular processes, including autophagy, antagonize it.

Autophagy is a conserved intracellular process in which cytoplasmic components are degraded within lysosomes playing a central role in cell metabolism and homeostasis. There are different types of autophagy: micro-autophagy, selective autophagy, macro-autophagy and chaperone-mediated autophagy.³ Macro-autophagy is the main autophagic pathway and consists in the formation of double-membrane autophagosomes that sequester cellular components and then fuse with lysosomes for degradation and recycling of macromolecules and organelles. Autophagy normally operates at low, basal levels in cells but can be strongly induced by cellular stress. Defective autophagy is associated with human pathologies such as bacteria and virus infections, neurodegenerative diseases and cancer.⁴⁻⁶

Autophagy plays dual roles in cancer; it can function as either a tumor suppressor, by preventing the accumulation of damaged proteins and organelles, or a survival pathway, by suppressing apoptosis and promoting the growth of tumors.⁷⁻⁹ Recent studies showed that autophagy plays a causative role in chemotherapy resistance in leukemia¹⁰ and in solid cancers.^{7, 10} Nonetheless the molecular mechanisms underlying the effects of autophagy on tumorigenesis must be further elucidated.

Mammalian Target of Rapamycin Complex 1 (mTORC1) is the major regulator of autophagy. In the presence of nutrients, mTORC1 is activated, resulting in inhibition of the Ulk1 complex and repression of autophagy.¹¹ Following nutrient deprivation, mTORC1 is inhibited, and Ulk1 complexes can lead autophagosome formation. Given its pivotal role in autophagy regulation, mTORC1 is the main target for drugs development to modulate the autophagic pathway.^{12, 13}

Recently, several studies have demonstrated that autophagy is regulated by epigenetic alterations, including histone methylation and acetylation.¹⁴⁻¹⁶ The precise mechanisms through which cancer-associated epigenetic alterations modulate autophagy have not yet been elucidated. An epigenetic enzyme that has been target of drug discovery is the lysine-specific demethylase 1, LSD1. LSD1 (also known as KDM1A and AOF2) is an amine oxidase that catalyzes lysine demethylation in a flavin adenine dinucleotide (FAD)-dependent oxidative reaction¹⁷ and removes mono- and dimethyl groups from lysine K4 and, in specific circumstances, K9 on histone H3.¹⁷⁻¹⁹ More recently, it has been shown that the neuron-specific isoform LSD1n has a new substrate specificity, targeting histone H4 Lys 20.²⁰ Finally, LSD1 can also targets non-histone proteins such as p53, E2F1, and DNMT.²¹⁻²³ LSD1 has been demonstrated to play important roles in many important aspects of cell biology, such as cell proliferation, cell mobility and differentiation.²⁴⁻²⁶ Most importantly, LSD1 is overexpressed in a variety of cancers and tends to correlate with more aggressive cancers with poor prognosis. There is a large body of evidence that LSD1 is involved in maintaining the

undifferentiated, malignant phenotype of Neuroblastoma cells and that its overexpression correlates with aggressive disease, poor differentiation and infaust outcome.^{24, 27}

In the present study, we define a novel role of the epigenetic regulator LSD1 in the modulation of autophagy. We found that selective ablation of LSD1, or pharmacological inactivation of its catalytic function, inhibits mTORC1 activity enabling enhanced autophagy. Mechanistically, we found that LSD1 binds to the promoter region of Sestrin2 (SESN2) and represses its expression. LSD1 inhibition triggers SESN2 expression that hampers mTORC1 activity leading to Transcription Factor EB (TFEB) nuclear translocation driving the expression of the Coordinated Lysosomal Expression and Regulation (CLEAR) regulatory network. Taken together, our findings indicate that LSD1 regulates autophagy in Neuroblastoma cells via transcriptional regulation of SESN2 that serves as key positive regulator of mTORC1–dependent autophagy pathway.

RESULTS

LSD1 inhibition represses mTORC1 pathway

LSD1 is highly expressed in undifferentiated Neuroblastomas and its expression correlates with adverse outcome, however, the molecular mechanism underlying LSD1 effects is largely unknown. We initially undertook an unbiased approach to uncover how cells respond to the loss of LSD1 function looking at signaling alterations caused by treatment with tranylcypromine (TCP), a potent inhibitor of LSD1 in Tet-21/N Neuroblastoma cells. PathScan array was used to determine pathways involved in TCP response. In this assay mTORC1 pathway was the most responsive, evidenced by ribosomal protein S6 (Ser235/236), p70S6 Kinase (Thr389) and PRAS40 (Thr246) phosphorylation reduction (Fig. 1a). To verify PathScan array results, we performed Western blot analysis of mTORC1 downstream substrates, p70S6K and rpS6. Tet-21/N cells were also treated with SP2509, a reversible inhibitor of LSD1 that, differently from TCP does not target the catalytic activity of the enzyme, but attenuates the binding of LSD1 to CoREST.^{28,25} In addition, to address the specific role of LSD1 in mTORC1 activity, we inhibited LSD1 by siRNA-targeted knockdown and measured expression of mTORC1 downstream targets. Protein extracts were prepared at the indicated times and probed with antibodies recognizing phosphorylated and total protein forms of mTORC1 substrates. In agreement with the array data, phosphorylation levels of p70S6K, and consequently of its target rpS6, were down regulated by either TCP or SP2509 treatment as well as in LSD1 KD cells (Fig. 1b, c). In addition, similar results were observed in SH-SY5Y Neuroblastoma cells (Fig. 1d). Collectively these findings demonstrated that LSD1 inhibition downregulates mTORC1 signaling.

mTORC1 is known as a critical regulator of autophagy. In response to nutrient deprivation, mTORC1 is inactivated and dissociates from the ULK complex, inducing autophagy activation. In addition mTORC1 has been shown to control autophagy through the functional regulation of the Transcription Factor EB (TFEB), a master regulator of lysosomal and autophagic functions. Active mTORC1 phosphorylates and sequesters TFEB to the cytoplasm; on the contrary, mTORC1 inactivation leads to de-phosphorylation of TFEB, which translocates into the nucleus and drives the expression of lysosomal and autophagy genes that are part of the Coordinated Lysosomal Expression and Regulation (CLEAR) regulatory network.^{12, 29}

We sought to investigate the impact of LSD1 inhibition on TFEB subcellular localization. Tet-21/N and SH-SY5Y cells were treated with TCP for the indicated times and analyzed by immunofluorescence using a TFEB antibody. In untreated cells TFEB is localized mainly in the cytoplasm. Consistently with mTORC1 repression, pharmacological inhibition of LSD1 leads to a significant increase of TFEB nuclear levels along with a decreased cytosolic localization (Fig. 2a and b). This finding was further confirmed using specific siRNA against LSD1 (Fig. 2c).

Because SP2509 is a reversible inhibitor of LSD1, we used this drug to test whether TFEB nuclear shuttling was directly dependent upon LSD1 inhibition. We monitored whether nuclear shuttling of

TFEB was reversed in time after SP2509 wash out. Tet-21/N cells were treated with SP2509 for 48 hrs and then cells were washed and cultivated in fresh medium for additional 24 and 48 hrs after drug removal. The immunofluorescence results in Figure 2d show that TFEB nuclear localization decreases in a time dependent manner following SP2509 wash out, demonstrating that TFEB nuclear localization is directly dependent upon LSD1 inhibition.

LSD1 depletion induces autophagy

Autophagy begins with the sequestration of cytosolic proteins in a double membrane structure called autophagosome. Following fusion with a lysosome it becomes an autophagolysosomes, then lysosomal hydrolases degrade the content of the phagosome that is released in the cytosol for the recycling of macromolecules. During autophagosome formation, the cytosolic form of the microtubule-associated protein 1A/1B-light chain 3 (LC3-I) is conjugated to phosphatidylethanolamine to form lipidated-LC3 (LC3-II), which becomes associated with autophagosomal membranes. Tet-21/N cells were treated with TCP (Fig. 3a) or siLSD1 transfected (Fig. 3b) and then processed for Western blot analysis to monitor the conversion from LC3-I to lower-migrating form LC3-II, as well-established marker of autophagosomes formation.³⁰ TCP treatment induced LC3-II form accumulation over time compared with control cells (Fig. 3a). Moreover, LSD1-KD also increases LC3-II form level in a dose dependent manner (Fig. 3b). Similar findings were observed in SH-SY5Y cells (Supplementary Figure 1). Because LC3-II increment might also be interpreted as autophagosome accumulation due to the block of autophagosome-lysosome fusion, we evaluated the autophagic flux following LSD1 inhibition using a GFP-mRFP-tandem tagged LC3. Indeed, by taking advantage of the properties of these two fluorescent proteins (GFP signal is quenched inside the acidic lysosomal lumen, but not mRFP) we can discriminate between autophagic compartments before and after fusion with lysosomes.^{30, 31}

Tet-21N cells were transiently transfected with the GFP-mRFP-LC3 tandem construct and treated with TCP alone or in combination with NH₄Cl to block autophagolysosomal degradation by preventing its acidification. In untreated cells GFP and mRFP signals appear mainly diffused in the cytosol and with few puncta (Fig. 3c). Conversely, the number of green and red puncta was higher following TCP treatment, indicating that LSD1 inhibition enhanced the autophagic flux (Fig. 3c, upper graph). Moreover, a significant increase of autolysosomes (mRFP positive, but GFP-negative puncta) was observed upon TCP treatment (Fig. 3c, lower graph), indicating that the autophagosome maturation is occurring. Consistently, upon combined treatment of TCP and NH₄Cl green dots were augmented as expected by the fact that NH₄Cl, increasing the intralysosomal pH, prevents GFP quenching (Fig. 3c).

Taken together, these results clearly indicate that pharmacological inhibition of LSD1 activity triggers a functional autophagic flux induction, as demonstrated by the nuclear localization of autophagy master regulator TEFB and the mature autophagolysosomes formation.

LSD1 inhibition promotes autophagy by increasing SESN2 expression

To understand the mechanisms by which LSD1 inhibition induces autophagy, we analyzed data from our recent published RNA-seq from Tet-21/N cells treated with TCP or siLSD1.²⁵ Among the common up-regulated genes we identify Sestrin2 (SESN2) as a LSD1 repressed target gene. SESN2 is a member of an evolutionarily conserved stress-inducible Sestrin gene family and it has been shown that SESN2 directly inhibits mTORC1 activity via GATOR2 with a consequent inhibition of mTORC1 recruitment to the lysosomal membrane.^{32, 33} Through these functions, SESN2 serves as key positive regulator of the autophagic pathway. To validate RNA-seq data we inhibited LSD1 in Tet-21/N cells with TCP or siRNA against LSD1 and assayed SESN2 mRNA and protein expression. Accordingly, with our RNA-seq data, we found that LSD1 inhibition or silencing enhances SESN2 expression (Fig. 4a).

Next, we sought to determine whether LSD1 is directly involved in control of SESN2 gene expression. Public available ChIP-seq LSD1 data from SH-SY5Y cells as well as from mouse ES cells indicate a putative LSD1 binding to the promoter region of SESN2 (Supplementary Figure 2). We then carried out Chromatin IP assays to determine binding of LSD1 to SESN2 chromatin. LSD1 binding was analyzed in Tet-21/N cells treated with TCP or silenced for LSD1 expression. Chromatin isolated from Tet-21/N cells was immunoprecipitated with anti-LSD1 antibody and analyzed by qPCR, using primers corresponding to the 5' regulatory regions surrounding the transcription start site (TSS) of the SESN2 gene. As shown in Fig. 4b, LSD1 is recruited selectively at TSS of the SESN2 gene but not at distal sites (-10kb), indicating that LSD1 binds to the SESN2 promoter.

To better understand how LSD1 can affect chromatin organization at SESN2 promoter, we analyzed four different histone modifications, H3 pan-acetyl (H3Ac), H3K27Me3, H3K4Me2 and H3K9Me2 around TSS promoter region. Fig. 4c shows that both LSD1 silencing (siLSD1) and inhibition by TCP determine a significant increase in H3 acetylation. As a marker of transcriptional repression we analyzed Lysine 27 tri-methylation of Histone H3. Data presented in Fig. 4d demonstrate that both LSD1 silencing or its inhibition (TCP) determine an almost 2,5 fold decrease of the marker. Chromatin-IP assays were also performed on di-methylated Lysine 4 of histone H3 (Fig. 4e) and we found a significant increase of H3K4me2 at SESN2 TSS following LSD1 inhibition. Conversely, both inhibition and repression of LSD1 do not affect H3K9Me2 signature at TSS level of SESN2 (Fig. 4f). These findings highlight the critical role of LSD1 in the transcriptional regulation of SESN2 gene through direct binding to SESN2 promoter.

It has been recently shown that LSD1-depletion, synergistically with UBE4B inhibition, increases proteasomal and autophagy clearance activating the p53-mediated transcriptional program.³⁴ TP53/p53 is involved in the regulation of autophagy through two distinct mechanisms, according to its sub-cellular localization: cytoplasmic p53 inhibits autophagy through the inhibition

of AMPK and the subsequent mTOR activation; nuclear p53 induces the transcription of pro-autophagic genes, including SESN2.³⁵⁻³⁷ To verify that SESN2 up-regulation mediated by LSD1 inhibition occurs in a p53-independent manner, we employed SK-N-BE (2) neuroblastoma cell line, which expresses a non-functional p53.³⁸ Cell extracts from SK-N-BE (2) cells treated with TCP, SP2509 or vehicle were processed and assayed for SESN2 expression. As shown in Figure 5a, both inhibitors induce significant increase of SESN2 protein levels, together with a strong induction of LC3I/LC3II conversion. Furthermore, we found a SP2509 dose-dependent reduction in phosphorylation of mTORC1 targets, S6p70K and rpS6, confirming that LSD1-inhibition specifically impairs mTORC1 activity (Fig. 5b). These findings strongly suggest that p53 function was not essential for SESN2 transcriptional activation and mTORC1 inhibition triggered by pharmacological LSD1 depletion.

SESN2 is required for autophagy induced by LSD1 inhibition

The findings reported above demonstrated that LSD1 binds and represses SESN2 gene expression; thus, LSD1 inhibition triggers SESN2 expression. Because SESN2 serves as important regulator of mTORC1 activity, we hypothesized that its up-regulation may have a causative role in LSD1-mediated mTORC1 activity modulation and autophagy induction.

To substantiate the relationship between SESN2 and autophagy induction following LSD1 inhibition, we ectopically overexpressed SESN2 in SH-SY5Y cells, and assessed the effect of increased expression of SESN2 on autophagy. We found that overexpression of SESN2 reduced rpS6 phosphorylation, along with a concomitant increase of TFEB nuclear localization. These findings provide functional evidences that enhanced expression of SESN2 induces autophagy through mTORC1 inhibition and recapitulates the effects of TCP treatment in neuroblastoma cells (Fig. 6a and b). To further define the role of SESN2 in autophagy induced by LSD1 inhibition, we performed SESN2 knockdown experiments, using a specific siRNA in SH-SY5Y cells, and investigated the functional consequences on LSD1 inhibition in SESN2 silenced cells. Lacks of appreciable changes in phosphorylation level of mTORC1 downstream targets were seen in siRNA-SESN2 cells (Fig. 6c). In contrast, reduction of phosphorylation levels of p70S6K and rpS6 induced by TCP treatment is significantly weakened in SESN2 silenced cells; these data suggest that TCP requires SESN2 expression to decrease mTORC1 activity. Moreover, in SESN2 knockdown cells we found a reduced nuclear translocation of TEFB following TCP treatment (Fig. 6d), indicating that SESN2 knockdown prevents the LSD1 inhibition-mediated autophagy. Taken together, these results identified SESN2 as a key player in the autophagy activation mediated by LSD1 inhibition.

DISCUSSION

LSD1 is overexpressed in several types of cancers and its enhanced expression correlates with more aggressive cancers and poor prognosis. LSD1 is implicated in several biologic processes, such as cell proliferation, epithelial-mesenchymal transition, stem cell pluripotency and differentiation.^{24-27, 39} However, its involvement in autophagy regulation is still poorly characterized. Here we show that pharmacological and genetic inhibition of LSD1 induces autophagy via the mTORC1-dependent pathway.

The present work highlights a critical role of LSD1 in promoting autophagy in neuroblastoma cells; we provide for the first time evidences supporting the role of LSD1 as epigenetic regulator of autophagic pathway through the modulation of SESN2 expression.

We demonstrated that LSD1 binds and represses the SESN2 gene; alteration of chromatin structures following LSD1 inhibition leads to the de-repression of SESN2 gene, which resulted in a decreased mTORC1 activity. Thus, LSD1 inhibition triggers autophagy, as demonstrated by mTORC1 inhibition, nuclear translocation of TFEB, accumulation of LC3-II and finally the formation of autophagosomes, suggesting a direct link between LSD1-specific transcriptional regulation, mTORC1 cascade and autophagy.

Recent works highlight the involvement of LSD1 in the autophagic machinery. Indeed, in prostate⁴⁰ and ovarian cancer cells⁴¹ LSD1 inhibition triggers LC3-II accumulation and autophagosomes formation, however the molecular mechanism underlying these effects was not described.

Here, we identify SESN2 as an LSD1 repressed target gene involved in mTORC1 pathway control. We found that SESN2 promoter is directly bound and repressed by LSD1; pharmacological inhibition of LSD1 triggers a structural modeling in the chromatin surrounding the TSS of SESN2 gene, leading transcriptional activation of SESN2 expression. Moreover, we demonstrated that SESN2 enhanced expression suffices to promote autophagy in Neuroblastoma cells and SESN2 silencing attenuates mTORC1 suppression and autophagy induction by LSD1 inhibition, providing evidence that SESN2 has a critical role in the autophagy activation mediated by LSD1 depletion. SESN2 is a member of the sestrin family of PA26-related proteins, which plays an important role in regulating the cellular response to oxidative stress. TP53/p53 is the master transcriptional regulator of SESN2 under DNA damage and oxidative stress.^{37, 42} Interestingly, it has been recently shown that LSD1-depletion, synergistically with UBE4B inhibition, increases proteasomal and autophagic clearance activating the p53-mediated transcriptional program.³⁴ We find that depletion of LSD1 induces activation of SESN2 expression in SK-N-BE (2) cell line, which express non-functional p53. Thus, LSD1 appears to regulate transcription of SESN2 in both p53-dependent and p53-independent ways.

We recently reported that the MYCN/LSD1 complex inhibits the transcription of the molecular chaperone Clusterin³⁹, which is involved in the autophagic process through the stabilization of the LC3-Atg3 heterodimer, increasing the autophagosome biogenesis and autophagy progression⁴³;

we suggest that LSD1 orchestrates a broad-spectrum regulation of autophagic pathway via transcriptional regulation of several autophagy-related genes.

Autophagy is a catabolic process that, at basal levels, represents the major mechanism for the turnover of cytoplasm components and selective removal of unfolded proteins and damaged organelles. However, autophagy could be activated in response to several stimuli such as oxidative and nutrient stresses and the mTOR-pathway is the main regulator.^{12, 35} Recent studies suggest that the mTORC-pathway may be associated with cancer-related epigenetic alterations^{1, 44, 45}, unveiling a key role of the epigenetic network in the autophagy control. HDACi inhibitors have been shown to induce autophagy via FOXO1-dependent pathways⁴⁶; the methyltransferase EZH2 has been demonstrated to repress several negative regulators of the mTOR pathway and inhibits autophagy.⁴⁷ However, epigenetic role in autophagy regulation and its association with tumorigenesis continues to be uncovered.

The relationship between autophagy and cancer remains controversial. Autophagy seems to have a dual effect in cancer, depending on stage and cell type, and it could act as tumor suppressor or driver of cancer progression.^{7, 9} Some tumors are sensitive to hyper-activation of autophagy; in other circumstances, inhibition of mTORC1 increases cell survival and prevents apoptosis, inducing chemoresistance.⁴⁸ Although relationship between autophagy and tumor progression is disputed, during early stages of carcinogenesis autophagy seems to suppress tumor initiation and cancer development is often associated with defective autophagy.^{7, 9} We cannot exclude that LSD1 overexpression may contribute to tumor initiation by suppressing the expression of key regulators of autophagy induction, although further studies are required to clarify this issue.

In conclusion, data reported here establish the critical role of LSD1 in autophagy and indicate that, in neuroblastoma cells, LSD1 knockdown induces autophagy through the SESN2-mTORC1 pathway. Our results strongly support the concept that LSD1 dependent epigenetic alterations may influence the expression of autophagy-related-genes and provide a novel link among epigenetic regulation, mTOR pathway, and tumorigenesis.

MATERIALS AND METHODS

Cell culture and treatments

SH-SY5Y and SHEP Tet-21/N cells were cultured in Dulbecco's modified Eagle's Medium (DMEM) supplemented with antibiotics, 10% fetal calf serum. SK-N-BE (2) was cultured in 1:1 mixture DMEM/F-12 containing 10% FBS. All cell lines were incubated at 37°C in humidified atmosphere with 5% CO₂. When indicated, cells were treated with TCP (1mM, Enzo Life Sciences) or SP2509 (0,2/ 0,5 /1 μM, Cayman Chemical Company) for 6, 12, 24 or 48 hrs. 20 mM of NH₄Cl was administrated for 24h to block autophagic flux.

Transfection and silencing

For transient transfections of Tet-21/N and SH-SY5Y, cells cultured on 100 mm dishes were transfected with 12 μg of SESN2 plasmid, GFP-mRFP-LC3 (kind gift of Dr. A. Fraldi, Tigem Institute) construct or empty vector using Lipofectamine 2000 according to manufacturer's protocol. For LSD1 Knock-down 50 or 100 nM siRNA targeting LSD1 (GE Dharmacon) or scramble were transfected in Tet-21/N cells using a MicroPorator Digital Bio Technology, according to the recently described protocol.³⁹ Briefly, 2x10⁶ cells were collected by trypsin/EDTA digestion, washed once with calcium and magnesium-free PBS and resuspended in 100 μl of resuspension buffer, mixed with siRNA or scramble and electroporated according to the manufacturer's protocol. Transfected cells were seeded in a 100 mm dish in antibiotic-free DMEM supplemented with 10% FBS. The efficiency of siRNA to knockdown LSD1 protein expression was assayed 48h after transfection by western blot. For silencing assays 45 nM siRNA targeting SESN2 (GE Dharmacon) or scramble were transfected in SH-SY5Y cells using Viromer Green, according to the manufacturer's protocol. Cells were collected for analysis 48h after transfection.

Path Scan assay

For PathScan assay (PathScan® Intracellular Signaling Array Kit, Cell Signaling), cell lysates from Tet-21/N cells, treated with TCP or vehicle for 24h, were prepared according to manufacturer protocol; 75 μl of lysates was added to each well previously prepared with Blocking Buffer and slide was incubated 2h at room temperature. After incubation, slide was washed four times with Wash buffer and each well was incubated with 75 μl of Detection Antibody Cocktail for 1 hour at room temperature. Then, slide was washed three times and incubated for 30 minutes with 75 μl of HRP-linked Streptavidin reagent. Next, slide was washed, incubated with Lumi Glo/peroxide solution and displayed by biochemiluminescence acquisition. Protein expression levels were quantified and normalized by positive controls using ImageJ32 software.

Protein extraction and Western blot

Whole-cell extracts were obtained using buffer F (10 mM TrisHCl pH 7.5, 150 mM NaCl, 30 mM Na₄O₇P₂, 50 mM NaF, 5 mM ZnCl₂, 0.1 mM Na₃VO₄, 1% Triton, 0.1mM PMSF). 50 µg of protein extracts were loaded and separated by SDS-PAGE and WB was performed with indicated antibodies listed in Supplementary Table S1.

Immunofluorescence and microscopy

Immunofluorescence assay was carried out as previously described.²⁵ Briefly, 2x10⁴ cells were plated in a well of a 12-well plate, in which a coverslip had been placed, and treated as indicated. Cells were then washed, fixed in 4% paraformaldehyde in PBS, permeabilized in 0.1% Triton X-100 in PBS for 5 min, pre-blocked in 2% BSA for 30 min at room temperature, and then incubated for 1 h at 37° C with rabbit anti-TFEB. Cells were then incubated for 30 min at room temperature with Cy3-conjugated secondary antibody and nuclei were stained with DAPI. Images were acquired using a Nikon Eclipse TE 2000-U microscope.

In case of GFP-mRFP-LC3 experiments cells were just fixed in 4% paraformaldehyde and images were collected using a laser-scanning microscope (LSM 510 META, Carl Zeiss Microimaging, Inc.) equipped with a Plan Apo 63x oil-immersion (NA 1.4) objective lens. Moreover, we acquired the images with the same setting (laser power, detector gain) as well as we kept the same threshold of fluorescence intensity in all experimental conditions. Quantification analyses were carried out using LSM 510 software. We evaluated the autophagic flux counting the number of green and red puncta per cell (number of cells > 100). Student's t-test was used to determine the significance and error bars represent the standard deviation (SD) of the average.

RNA extraction and qRT-PCR

Total RNA was extracted from Tet-21/N cells using EuroGold Trifast (EuroClone). The reverse transcription reaction was performed using Quantitect Reverse Transcription Kit (Qiagen), according to manufacturer's protocol. cDNA thus obtained was analyzed by quantitative-PCR using SYBR Green 2X PCR Master Mix (Applied Biosystem). Each sample was run in triplicate and normalized to the expression of housekeeping beta-glucuronidase (GUSb) gene as previously described.³⁹ Primers are presented in Supplementary Table S1.

Chromatin Immunoprecipitation assay

For ChIP assays, 1x10⁷ cells treated as indicated were cross-linked using 1% formaldehyde. Cell pellet was lysed and sonicated into 200 bp fragments using Bioruptor (Diagenode). A small aliquot of sonicated material was put aside as input. Remaining samples were incubated overnight with rotation at 4°C with 5 µg of ChIP-grade antibodies listed in Table S2; 50 µl of Rec-sepharose Protein A/G beads (Invitrogen) were used to immobilize immuno-complexes. After RNase-A treatment (37°C for 1 hour) reverse cross-linking were performed using Proteinase K (Roche) for 6

hours at 65°C. Immunoprecipitated DNA was purified and quantified by qPCR with the primer sets described in Table S1 and normalized to input DNA.

Statistical analysis

All experiments were repeated at least two times. Graphs representing data express mean \pm SD. Statistical significance was obtained by unpaired, two-tailed Student *t* test. $P < 0,05$ was considered statistically significant.

ACKNOWLEDGEMENTS

We thank A. Feliciello for helpful discussions, constructive criticisms and Dr P. Chumakov for providing us the SESN2-Flag expression vector. This work was supported by following grants: AIRC (IG13173 to B.M.), Epigenomics Flagship Project— EPIGEN, C.N.R. and from Grant MOVIE of the Rete delle Biotecnologie, Campania.

CONFLICT OF INTEREST

The authors declare no conflict of interest.

FIGURE LEGENDS

Figure 1.

LSD1 inhibition represses mTORC1 activity. **(a)** Protein extract from Tet-21/N treated with 1 mM TCP or vehicle (Ctrl) for 24 h were analyzed for the signaling activation using the PathScan antibody arrays. Graph shows the pixel density ratio of signaling molecules dots. Values represent the means of two independent experiments (\pm s.d.). **(b)** Western blotting of protein extracts from Tet-21/N cells treated for 0, 12 or 24 h with TCP or SP2509 (1 μ M) using the indicated antibodies. **(c)** Tet-21/N cells were transfected with siRNA against LSD1 at different concentration, or scramble (0). Cells were collected 48h after transfection and protein extracts were prepared and stained with the indicated antibodies. **(d)** Western blotting of protein extracts from SH-SY5Y cells treated for 24 h with TCP using the indicated antibodies. Actinin was probed as loading control.

Figure 2.

LSD1 inhibition leads to TFEB nuclear sub-localization. Tet-21/N **(a)** and SH-SY5Y **(b)** cells were treated with TCP or vehicle for the indicated times fixed and processed for anti-TFEB immunofluorescence and DAPI staining. **(c)** Tet-21/N cells were transfected with scramble (Ctrl) or siRNA against LSD1 (100 nM), fixed and stained with anti-TFEB and DAPI **(d)** Tet-21/N cells were treated for 48 h with SP2509 or vehicle and then released into fresh medium for the indicated times before immuno-staining with TFEB antibody and DAPI. Histograms show the percentage of TFEB nuclear translocation (mean \pm s.d., n=200 cells)

Figure 3.

LSD1 inhibition induces autophagy. Tet-21/N cells were treated with TCP for the indicated times **(a)**, or siLSD1 at different concentrations as indicated **(b)**, and protein extract were prepared and probed using anti-LC3 antibody. LSD1 protein level in cells transfected with siLSD1 or control (0) was shown. Actinin was probed as loading control. **(c)** Tet-21/N were transiently transfected with GFP-mRFP-LC3 tandem construct and treated with TCP alone or in combination with 20mM NH₄CL for 24 h. After treatment, cells were fixed and analyzed by confocal microscopy. Bar, 10 μ m. Histograms show the number of GFP or mCherry puncta (upper graph) or the number of only-red positive (GFP-negative) puncta (lower graph). The values are expressed as means \pm s.d. (n>100 cells). * p<0.00001.

Figure 4.

LSD1 represses SESN2 expression. SESN2 expression was analyzed by qRT-PCR and Western blotting **(a)** using samples prepared from Tet-21/N cells treated with TCP or siLSD1 (100nM). **(b)** LSD1 binding to SESN2 chromatin. Cell treatments are indicated at the bottom of the figure. qPCR was performed with primers for SESN2 TSS, and -10kb. **(c-f)** Histone modifications at SESN2

chromatin; ChIPs were carried out using the indicated antibodies and analyzed with primers encompassing the TSS region and -10kb from TSS. Values from three independent ChIP assays are presented along with standard deviations, n=3. Changes in % input are shown normalized over IgG controls (*p < 0,05; **p<0,01; Student t test).

Figure 5.

LSD1 depletion-mediated autophagy does not rely on p53 activity. **(a)** Cell extracts from SK-N-BE (2) treated with TCP (1 mM) or SP2509 (1 μ M) for 48 h were prepared and probed with specific SESN2 and LC3 antibodies. **(b)** SK-N-BE (2) were treated with different concentration of SP2509 (0, 0,2, 0,5, 1 μ M) for 48 h and protein extract were prepared and probed with the indicated antibody. Actinin was probed as loading control.

Figure 6.

LSD1 regulates autophagy through SESN2 expression. **(a)** SH-SY5Y were transfected with a SESN2 expression plasmid or empty vector and protein extract were prepared and stained with indicated antibody. **(b)** Localization of TFEB was analyzed in cells treated as described in A by immuno-staining with TFEB antibody. **(c)** SH-SY5Y cells were transfected with siRNA against SESN2 or scramble. 24h after transfection cells were treated with TCP or vehicle for 24h, and protein extract were probed with the indicated antibody. Actinin was probed as loading control. Graphs show quantitative analysis of western blot experiments. A mean value \pm s.d. of four independent experiments is shown (*p<0,05; **p<0,005). **(d)** SH-SY5Y treated as described in c were fixed and stained with anti-TEFB and DAPI. Histograms show the percentage of TFEB nuclear translocation (mean \pm s.d., n=200 cells). * p<0.0001.

REFERENCES

1. Galluzzi L, Pietrocola F, Bravo-San Pedro JM, Amaravadi RK, Baehrecke EH, Cecconi F *et al.* Autophagy in malignant transformation and cancer progression. *EMBO J* 2015; **34**: 856-80.
2. Rebecca VW, Amaravadi RK. Emerging strategies to effectively target autophagy in cancer. *Oncogene* 2016; **35**: 1-11.
3. Mizushima N, Levine B, Cuervo AM, Klionsky DJ. Autophagy fights disease through cellular self-digestion. *Nature* 2008; **451**: 1069-1075.
4. Levine B, Mizushima N, Virgin HW. Autophagy in immunity and inflammation. *Nature* 2011; **469**: 323-335.
5. Maiese K. Targeting molecules to medicine with mTOR, autophagy and neurodegenerative disorders. *Br J Clin Pharmacol* 2016; **82**: 1245-1266.
6. Jiang P, Mizushima N. Autophagy and human diseases. *Cell Res* 2014; **24**: 69-79.
7. Eisenberg-Lerner A, Kimchi A. The paradox of autophagy and its implication in cancer etiology and therapy. *Apoptosis* 2009; **14**: 376-391.
8. Maiuri MC, Zalckvar E, Kimchi A, Kroemer G. Self-eating and self-killing: crosstalk between autophagy and apoptosis. *Nat Rev Mol Cell Biol* 2007; **8**: 741-752.
9. White E. The role for autophagy in cancer. *J Clin Invest* 2015; **125**: 42-46.
10. Sehgal AR, Konig H, Johnson DE, Tang D, Amaravadi RK, Boyiadzis M *et al.* You eat what you are: autophagy inhibition as a therapeutic strategy in leukemia. *Leukemia* 2015; **29**: 517-525.
11. Kim J, Kundu M, Viollet B, Guan KL. AMPK and mTOR regulate autophagy through direct phosphorylation of Ulk1. *Nat Cell Biol* 2011; **13**: 132-141.
12. Martina JA, Chen Y, Gucek M, Puertollano R. MTORC1 functions as a transcriptional regulator of autophagy by preventing nuclear transport of TFEB. *Autophagy* 2012; **8**: 903-914.
13. Gallagher LE, Williamson LE, Chan EY. Advances in Autophagy Regulatory Mechanisms. *Cells* 2016; **5**: 24
14. Artal-Martinez de Narvajas A, Gomez TS, Zhang JS, Mann AO, Taoda Y, Gorman JA *et al.* Epigenetic regulation of autophagy by the methyltransferase G9a. *Mol Cell Biol* 2013; **33**: 3983-3993.
15. Eisenberg T, Schroeder S, Andryushkova A, Pendl T, Küttner V, Bhukel A *et al.* Nucleocytosolic depletion of the energy metabolite acetyl-coenzyme a stimulates autophagy and prolongs lifespan. *Cell Metab* 2014; **19**: 431-444.
16. Lapierre LR, Kumsta C, Sandri M, Ballabio A, Hansen M. Transcriptional and epigenetic regulation of autophagy in aging. *Autophagy* 2015; **11**: 867-880.
17. Shy Y, Lan F, Matson C, Mulligan P, Whetstine JR, Cole PA *et al.* Histone demethylation

- mediated by the nuclear amine oxidase homolog LSD1. *Cell* 2004; **119**: 941-953
18. Lan F, Nottke AC, Shi Y. Mechanisms involved in the regulation of histone lysine demethylases. *Curr Opin Cell Biol* 2008; **20**: 316-325.
 19. Metzger E, Wissmann M, Yin N, Muller JM, Schneider R, Peters AH *et al.* LSD1 demethylates repressive histone marks to promote androgen-receptor dependent transcription. *Nature* 2005; **437**: 436-439.
 20. Wang J, Telese F, Tan Y, Li W, Jin C, He X *et al.* LSD1n is an H4K20 demethylase regulating memory formation via transcriptional elongation control. *Nat Neurosci* 2015; **18**:1256-1264
 21. Huang J, Sengupta R, Espejo AB, Lee MG, Dorsey JA, Richter M *et al.* p53 is regulated by the lysine demethylase LSD1. *Nature* 2007; **449**: 105-108.
 22. Kontaki H, Talianidis I. Lysine methylation regulates E2F1-induced cell death. *Mol Cell* 2010; **39**: 152-160.
 23. Wang J, Hevi S, Kurash JK, Lei H, Gay F, Bajko J *et al.* The lysine demethylase LSD1 (KDM1) is required for maintenance of global DNA methylation. *Nat Genet* 2009; **41**: 125-129.
 24. Amente S, Lania L, Majello B. The histone LSD1 demethylase in stemness and cancer transcription programs. *Biochim Biophys Acta* 2013; **1829**: 981-986.
 25. Ambrosio S, Amente S, Saccà CD, Capasso M, Calogero RA, Lania L, Majello B. LSD1 mediates MYCN control of epithelial-mesenchymal transition through silencing of metastatic suppressor NDRG1 gene. *Oncotarget* 2017; **8**:3854-3869
 26. Han X, Gui B, Xiong C, Zhao L, Liang J, Sun L *et al.* Destabilizing LSD1 by Jade-2 promotes neurogenesis: an antibraking system in neural development. *Mol Cell* 2014; **55**: 482-494.
 27. Schulte JH, Lim S, Schramm A, Friedrichs N, Koster J, Versteeg R *et al.* Lysine-specific demethylase 1 is strongly expressed in poorly differentiated neuroblastoma: implications for therapy. *Cancer Res* 2009; **69**: 2065-2071.
 28. Fiskus W, Sharma S, Shah B, Portier BP, Devaraj SG, Liu K *et al.* Highly effective combination of LSD1 (KDM1A) antagonist and pan-histone deacetylase inhibitor against human AML cells. *Leukemia* 2014; **28**: 2155–2164.
 29. Settembre C, Zoncu R, Medina DL, Vetrini F, Erdin S, Erdin S *et al.* A lysosome-to-nucleus signalling mechanism senses and regulates the lysosome via mTOR and TFEB. *EMBO J* 2012; **31**: 1095-1108.
 30. Klionsky, D. J. *et al.* Guidelines for the use and interpretation of assays for monitoring autophagy (3rd edition). *Autophagy* 2016; **12**: 1-222.
 31. Mizushima N, Yoshimori T, Levine B. Methods in Mammalian Autophagy Research. *Cell* 2010; **140**: 313-326.

32. Parmigiani A, Nourbakhsh A, Ding B, Wang W, Kim YC, Akopiants K *et al.* Sestrins inhibit mTORC1 kinase activation through the GATOR complex. *Cell Rep* 2014; **9**: 1281-1291.
33. Wolfson RL, Chantranupong L, Saxton RA, Shen K, Scaria SM, Cantor JR *et al.* Sestrin2 is a leucine sensor for the mTORC1 pathway. *Science* 2016; **351**: 43-48.
34. Periz G, Lu J, Zhang T, Kankel MW, Jablonski AM, Kalb R *et al.* Regulation of protein quality control by UBE4B and LSD1 through p53-mediated transcription. *PLoS Biol* 2015; **13**: e1002114; doi: 10.1371/journal.pbio.1002114.
35. Cam M, Bid HK, Xiao L, Zambetti GP, Houghton PJ, Cam H. p53/TAp63 and AKT regulate mammalian target of rapamycin complex 1 (mTORC1) signaling through two independent parallel pathways in the presence of DNA damage. *J Biol Chem* 2014; **289**: 4083-4094.
36. Maiuri MC, Malik SA, Morselli E, Kepp O, Criollo A, Mouchel PL *et al.* Stimulation of autophagy by the p53 target gene Sestrin2. *Cell Cycle* 2009; **8**: 1571-1576.
37. Budanov AV, Karin M. p53 target genes sestrin1 and sestrin2 connect genotoxic stress and mTOR signaling. *Cell* 2008; **134**: 451-60.
38. Goldschneider D, Horvilleur E, Plassa LF, Guillaud-Bataille M, Million K, Wittmer-Dupret E *et al.* Expression of C-terminal deleted p53 isoforms in neuroblastoma. *Nucleic Acids Res* 2006; **34**: 5603-5612.
39. Amente S, Milazzo G, Sorrentino MC, Ambrosio S, Di Palo G, Lania L *et al.* Lysine-specific demethylase (LSD1/KDM1A) and MYCN cooperatively repress tumor suppressor genes in neuroblastoma. *Oncotarget* 2015; **6**: 14572-14583.
40. Etani T, Suzuki T, Naiki T, Naiki-Ito A, Ando R, Iida K *et al.* NCL1, a highly selective lysine-specific demethylase 1 inhibitor, suppresses prostate cancer without adverse effect. *Oncotarget* 2015; **6**: 2865-2878.
41. Feng S, Jin Y, Cui M, Zheng J. Lysine-Specific Demethylase 1 (LSD1) Inhibitor S2101 Induces Autophagy via the AKT/mTOR Pathway in SKOV3 Ovarian Cancer Cells. *Med Sci Monit* 2016; **22**: 4742-4748.
42. Kim H, An S, Ro SH, Teixeira F, Park GJ, Kim C *et al.* Janus-faced Sestrin2 controls ROS and mTOR signalling through two separate functional domains. *Nat Commun* 2015; **6**: 10025.
43. Zhang F, Kumano M, Beraldi E, Fazli L, Du C, Moore S *et al.* Clusterin facilitates stress-induced lipidation of LC3 and autophagosome biogenesis to enhance cancer cell survival. *Nat Commun* 2014; **5**: 5775.
44. Füllgrabe J, Klionsky DJ, Joseph B. The return of the nucleus: transcriptional and epigenetic control of autophagy. *Nat Rev Mol Cell Biol* 2014; **15**: 65-74.
45. Maiuri MC, Tasdemir E, Criollo A, Morselli E, Vicencio JM, Carnuccio R *et al.* Control of autophagy by oncogenes and tumor suppressor genes. *Cell Death Differ* 2009; **16**: 87-93.

46. Zhang J, Ng S, Wang J, Zhou J, Tan SH, Yang N *et al.* Histone deacetylase inhibitors induce autophagy through FOXO1-dependent pathways. *Autophagy* 2015; **11**: 629-642.
47. Wei FZ, Cao Z, Wang X, Wang H, Cai MY, Li T *et al.* Epigenetic regulation of autophagy by the methyltransferase EZH2 through an MTOR-dependent pathway. *Autophagy* 2015; **11**: 2309-2322.
48. Belounis A, Nyalendo C, Le Gall R, Imbriglio TV, Mahma M, Teira P *et al.* Autophagy is associated with chemoresistance in neuroblastoma. *BMC Cancer* 2016; **16**: 891.

Figure 1

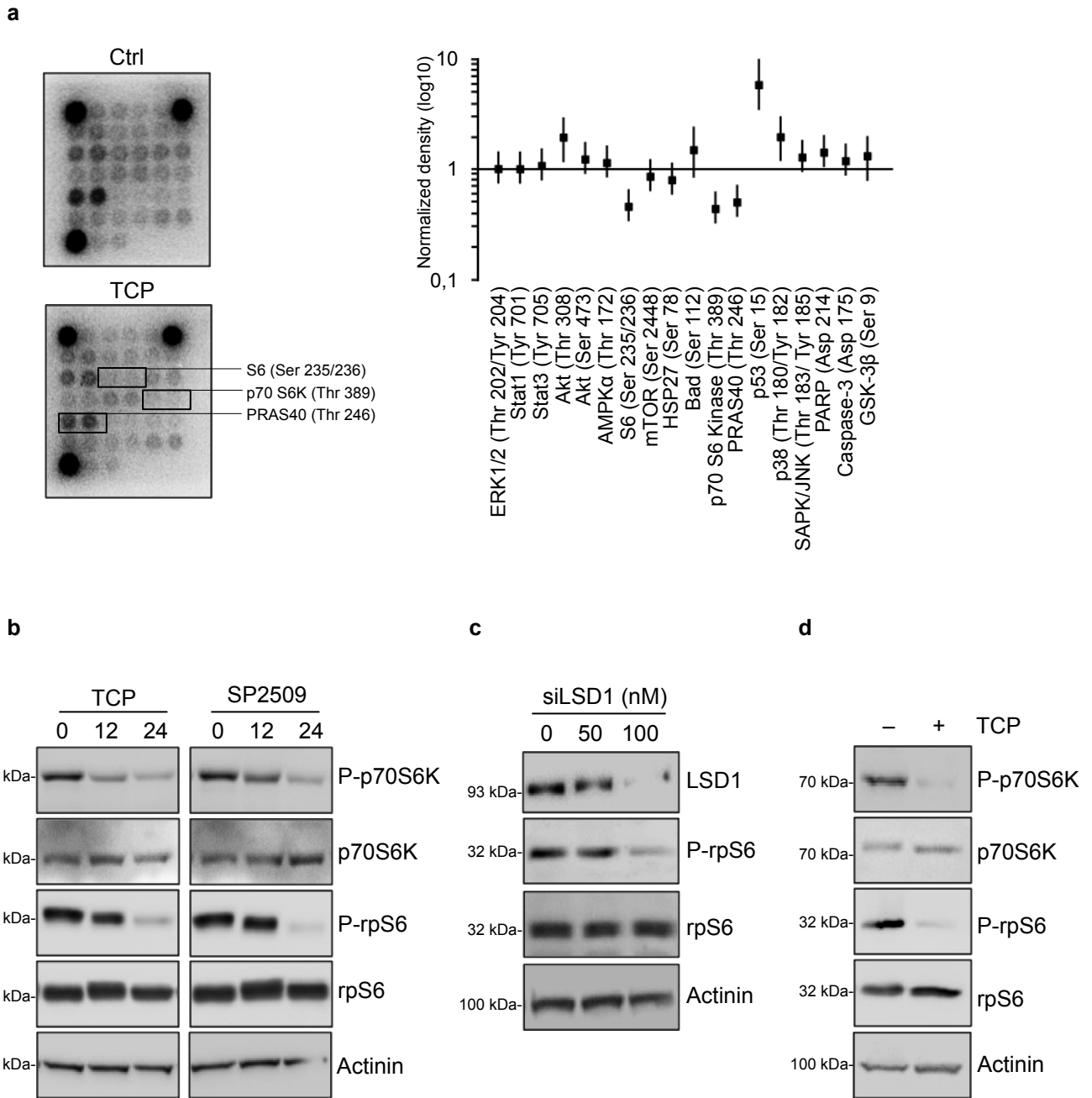


Figure 2

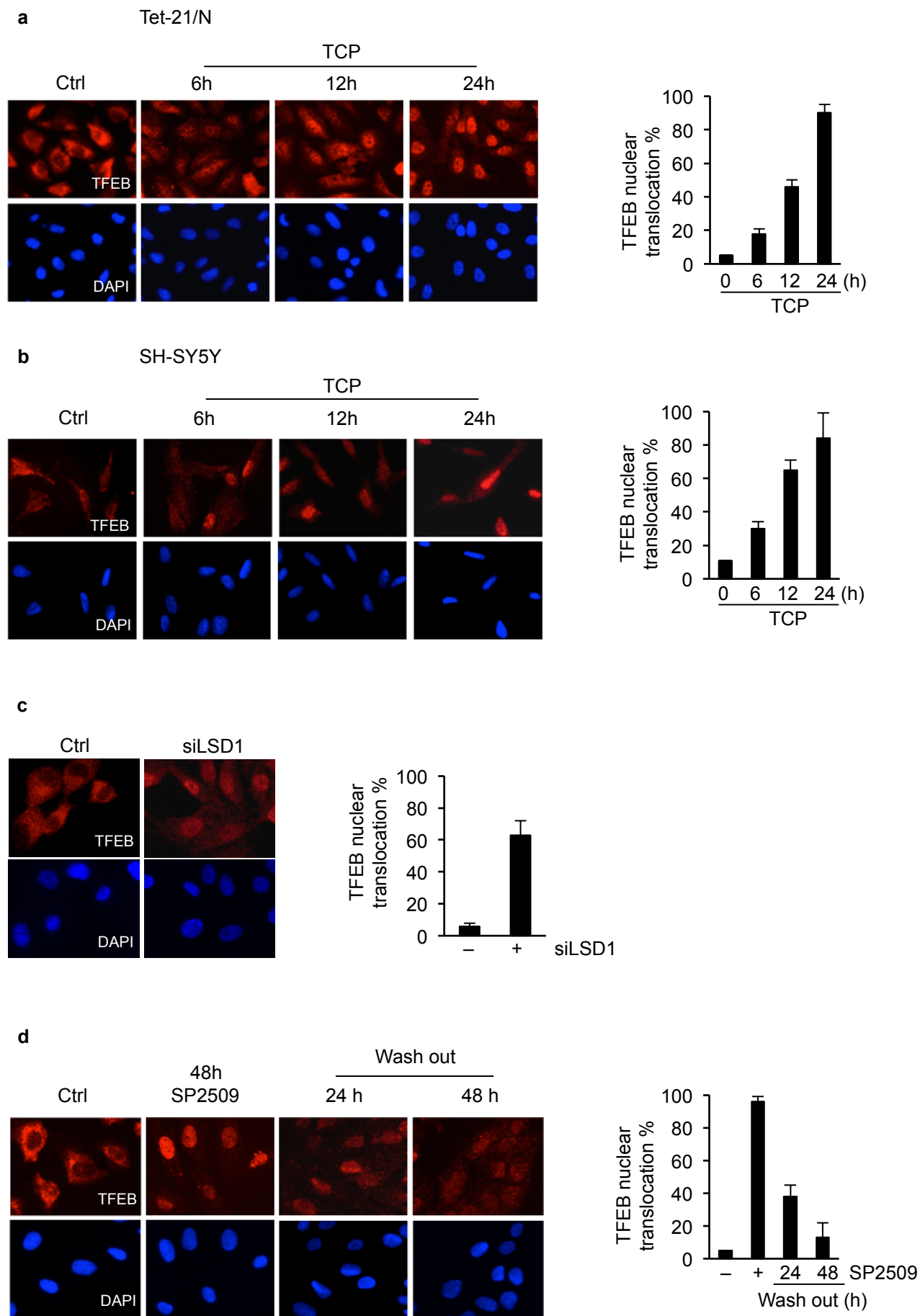


Figure 3

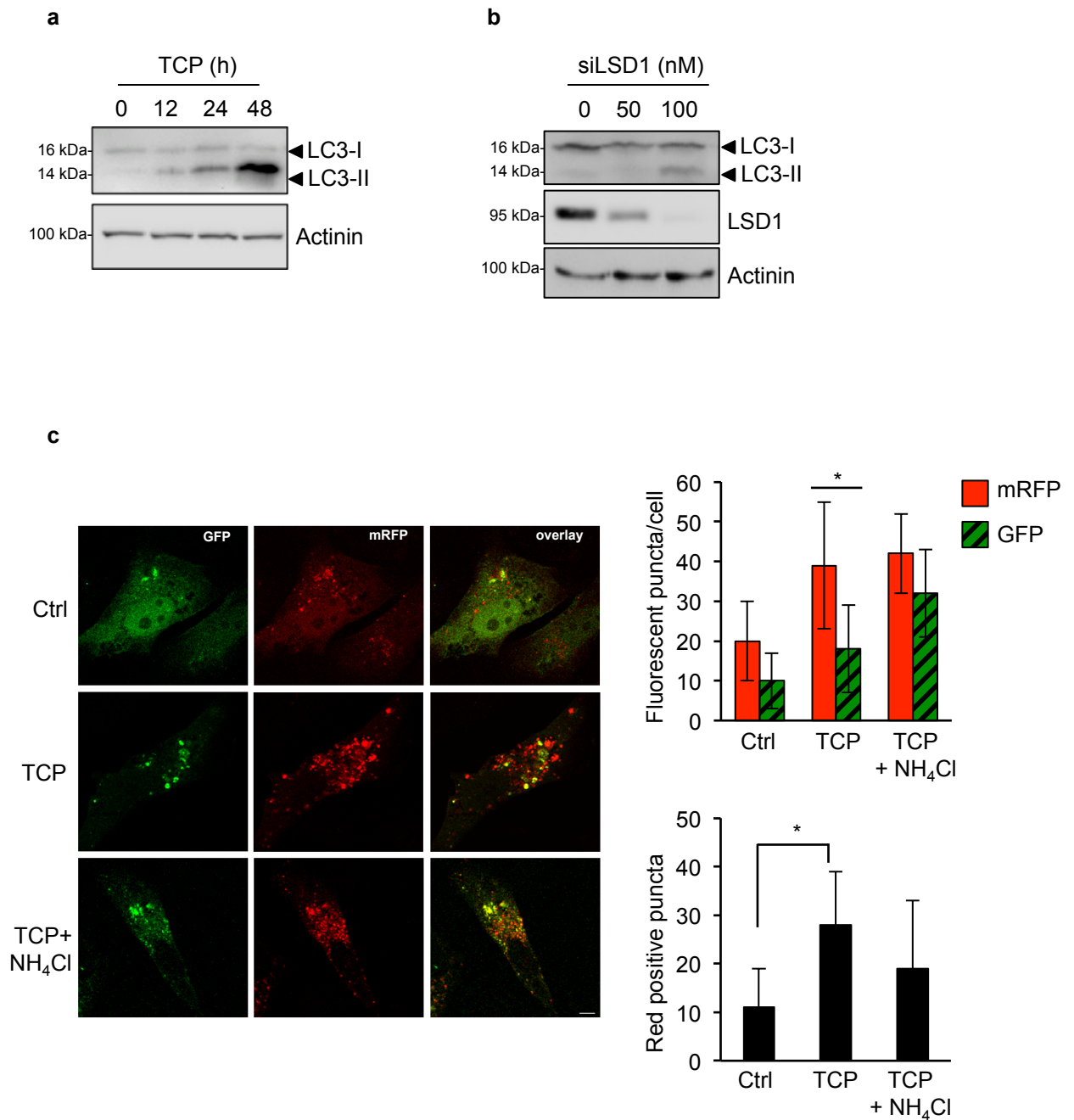


Figure 4

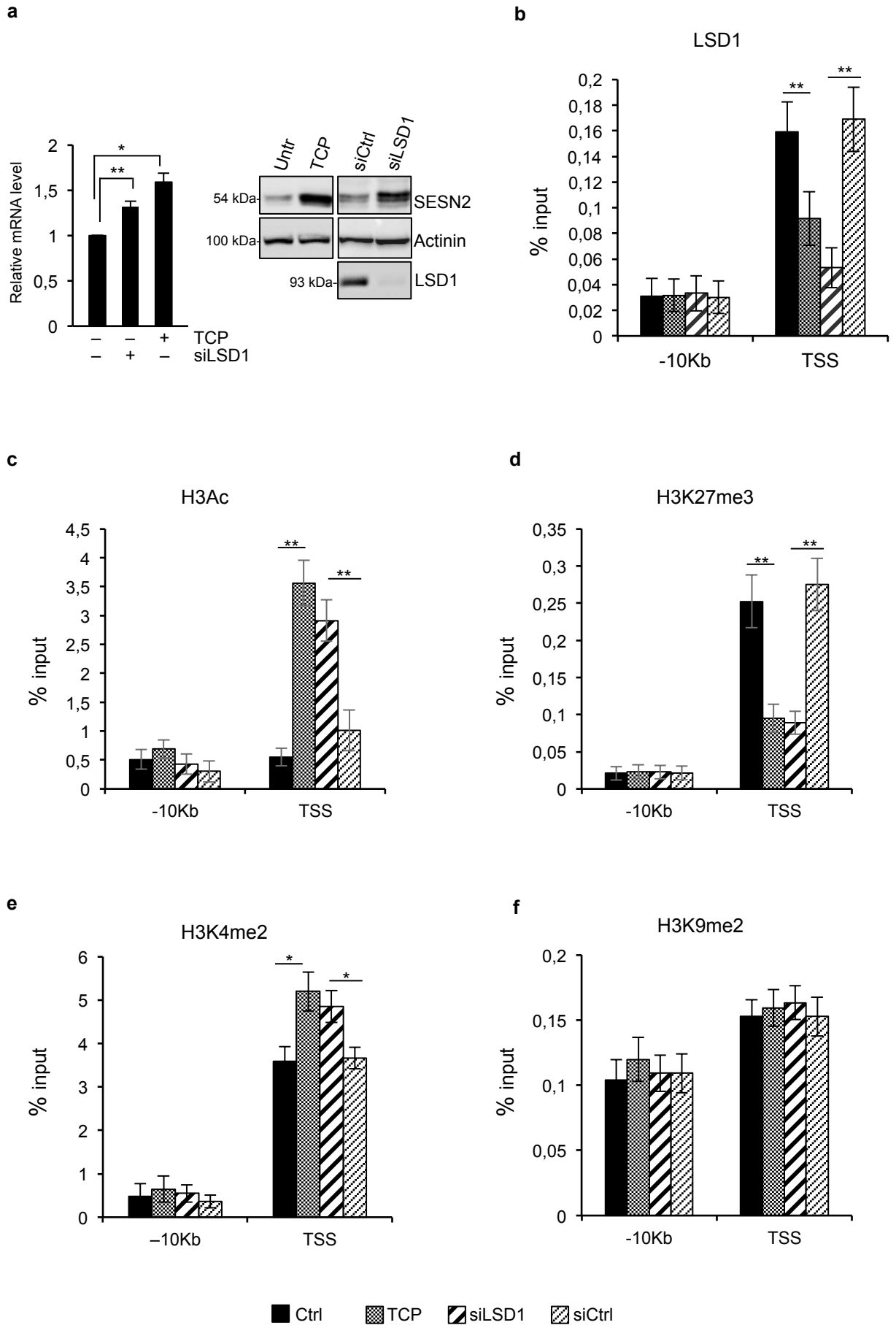


Figure 5

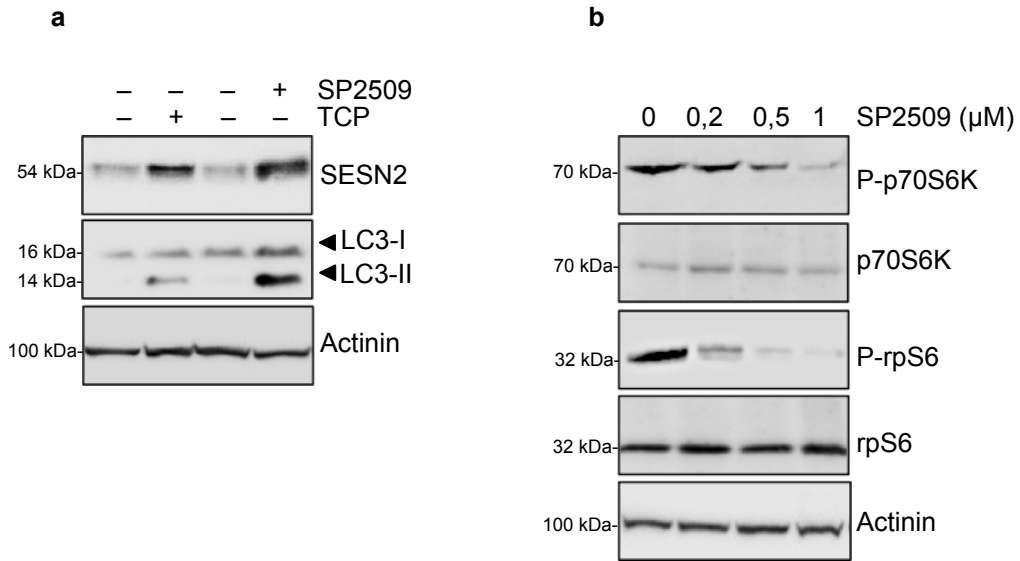
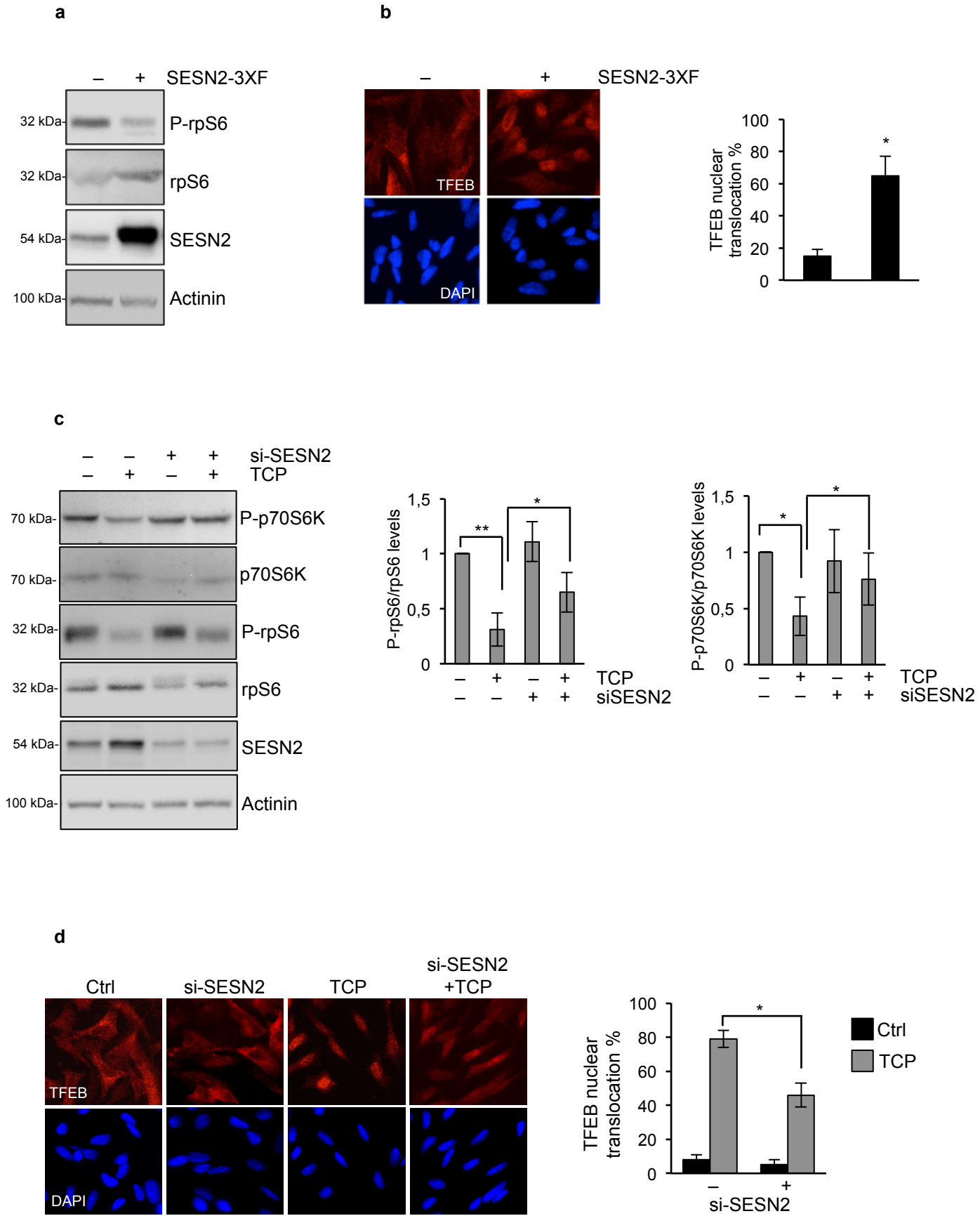
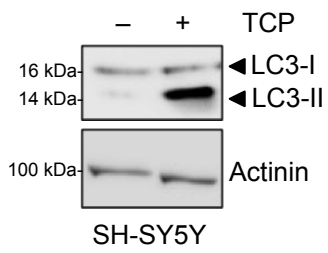


Figure 6



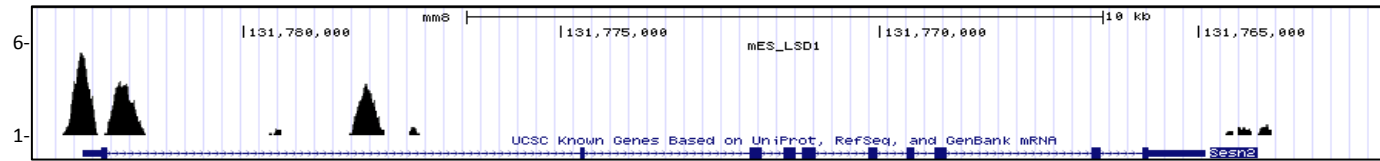
Supplementary Figure 1



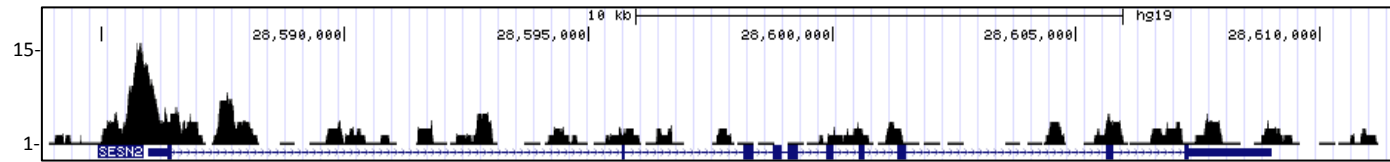
Supplementary Figure 1: SH-SY5Y cells were treated with TCP for 24 h and protein extract were prepared and probed using anti-LC3 antibody. Actinin was probed as loading control.

Supplementary Figure 2

A



B



Supplementary Figure 2: Screenshots of UCSC genome browser of SESN2 gene are shown. (A) and (B) the peaks represent the LSD1 binding on the promoter region and TSS of SENS2 gene in mouse and human cells respectively.

Supplementary Figure 3

Fig. 1b (*)

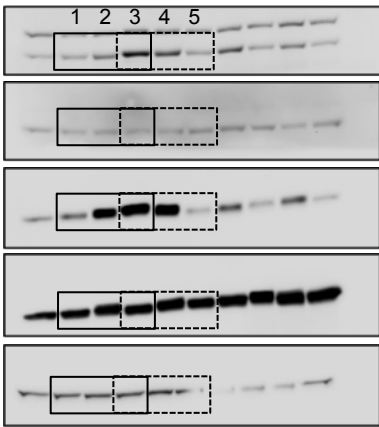


Fig. 1c

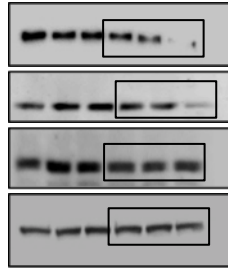


Fig. 1d

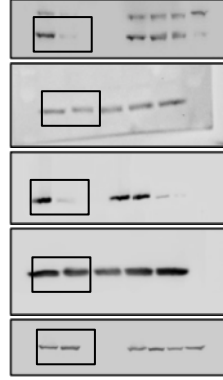


Fig. 3a

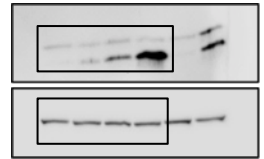


Fig. 3b



Fig. 4a

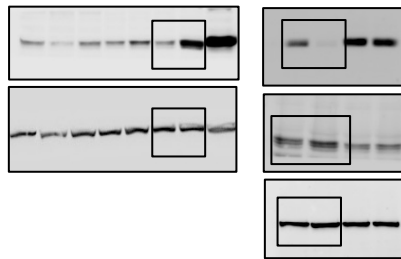


Fig. 5a

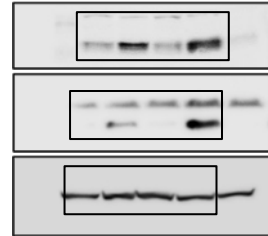


Fig. 5b

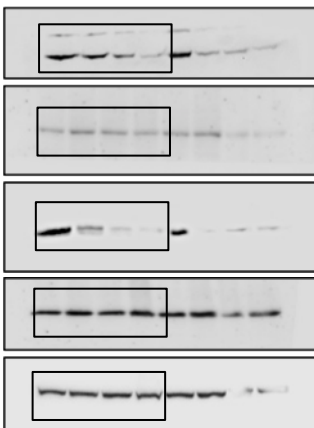


Fig. 6a

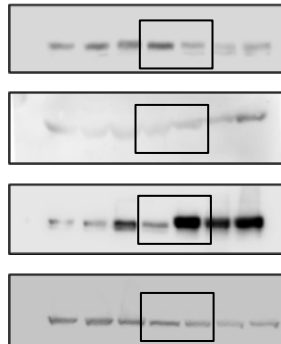
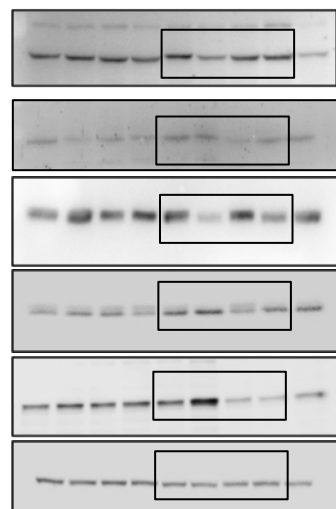


Fig. 6c



Supplementary Figure 3: Full scans of Western data. (*) Only in Fig. 1B, for better results presentation, lanes have been separated into two panels that share the control sample (lane 3).

Table S1: antibodies and oligos used in this work

Protein	Used for	Manufacturer
Actinin	WB	sc-17829, Santa Cruz
Sestrin 2	WB	10795-1-AP, Proteintech
Phospho-S6 Ribosomal Protein	WB	2215, Cell Signaling
S6 Ribosomal Protein	WB	2217, Cell Signaling
Phospho-p70 S6 Kinase (Thr 389)	WB	9205, Cell Signaling
p70 S6 Kinase	WB	2708, Cell Signaling
LC3A/B	WB	4108, Cell Signaling
LSD1	ChIP, WB	ab17721, Abcam
TFEB	IF	4240, Cell Signaling
H3Ac	ChIP	06-599, Millipore
H3K27me3	ChIP	07-449, Millipore
H3K4me2	ChIP	ab32356, Abcam
H3K9me2	ChIP	ab1220, Abcam

	Gene	FW	Rev
qChiP	SESN2 (-10Kb)	CCAAGTTGTGAATGCAAAGG	AGCCGAGATCAGGCCACT
qChiP	SESN2 (TSS)	AGTCCCTCCAGGAACTGAAA	GTCATTAGGGTTGCGTGATG
qRT-PCR	SESN2	GTGGACACCTCCGTGCTC	GGTTCACCTCCCCATAATCA
qRT-PCR	GUSb	GTGGGCATTGTGCTACCTC	ATTTTTGTCCCGGCGAAC

CHAPTER 6
CONCLUSIONS

Conclusions

Oncogenic activation of MYC proteins affects multiple intracellular pathways, culminating in neoplastic transformation in many cell types (6-9). MYC overexpression is involved in all aspects of tumor cell biology including cellular proliferation and growth, altered cellular metabolism, cellular senescence and differentiation blockage. Additionally, MYC orchestrates changes in the tumor microenvironment, such as activation of angiogenesis and suppression of the host immune response (27, 28, 32, 48, 49).

Tumor maintenance machinery depends in large part on the accumulation of mutations in the genome of neoplastic cells. Chromosomal instability is a common feature of many human cancers (92). As in the case of other oncogenes, aberrant MYC activity is associated with the appearance of DNA damage-associated markers and karyotypic abnormalities (41, 42). This phenomenon can be explained through different mechanisms. First, metabolic effects of MYC might lead to DNA damage. Specifically, oxygen radicals produced following MYC activation could lead to oxidative base modifications (43). An additional source of MYC-induced DNA damage is replication stress, a poorly understood perturbation of DNA replication (45). In addition, MYC seems to be involved in the modulation of DNA repair pathways. Indeed, it has been demonstrated that MYC plays a role in regulating the repair of IR-induced DSBs, through direct suppression of the NHEJ pathway and consequently enhanced chromosomal breaks. (46, 47)

Findings reported in this study add further support to the role of MYC proteins in DNA damage repair. In this work we used a dedicated cell system, in which inducible specific DSBs may occur, to investigate the role of MYC oncoproteins (MYC and MYCN) overexpression on repair of DNA double-strand breaks in osteosarcoma and neuroblastoma cells. Our data show that damaged MYC overexpressing cells undergo a prolonged cell cycle arrest and sustained DDR response, compared to cell expressing physiological level of MYC, suggesting that overexpression of MYC proteins impairs the wave of DSBs repair at the DNA lesions. We found that MYC does not prevent appropriate γ -H2AX foci formation, indicating that aberrant MYC expression does not affect the initial recognition of DSBs. Proper DNA repair relies on the precise orchestration of DDR, DNA replication and transcription, along with cell cycle progression and MYC could

Conclusions

interfere with repair pathways at several different layers. First, MYC regulates expression of several repair factors and it has been shown to interact with many of these, such as TIP60, DNA-PK and MRE11 (93, 94). Replication stress induced by MYC over-expression could lead to an aberrant activation of DDR at sites of active DNA replication that impairs resolution of DNA repair. MYC has been shown to have a profound impact on the global chromatin structure and it is reasonable to think that MYC proteins could influence DNA repair substantially influencing histone modifications surrounding DSBs (94-96). Noteworthy, high level of MYC proteins could abrogate DSB resolution altering the cell cycle regulatory machinery.

It is well established the interdependence between DNA repair and cell cycle machineries. Different molecular mechanisms involved in DNA repair occurring at specific cell cycle phases, regulated by the activity of cyclin-dependent kinases and by the cell cycle-dependent expression of required factors. DNA damage induces cell cycle arrest, providing time for repair pathways before DNA replication and segregation, whereas cells with unreparable DNA lesions undergo permanent cell cycle arrest or apoptosis (97).

In this study we propose that cell cycle phase in which DNA damage occurs do not interfere with DSBs recognition and recruitment of repair factors, but rather that DNA damage repair competence strictly depend on cell proliferative status. Thus, DNA repair is deeply reliant on fine regulation of cell-cycle progression and disruption of these regulation systems can lead to defective DNA repair pathways and DNA damage accumulation.

Control of cell proliferation is one of the major rules of MYC biology and likely the most relevant for its oncogenic activity (28). MYC influences all levels of the cell cycle regulatory machinery and facilitates transit through the cell cycle. High MYC levels accelerate cell division and mediate unscheduled entry into S-phase. Moreover, MYC could lead to abrogation of DNA damage-induced cell cycle checkpoint through the suppression of genes that encode inhibitors of cellular proliferation, such as p21 and p27 (29-31). Thus, MYC overexpressing cells experience oxidative stress, damage at replication forks and loss of DNA damage-based checkpoints and repair capacity. Consequently, MYC pathological activation may drive cells with unrepaired DNA damage into cell cycle and

Conclusions

escape from normal cellular barriers to establishment and tumorigenesis maintenance.

Due to its ability to impact genetic stability, MYC is carefully controlled in non-pathological state through multiple genetic and epigenetically controlled checkpoint mechanisms. Thus, MYC activation alone is restrained from causing tumorigenesis, unless MYC is pathologically activated in a permissive context; in this case, MYC bypasses control mechanisms and may lead to the acquisition of additional genomic lesions that could enforce many of the “hallmark” of cancer and drive malignant transformation. This process can be enhanced by compromised surveillance systems that normally monitor genomic integrity. Consistent with this notion, genetic events that abrogate cell cycle arrest, apoptosis, and senescence frequently occur during cancer progression and synergize with MYC overexpression to create a permissive environment for malignant transformation. Examples include loss of p53 and p19ARF functions and BCL-2 overexpression (98-101).

A central tenet of molecular oncology asserts that these tumors, once established, remain dependent on elevated MYC levels to sustain proliferation and viability and, therefore, could be treated by targeting MYC activity (57). Supporting this notion, knock-down of MYC in established tumors, using small interfering RNA, short hairpin RNA and antisense oligonucleotides, appears to reduce cell proliferation and induce apoptosis; in transgenic mouse models with inducible MYC, when expression of the oncogene is switched off, tumor cells undergo apoptosis (58-60); finally, in vivo expression of the dominant negative inhibitor of MYC heterodimerization, OmoMYC, has resulted in tumor regression by competing with MYC/MAX for binding to promoter of specific genes involved in MYC driven tumorigenesis (102). MYC inactivation could lead tumor cells to lose their neoplastic properties, for example reducing tumor nutrient providing and restoring differentiation signals. Beyond these effects, MYC targeting may reduce survive capacity also due to the consequent restoration of some critical aspects of cell cycle checkpoint and repair functions that force damaged cells into either senescence or apoptosis. For all these reasons, targeting MYC activity appears to have significant therapeutic value for cancers that involve gain of function in MYC. Despite many efforts have been made (103), targeting MYC is

Conclusions

not child's play; since MYC lacks enzymatic activity or any deep pocket, pharmacological targeting by small-molecules has limited applicability; furthermore, at physiological level, MYC acts as a vital transcription regulator, and its inhibition could be associated with high toxicity. Although MYC is widely considered "undruggable", a promising approach to circumvent blocking MYC is selectively targeting chromatin modifiers that drive MYC-dependent transcription.

MYC proteins orchestrate epigenetic alterations by recruitment of several chromatin complexes that activate or repress transcription. In 2010, Amente et al. demonstrated that LSD1 drives transcription of MYC target genes (71); these findings give rise to the interest of Majello laboratory on how LSD1/MYC complex transcriptional activity could be exploited in the context of particular types of MYC-driven cancers. Recently, we demonstrated that MYCN interacts with LSD1 and that, accordingly with LSD1 role exerted in transcriptional repression events, the MYCN/LSD1 complex is involved in repression of MYCN target genes in neuroblastoma cell lines (91). Importantly, we reported that LSD1 inhibition reduces neuroblastoma cell proliferation and causes reactivation of p21, CLU and, plausibly, other potential tumor suppressor genes involved in MYCN-driven oncogenesis with therapeutic effects, suggesting that LSD1 inhibition could be therapeutically used, alone or in combination with other therapeutic tools, to counteract MYCN-amplified neuroblastomas.

LSD1 has been shown to be involved in maintaining the undifferentiated, malignant phenotype of neuroblastoma cells and its overexpression correlated with aggressive disease, poor differentiation and infaust outcome (85), suggesting that the employ of LSD1 pharmacological inhibitors could be taken under consideration as a valid therapeutic approach directed against neuroblastomas with MYCN amplification. For these reasons our work has been focused on understanding of LSD1 role in MYCN-driven transcription, and uncovering its potential as a new perspective for therapy in neuroblastoma. We found that, in neuroblastoma cells, LSD1 is deeply involved in two major processes in cancers, epithelial-mesenchymal-transition and mTORC-mediated autophagy. Recent observations indicate that these two important processes in cancer are linked in an intricate relationship (104). While EMT requires

Conclusions

autophagy to support viability of potentially metastatic cancer cells, autophagy acts to prevent EMT. Indeed, it has been shown that induction of autophagy by mTOR pathway inhibition leads to reduced migration and invasion in glioblastoma cells, while autophagy impairment results in enhanced cell motility and invasiveness (104). Moreover, activation of the autophagic process leads to SNAIL degradation, a critical transcription factors which promotes the EMT process. Here we propose the LSD1-specific transcriptional regulation as a novel link between EMT and autophagy.

We described a novel role for MYCN/LSD1 complex in migration and invasiveness of neuroblastoma cells through the transcriptional control of the metastatic suppressor NDRG1. Neuroblastoma is a high metastatic tumor and MYCN overexpression correlates with invasive and metastatic behavior. MYCN contributes to all facets of metastasis: adhesion, motility, invasion, and degradation of surrounding matrices (105). We propose that LSD1 pharmacological targeting by small molecules could modulate cell migration capability and invasiveness of cancer cells through NDRG1 de-repression and impair the ability of MYCN-amplified neuroblastomas to metastasize.

Intriguingly, we found that LSD1 inhibition also lead to NDRG1 phosphorylation at Thr346. Phosphorylation of NDRG1 is mediated through the serum/glucocorticoid regulated kinase 1 (SGK1) and glycogen synthase kinase 3 beta (GSK3b), and seems to be under control of the Mammalian target of rapamycin complex 2 (mTORC2) cascade (106). The impact of NDRG1 phosphorylation is largely unknown; NDRG1 phosphorylation mediated by LSD1-inhibition may be related to the modulation of the Wnt/ β -catenin signaling pathway and contribute to NDRG1 anti-metastatic effects in NB cells. However, additional investigation is needed to unequivocally determine whether NDRG1 phosphorylation has a role in the modulation of NDRG1 anti-metastatic functions.

Moreover, we found that LSD1 inhibition triggers autophagy through the impairment of the Mammalian target of rapamycin complex 1 (mTORC1) cascade. mTORC1 has essential functions in translational control, metabolism, proliferation and tumorigenesis, and proteins involved in mTORC1 signaling are frequently altered in human cancers (107, 108). We identified Sestrin2 (SESN2)

Conclusions

as an LSD1 negative transcriptional target. SESN2 acts as mTORC1 inhibitor through the GATOR complex via interaction with GATOR2 (109). We found that SESN2 enhanced expression suffices to promote autophagy in neuroblastoma cells and SESN2 silencing attenuates mTORC1 suppression and autophagy induction by LSD1 inhibition, indicating that SESN2 has a critical role in the autophagy activation mediated by LSD1 depletion.

Emerging evidences has established mTORC1 as a major link in development and progression of neuroblastoma. mTORC1 inhibition seems to have antiproliferative effects and increased apoptosis in neuroblastoma cells in vitro (110). Additionally, mTOR inhibition has been shown to inhibit angiogenesis decreasing VEGF-A secretion and downregulate expression of MYCN and cyclin D1 proteins. (111). Indeed, mTORC pathway seems to be involved in MYC proteins stability. Turnover of MYC is largely dependent on phosphorylation at T58 and S62; phosphorylation at S62 stabilizes MYC, and priming these proteins for phosphorylation at T58 via GSK3b; dephosphorylation of S62 via protein phosphatase 2A (PP2A) sensitizes MYC phosphorylated at T58 to bind F-box and WD repeat domain-containing 7 (FBW7), leading to the ubiquitination and degradation in the proteasome. It has been shown that AMBRA1, a pro-autophagic mTORC downstream target protein, promotes the interaction between MYC and its phosphatase PP2A, facilitating the dephosphorylation and degradation of the proto-oncogene MYC (112). These evidences suggest that mTORC1 inhibition represent a viable strategy to targeting MYCN amplified neuroblastoma.

However, the induction of autophagy may be a double-edged sword in cancer: it represents a suppressive mechanism against tumor formation, counteracting the accumulation of damaged organelles and misfolded proteins; on the other hand, autophagy provides a survival strategy for established tumor growth and maintenance (113). Thus, autophagy might have different effects in tumors depending on the cell type and the stage of progression. Recent studies showed that autophagy predicts resistance to chemotherapy and survival in neuroblastoma (114) and this should be taken in consideration. Future investigations may clarify whether combinatory LSD1 and autophagy inhibition

Conclusions

could be a strategy to increase cytotoxic effects and improve the efficacy of LSD1 inhibitors in neuroblastoma cells.

Concluding, this study expands our knowledge about the impact of MYC oncogenes alterations on damage response and repair networks. Moreover, our findings establish the major role of the MYCN/LSD1 complex in neuroblastoma and elucidate the critical function of LSD1 in the control of many important aspects of cell biology, through transcription regulation of specific target genes, suggesting that LSD1 inhibition may have strong therapeutic relevance to counteract MYCN-driven oncogenesis.

Future elucidation of MYC-driven transcriptional network in cancers may have important implication for the development of new therapeutic approaches directed against malignancies with deregulated MYC.

CHAPTER 7
BIBLIOGRAPHY

Bibliography

- 1) Blackwood EM, Eisenman RN. Max: a helix-loop-helix zipper protein that forms a sequence-specific DNA-binding complex with Myc. *Science*. 1991;251(4998):1211-7.
- 2) Amati B, Dalton S, Brooks MW, Littlewood TD, Evan GI, Land H. Transcriptional activation by the human c-Myc oncoprotein in yeast requires interaction with Max. *Nature*. 1992;359(6394):423-6.
- 3) Rahl PB, Lin CY, Seila AC, et al. c-Myc regulates transcriptional pause release. *Cell*. 2010;141(3):432-45.
- 4) Gartel AL, Shchors K. Mechanisms of c-myc-mediated transcriptional repression of growth arrest genes. *Exp Cell Res*. 2003;283(1):17-21.
- 5) Wu S, Cetinkaya C, Munoz-alonso MJ, et al. Myc represses differentiation-induced p21CIP1 expression via Miz-1-dependent interaction with the p21 core promoter. *Oncogene*. 2003;22(3):351-60.
- 6) Escot C, Theillet C, Lidereau R, et al. Genetic alteration of the c-myc protooncogene (MYC) in human primary breast carcinomas. *Proc Natl Acad Sci USA*. 1986;83(13):4834-8.
- 7) Boxer LM, Dang CV. Translocations involving c-myc and c-myc function. *Oncogene*. 2001;20(40):5595-610.
- 8) Nesbit CE, Tersak JM, Prochownik EV. MYC oncogenes and human neoplastic disease. *Oncogene*. 1999;18(19):3004-16.
- 9) Vita M, Henriksson M. The Myc oncoprotein as a therapeutic target for human cancer. *Semin Cancer Biol*. 2006;16(4):318-30.
- 10) Lönn U, Lönn S, Nilsson B, Stenkvist B. Prognostic value of erb-B2 and myc amplification in breast cancer imprints. *Cancer*. 1995;75(11):2681-7.
- 11) Roncalli M, Viale G, Grimelius L, et al. Prognostic value of N-myc immunoreactivity in medullary thyroid carcinoma. *Cancer*. 1994;74(1):134-41.
- 12) Bourhis J, Le MG, Barrois M, et al. Prognostic value of c-myc proto-oncogene overexpression in early invasive carcinoma of the cervix. *J Clin Oncol*. 1990;8(11):1789-96.
- 13) Bourhis J, Le MG, Barrois M, et al. Prognostic value of c-myc proto-oncogene overexpression in early invasive carcinoma of the cervix. *J Clin Oncol*. 1990;8(11):1789-96.
- 14) Shen-ong GL, Keath EJ, Piccoli SP, Cole MD. Novel myc oncogene RNA from abortive immunoglobulin-gene recombination in mouse plasmacytomas. *Cell*. 1982;31(2 Pt 1):443-52.
- 15) Crews S, Barth R, Hood L, Prehn J, Calame K. Mouse c-myc oncogene is located on chromosome 15 and translocated to chromosome 12 in plasmacytomas. *Science*. 1982;218(4579):1319-21.
- 16) Dalla-favera R, Bregni M, Erikson J, Patterson D, Gallo RC, Croce CM. Human c-myc oncogene is located on the region of chromosome 8 that is translocated in Burkitt lymphoma cells. *Proc Natl Acad Sci USA*. 1982;79(24):7824-7.

Bibliography

- 17) Neel BG, Jhanwar SC, Chaganti RS, Hayward WS. Two human c-onc genes are located on the long arm of chromosome 8. *Proc Natl Acad Sci USA*. 1982;79(24):7842-6.
- 18) Taub R, Kirsch I, Morton C, et al. Translocation of the c-myc gene into the immunoglobulin heavy chain locus in human Burkitt lymphoma and murine plasmacytoma cells. *Proc Natl Acad Sci USA*. 1982;79(24):7837-41.
- 19) Dalla-favera R, Wong-staal F, Gallo RC. Onc gene amplification in promyelocytic leukaemia cell line HL-60 and primary leukaemic cells of the same patient. *Nature*. 1982;299(5878):61-3.
- 20) Collins S, Groudine M. Amplification of endogenous myc-related DNA sequences in a human myeloid leukaemia cell line. *Nature*. 1982;298(5875):679-81.
- 21) Payne GS, Courtneidge SA, Crittenden LB, Fadly AM, Bishop JM, Varmus HE. Analysis of avian leukosis virus DNA and RNA in bursal tumours: viral gene expression is not required for maintenance of the tumor state. *Cell*. 1981;23(2):311-22.
- 22) Hayward WS, Neel BG, Astrin SM. Activation of a cellular onc gene by promoter insertion in ALV-induced lymphoid leukosis. *Nature*. 1981;290(5806):475-80.
- 23) Singhi AD, Cimino-mathews A, Jenkins RB, et al. MYC gene amplification is often acquired in lethal distant breast cancer metastases of unamplified primary tumors. *Mod Pathol*. 2012;25(3):378-87.
- 24) Eilers M, Picard D, Yamamoto KR, Bishop JM. Chimaeras of myc oncoprotein and steroid receptors cause hormone-dependent transformation of cells. *Nature*. 1989;340(6228):66-8.
- 25) Kaczmarek L, Hyland JK, Watt R, Rosenberg M, Baserga R. Microinjected c-myc as a competence factor. *Science*. 1985;228(4705):1313-5.
- 26) Amati B, Alevizopoulos K, Vlach J. Myc and the cell cycle. *Front Biosci*. 1998;3:d250-68.
- 27) Lutz W, Leon J, Eilers M. Contributions of Myc to tumorigenesis. *Biochim Biophys Acta*. 2002;1602(1):61-71.
- 28) Bretones G, Delgado MD, León J. Myc and cell cycle control. *Biochim Biophys Acta*. 2015;1849(5):506-16.
- 29) Seoane J, Le HV, Massagué J. Myc suppression of the p21(Cip1) Cdk inhibitor influences the outcome of the p53 response to DNA damage. *Nature*. 2002;419(6908):729-34.
- 30) Wu S, Cetinkaya C, Munoz-alonso MJ, et al. Myc represses differentiation-induced p21CIP1 expression via Miz-1-dependent interaction with the p21 core promoter. *Oncogene*. 2003;22(3):351-60.
- 31) Acosta JC, Ferrándiz N, Bretones G, et al. Myc inhibits p27-induced erythroid differentiation of leukemia cells by repressing erythroid master genes without reversing p27-mediated cell cycle arrest. *Mol Cell Biol*. 2008;28(24):7286-95.

Bibliography

- 32) Wahlström T, Henriksson MA. Impact of MYC in regulation of tumor cell metabolism. *Biochim Biophys Acta*. 2015;1849(5):563-9.
- 33) Dunn S, Cowling VH. Myc and mRNA capping. *Biochim Biophys Acta*. 2015;1849(5):501-5.
- 34) Arabi A, Wu S, Ridderstråle K, et al. c-Myc associates with ribosomal DNA and activates RNA polymerase I transcription. *Nat Cell Biol*. 2005;7(3):303-10.
- 35) Grandori C, Gomez-roman N, Felton-edkins ZA, et al. c-Myc binds to human ribosomal DNA and stimulates transcription of rRNA genes by RNA polymerase I. *Nat Cell Biol*. 2005;7(3):311-8.
- 36) Gomez-roman N, Grandori C, Eisenman RN, White RJ. Direct activation of RNA polymerase III transcription by c-Myc. *Nature*. 2003;421(6920):290-4.
- 37) Pourdehnad M, Truitt ML, Siddiqi IN, Ducker GS, Shokat KM, Ruggero D. Myc and mTOR converge on a common node in protein synthesis control that confers synthetic lethality in Myc-driven cancers. *Proc Natl Acad Sci USA*. 2013;110(29):11988-93.
- 38) Pusapati RV, Rounbehler RJ, Hong S, et al. ATM promotes apoptosis and suppresses tumorigenesis in response to Myc. *Proc Natl Acad Sci USA*. 2006;103(5):1446-51.
- 39) Reimann M, Loddenkemper C, Rudolph C, et al. The Myc-evoked DNA damage response accounts for treatment resistance in primary lymphomas in vivo. *Blood*. 2007;110(8):2996-3004.
- 40) Gorrini C, Squatrito M, Luise C, et al. Tip60 is a haplo-insufficient tumour suppressor required for an oncogene-induced DNA damage response. *Nature*. 2007;448(7157):1063-7.
- 41) Prochownik EV. c-Myc: linking transformation and genomic instability. *Curr Mol Med*. 2008;8(6):446-58.
- 42) Kuzyk A, Mai S. c-MYC-induced genomic instability. *Cold Spring Harb Perspect Med*. 2014;4(4):a014373.
- 43) Vafa O, Wade M, Kern S, et al. c-Myc can induce DNA damage, increase reactive oxygen species, and mitigate p53 function: a mechanism for oncogene-induced genetic instability. *Mol Cell*. 2002;9(5):1031-44.
- 44) Louis SF, Vermolen BJ, Garini Y, et al. c-Myc induces chromosomal rearrangements through telomere and chromosome remodeling in the interphase nucleus. *Proc Natl Acad Sci USA*. 2005;102(27):9613-8.
- 45) Rohban S, Campaner S. Myc induced replicative stress response: How to cope with it and exploit it. *Biochim Biophys Acta*. 2015;1849(5):517-24.
- 46) Li Z, Owonikoko TK, Sun SY, et al. c-Myc suppression of DNA double-strand break repair. *Neoplasia*. 2012;14(12):1190-202.
- 47) Karlsson A, Deb-basu D, Cherry A, Turner S, Ford J, Felsher DW. Defective double-strand DNA break repair and chromosomal translocations by MYC overexpression. *Proc Natl Acad Sci USA*. 2003;100(17):9974-9.
- 48) Cavin LG, Wang F, Factor VM, et al. Transforming growth factor-alpha inhibits the intrinsic pathway of c-Myc-induced apoptosis through activation of

Bibliography

- nuclear factor-kappaB in murine hepatocellular carcinomas. *Mol Cancer Res.* 2005;3(7):403-12.
- 49)Baudino TA, Mckay C, Pendeville-samain H, et al. c-Myc is essential for vasculogenesis and angiogenesis during development and tumor progression. *Genes Dev.* 2002;16(19):2530-43.
- 50)Dews M, Homayouni A, Yu D, et al. Augmentation of tumor angiogenesis by a Myc-activated microRNA cluster. *Nat Genet.* 2006;38(9):1060-5.
- 51)Smith AP, Verrecchia A, Fagà G, et al. A positive role for Myc in TGFbeta-induced Snail transcription and epithelial-to-mesenchymal transition. *Oncogene.* 2009;28(3):422-30.
- 52)Cho KB, Cho MK, Lee WY, Kang KW. Overexpression of c-myc induces epithelial mesenchymal transition in mammary epithelial cells. *Cancer Lett.* 2010;293(2):230-9.
- 53)Ma L, Young J, Prabhala H, et al. miR-9, a MYC/MYCN-activated microRNA, regulates E-cadherin and cancer metastasis. *Nat Cell Biol.* 2010;12(3):247-56.
- 54)Zhang J, Chen S, Zhang W, et al. Human differentiation-related gene NDRG1 is a Myc downstream-regulated gene that is repressed by Myc on the core promoter region. *Gene.* 2008;417(1-2):5-12.
- 55)Laurenti E, Varnum-finney B, Wilson A, et al. Hematopoietic stem cell function and survival depend on c-Myc and N-Myc activity. *Cell Stem Cell.* 2008;3(6):611-24.
- 56)Wong DJ, Liu H, Ridky TW, Cassarino D, Segal E, Chang HY. Module map of stem cell genes guides creation of epithelial cancer stem cells. *Cell Stem Cell.* 2008;2(4):333-44.
- 57)Gabay M, Li Y, Felsher DW. MYC activation is a hallmark of cancer initiation and maintenance. *Cold Spring Harb Perspect Med.* 2014;4(6)
- 58)Felsher DW, Bishop JM. Reversible tumorigenesis by MYC in hematopoietic lineages. *Mol Cell.* 1999;4(2):199-207.
- 59)Pelengaris S, Littlewood T, Khan M, Elia G, Evan G. Reversible activation of c-Myc in skin: induction of a complex neoplastic phenotype by a single oncogenic lesion. *Mol Cell.* 1999;3(5):565-77.
- 60)Pelengaris S, Khan M, Evan GI. Suppression of Myc-induced apoptosis in beta cells exposes multiple oncogenic properties of Myc and triggers carcinogenic progression. *Cell.* 2002;109(3):321-34.
- 61)Mcmahon SB, Wood MA, Cole MD. The essential cofactor TRRAP recruits the histone acetyltransferase hGCN5 to c-Myc. *Mol Cell Biol.* 2000;20(2):556-62.
- 62)Vervoorts J, Lüscher-firzlauff JM, Rottmann S, et al. Stimulation of c-MYC transcriptional activity and acetylation by recruitment of the cofactor CBP. *EMBO Rep.* 2003;4(5):484-90.
- 63)Frank SR, Parisi T, Taubert S, et al. MYC recruits the TIP60 histone acetyltransferase complex to chromatin. *EMBO Rep.* 2003;4(6):575-80.
- 64)Knoepfler PS, Zhang XY, Cheng PF, Gafken PR, McMahan SB, Eisenman RN. Myc influences global chromatin structure. *EMBO J.* 2006;25(12):2723-34.

Bibliography

- 65) Kurland JF, Tansey WP. Myc-mediated transcriptional repression by recruitment of histone deacetylase. *Cancer Res.* 2008;68(10):3624-9.
- 66) Iraci N, Diolaiti D, Papa A, et al. A SP1/MIZ1/MYCN repression complex recruits HDAC1 at the TRKA and p75NTR promoters and affects neuroblastoma malignancy by inhibiting the cell response to NGF. *Cancer Res.* 2011;71(2):404-12.
- 67) Kleine-kohlbrecher D, Adhikary S, Eilers M. Mechanisms of transcriptional repression by Myc. *Curr Top Microbiol Immunol.* 2006;302:51-62.
- 68) Secombe J, Li L, Carlos L, Eisenman RN. The Trithorax group protein Lid is a trimethyl histone H3K4 demethylase required for dMyc-induced cell growth. *Genes Dev.* 2007;21(5):537-51.
- 69) Brenner C, Deplus R, Didelot C, et al. Myc represses transcription through recruitment of DNA methyltransferase corepressor. *EMBO J.* 2005;24(2):336-46.
- 70) Corvetta D, Chayka O, Gherardi S, et al. Physical interaction between MYCN oncogene and polycomb repressive complex 2 (PRC2) in neuroblastoma: functional and therapeutic implications. *J Biol Chem.* 2013;288(12):8332-41.
- 71) Amente S, Bertoni A, Morano A, Lania L, Avvedimento EV, Majello B. LSD1-mediated demethylation of histone H3 lysine 4 triggers Myc-induced transcription. *Oncogene.* 2010;29(25):3691-702.
- 72) Shi Y, Lan F, Matson C, et al. Histone demethylation mediated by the nuclear amine oxidase homolog LSD1. *Cell.* 2004;119(7):941-53.
- 73) Lan F, Nottke AC, Shi Y. Mechanisms involved in the regulation of histone lysine demethylases. *Curr Opin Cell Biol.* 2008;20(3):316-25.
- 74) Chen Y, Yang Y, Wang F, et al. Crystal structure of human histone lysine-specific demethylase 1 (LSD1). *Proc Natl Acad Sci USA.* 2006;103(38):13956-61.
- 75) Humphrey GW, Wang Y, Russanova VR, et al. Stable histone deacetylase complexes distinguished by the presence of SANT domain proteins CoREST/kiaa0071 and Mta-L1. *J Biol Chem.* 2001;276(9):6817-24.
- 76) Shi Y, Sawada J, Sui G, et al. Coordinated histone modifications mediated by a CtBP co-repressor complex. *Nature.* 2003;422(6933):735-8.
- 77) Wang J, Hevi S, Kurash JK, et al. The lysine demethylase LSD1 (KDM1) is required for maintenance of global DNA methylation. *Nat Genet.* 2009;41(1):125-9.
- 78) Huang J, Sengupta R, Espejo AB, et al. p53 is regulated by the lysine demethylase LSD1. *Nature.* 2007;449(7158):105-8.
- 79) Luo H, Shenoy AK, Li X, et al. MOF Acetylates the Histone Demethylase LSD1 to Suppress Epithelial-to-Mesenchymal Transition. *Cell Rep.* 2016;15(12):2665-78.
- 80) Tang M, Shen H, Jin Y, et al. The malignant brain tumor (MBT) domain protein SFMBT1 is an integral histone reader subunit of the LSD1 demethylase

Bibliography

- complex for chromatin association and epithelial-to-mesenchymal transition. *J Biol Chem.* 2013;288(38):27680-91.
- 81) Lin T, Ponn A, Hu X, Law BK, Lu J. Requirement of the histone demethylase LSD1 in Snai1-mediated transcriptional repression during epithelial-mesenchymal transition. *Oncogene.* 2010;29(35):4896-904.
- 82) Lin Y, Wu Y, Li J, et al. The SNAG domain of Snail1 functions as a molecular hook for recruiting lysine-specific demethylase 1. *EMBO J.* 2010;29(11):1803-16.
- 83) Kahl P, Gullotti L, Heukamp LC, et al. Androgen receptor coactivators lysine-specific histone demethylase 1 and four and a half LIM domain protein 2 predict risk of prostate cancer recurrence. *Cancer Res.* 2006;66(23):11341-7.
- 84) Kauffman EC, Robinson BD, Downes MJ, et al. Role of androgen receptor and associated lysine-demethylase coregulators, LSD1 and JMJD2A, in localized and advanced human bladder cancer. *Mol Carcinog.* 2011;50(12):931-44.
- 85)
- 86) Lv T, Yuan D, Miao X, et al. Over-expression of LSD1 promotes proliferation, migration and invasion in non-small cell lung cancer. *PLoS ONE.* 2012;7(4):e35065.
- 87) Schulte JH, Lim S, Schramm A, et al. Lysine-specific demethylase 1 is strongly expressed in poorly differentiated neuroblastoma: implications for therapy. *Cancer Res.* 2009;69(5):2065-71.
- 88) Maris JM, Hogarty MD, Bagatell R, Cohn SL. Neuroblastoma. *Lancet.* 2007;369(9579):2106-20.
- 89) Huang M, Weiss WA. Neuroblastoma and MYCN. *Cold Spring Harb Perspect Med.* 2013;3(10):a014415.
- 90) Schwab M. MYCN in neuronal tumours. *Cancer Lett.* 2004;204(2):179-87.
- 91) Amente S, Milazzo G, Sorrentino MC, et al. Lysine-specific demethylase (LSD1/KDM1A) and MYCN cooperatively repress tumor suppressor genes in neuroblastoma. *Oncotarget.* 2015;6(16):14572-83.
- 92) Tanaka K, Hirota T. Chromosomal instability: A common feature and a therapeutic target of cancer. *Biochim Biophys Acta.* 2016;1866(1):64-75.
- 93) Koch HB, Zhang R, Verdoodt B, et al. Large-scale identification of c-MYC-associated proteins using a combined TAP/MudPIT approach. *Cell Cycle.* 2007;6(2):205-17.
- 94) Gospodinov A, Herceg Z. Chromatin structure in double strand break repair. *DNA Repair (Amst).* 2013;12(10):800-10.
- 95) Gospodinov A, Herceg Z. Shaping chromatin for repair. *Mutat Res.* 2013;752(1):45-60.
- 96) Miller KM, Jackson SP. Histone marks: repairing DNA breaks within the context of chromatin. *Biochem Soc Trans.* 2012;40(2):370-6.
- 97) Hustedt N, Durocher D. The control of DNA repair by the cell cycle. *Nat Cell Biol.* 2016;19(1):1-9.

Bibliography

- 98) Jacobs JJ, Scheijen B, Voncken JW, Kieboom K, Berns A, Van IJcken M. Bmi-1 collaborates with c-Myc in tumorigenesis by inhibiting c-Myc-induced apoptosis via INK4a/ARF. *Genes Dev.* 1999;13(20):2678-90.
- 99) Schmitt CA, Lowe SW. Bcl-2 mediates chemoresistance in matched pairs of primary E(mu)-myc lymphomas in vivo. *Blood Cells Mol Dis.* 2001;27(1):206-16.
- 100) Schmitt CA, Mccurrach ME, De Stanchina E, Wallace-brodeur RR, Lowe SW. INK4a/ARF mutations accelerate lymphomagenesis and promote chemoresistance by disabling p53. *Genes Dev.* 1999;13(20):2670-7.
- 101) Zindy F, Eischen CM, Randle DH, et al. Myc signaling via the ARF tumor suppressor regulates p53-dependent apoptosis and immortalization. *Genes Dev.* 1998;12(15):2424-33.
- 102) Soucek L, Jucker R, Panacchia L, Ricordy R, Tatò F, Nasi S. Omomyc, a potential Myc dominant negative, enhances Myc-induced apoptosis. *Cancer Res.* 2002;62(12):3507-10.
- 103) Müller I, Larsson K, Frenzel A, et al. Targeting of the MYCN protein with small molecule c-MYC inhibitors. *PLoS ONE.* 2014;9(5):e97285.
- 104) Gugnoni M, Sancisi V, Manzotti G, Gandolfi G, Ciarrocchi A. Autophagy and epithelial-mesenchymal transition: an intricate interplay in cancer. *Cell Death Dis.* 2016;7(12):e2520.
- 105) Wolfer A, Ramaswamy S. MYC and metastasis. *Cancer Res.* 2011;71(6):2034-7.
- 106) Weiler M, Blaes J, Pusch S, et al. mTOR target NDRG1 confers MGMT-dependent resistance to alkylating chemotherapy. *Proc Natl Acad Sci USA.* 2014;111(1):409-14.
- 107) Xie J, Wang X, Proud CG. mTOR inhibitors in cancer therapy. *F1000Res.* 2016;5
- 108) Li J, Kim SG, Blenis J. Rapamycin: one drug, many effects. *Cell Metab.* 2014;19(3):373-9.
- 109) Parmigiani A, Nourbakhsh A, Ding B, et al. Sestrins inhibit mTORC1 kinase activation through the GATOR complex. *Cell Rep.* 2014;9(4):1281-91.
- 110) Segerström L, Baryawno N, Sveinbjörnsson B, et al. Effects of small molecule inhibitors of PI3K/Akt/mTOR signaling on neuroblastoma growth in vitro and in vivo. *Int J Cancer.* 2011;129(12):2958-65.
- 111) Johnsen JI, Segerström L, Orrego A, et al. Inhibitors of mammalian target of rapamycin downregulate MYCN protein expression and inhibit neuroblastoma growth in vitro and in vivo. *Oncogene.* 2008;27(20):2910-22.
- 112) Cianfanelli V, Fuoco C, Lorente M, et al. AMBRA1 links autophagy to cell proliferation and tumorigenesis by promoting c-Myc dephosphorylation and degradation. *Nat Cell Biol.* 2015;17(1):20-30.
- 113) White E, Dipaola RS. The double-edged sword of autophagy modulation in cancer. *Clin Cancer Res.* 2009;15(17):5308-16.

Bibliography

- 114) Belounis A, Nyalendo C, Le gall R, et al. Autophagy is associated with chemoresistance in neuroblastoma. *BMC Cancer*. 2016;16(1):891.